

# High tire pressure test

Technical report



Ressources, territoires, habitats et logement  
Énergies et climat  
Prévention des risques  
Développement durable  
Infrastructures, transports et mer

Présent  
pour  
l'avenir



service technique de l'Aviation civile

Photo de Couverture: © Airbus Industrie

# HIGH TIRE PRESSURE TEST

## Technical Report

**SUMMARY:**

This report describes an outdoor full-scale test led by Airbus S.A.S in partnership with the French authorities DGAC-STAC, LCPC, LRPC-T, MICHELIN and VANCOUVER<sup>2</sup> to improve experimental and theoretical knowledge related to the effects of aircraft internal tire inflation pressure on the behavior of and damage to flexible pavement. Since some modern aircraft have tire pressures exceeding 15 bar, the tests focus on pressures from 15 bar to 17.5 bar. The experimental pavement located on the Toulouse-Blagnac airport in France includes up to seven different test sections, representative of current airfield flexible pavement world-wide. Variant parameters from one section to another are thickness of AC surface layer and its performance in respect of rutting, and surface treatment as grooving. The aircraft simulation vehicle drives four dual-wheel gears sufficiently spaced enough in order to prevent from any interaction between them, making it possible to test two different tire pressures (15 and 17.5 bar) and two weights per wheel (ultimate weights, 28.7 and 33.2 tons) simultaneously. The seven test sections are instrumented to measure resilient strains, and resilient and permanent displacements (rutting). The structure has been designed according to the French airport pavement design method, for 10,000 passes of B747-400 gear. Tests will continue until the simulator runs are no longer possible due to the high rut depth level. The tests have been presented in renowned airfield pavement seminars, conferences and journals., The US Federal Aviation Administration, the Boeing Company and a panel of Universities and private companies have been continuously kept informed of the test progress and the final test results, especially during the two HTPT workshops done in April 21<sup>st</sup>/22<sup>nd</sup>, 2009 and June 24<sup>th</sup>/25<sup>th</sup>, 2010

<b>KEYWORDS</b>	Pavement, Tire Pressure, regulation, ACN, PCN
<b>RELATED DOCUMENTS</b>	ICAO, Annex 14 -- Aerodromes, Volume I – Aerodrome Design and Operations ICAO, Doc 9157-AN/901 Part.3

## TABLE OF CONTENTS

1	Introduction.....	7
1.1	AOSWG / Pavement subgroup task.....	7
1.1.1	Composition .....	7
1.1.2	Task .....	7
1.1.3	Procedures .....	8
1.2	Aircraft Classification Number / Pavement Classification Number system (ACN / PCN).....	9
1.3	Aircraft load trends.....	10
1.4	Consistency of current “allowable tire pressure” category? .....	12
1.5	How to manage tire pressure? .....	13
1.5.1	Tire characteristics .....	13
1.5.2	Definitions.....	13
1.5.3	Example of in-service tire pressure calculation .....	13
2	Partnership .....	16
3	Test facilities.....	17
3.1	Design .....	17
3.1.1	Initial phase .....	17
3.1.2	Update phase: flexible overlay .....	24
3.2	Construction and acceptance .....	25
3.2.1	Natural soil .....	25
3.2.2	Capping layer .....	26
3.2.3	Sub-base layer .....	29
3.2.4	AC material.....	29
3.3	Simulator .....	38
3.4	Tires technology and specifications .....	38
3.4.1	Specifications .....	38
3.4.2	Element of tire mechanic .....	39
3.4.3	Specifications and tire technology.....	45
3.5	Instrumentation and data acquisition .....	46
3.5.1	Surface layer rutting sensors .....	48
3.5.2	Horizontal strain gauges .....	48
3.5.3	Vertical strain gauges .....	49
3.5.4	Absolute vertical displacement .....	50
3.5.5	Temperature profiles.....	50
3.5.6	Acquisition unit .....	51
4	Tests.....	52
4.1	Objectives.....	52
4.2	Test principles .....	52
4.2.1	General simulator specification .....	52
4.2.2	Loading cases principle .....	53
4.3	Consolidation phase: C0.....	54
4.3.1	Objectives.....	54
4.3.2	Simulator’s configuration .....	54
4.3.3	Procedure.....	55
4.4	Fatigue tests .....	57
4.4.1	Objectives.....	57
4.4.2	Simulator’s configuration .....	57
4.4.3	Procedure.....	59
5	Data analysis .....	60
5.1	Introduction.....	60

5.2	Thermal conditions of the tests .....	60
5.3	Strain-gauge signals .....	61
5.3.1	Wearing course-base AC interface .....	62
5.3.2	Vertical strains gauges and vertical displacement sensors .....	62
5.4	Rutting deformation .....	66
5.4.1	Rutting measurement and evolution curves with traffic .....	66
5.4.2	Observation on sample caught from the section B and G .....	71
5.4.3	Main results drawn from rutting measurement and core samples .....	72
6	General conclusions and recommendations .....	75
Appendix 1.	Glossary .....	77
Appendix 2.	Untreated gravel material (sub-base and capping layer) specification .....	79
Appendix 3.	Untreated gravel material control by sieving .....	80
Appendix 4.	EB14-GB Class 3 Base product specifications.....	81
Appendix 5.	EB14-GB Class 3 Base control.....	82
Appendix 6.	EB14-GB Class 4 Base product specifications.....	84
Appendix 7.	EB14-GB Class 4 Base control.....	86
Appendix 8.	Sections A,B,C,E and F asphalt material (EB14-BBA C Class 3 Surface) specifications .....	88
Appendix 9.	Sections A,B,C,E and F asphalt material (EB14-BBA C Class 3 Surface) control.....	89
Appendix 10.	Section D asphalt material (EB14-BBME C Class 3 Surface) product specifications .....	91
Appendix 11.	Section D asphalt material (EB14-BBME C Class 3 Surface) control.....	93
Appendix 12.	Section G asphalt material (EB14-BB C Surface) product specifications .....	95
Appendix 13.	Section G Asphalt material (EB14-BB C Surface) control .....	96
Appendix 14.	Schematics of the simulator.....	98
Appendix 15.	Dynaplaque, measurement of dynamic modulus of ground .....	100
Appendix 16.	Portancemetre, continuous capacity measurement .....	101
Appendix 17.	Evolution curves of rutting depth measured by the transverse-profilometer .....	102

## TABLE OF FIGURES

Figure 1: Individual wheel load of various aircraft – History (FAA, R. Joel courtesy).....	11
Figure 2: Aircraft internal tire pressure inflation trend .....	12
Figure 3: Bulges at bead area .....	14
Figure 4: Tire pressure category repartition for LR aircraft operations .....	15
Figure 5: HTPT site location .....	17
Figure 6: B747-400 gear geometry .....	18
Figure 7: Design chart of the B747-400 .....	20
Figure 8: Chart for determining the minimum granular thickness of base and surface materials....	21
Figure 9: Longitudinal typical cross-section showing the 7 tested sections .....	21
Figure 10: Pavement materials of the 7 test sections .....	24
Figure 11: EV2 modulus controls on stabilized sub-grade .....	25
Figure 12: EV2 modulus controls on capping layer (LCPC's plate) .....	26
Figure 13: EV2 modulus controls on capping layer (LCPC's Dynaplaque).....	27
Figure 14: EV2 modulus controls on capping layer (LCPC's Portancemètre) .....	28
Figure 15: Horizontal strains observed at bottom of base asphalt layer prior to reinforcement.....	31
Figure 16: Vertical strains observed at top of sub-base prior to reinforcement.....	31
Figure 17 : Water contamination under the pavement .....	33
Figure 18: strains observed at bottom of base asphalt layer post reinforcement.....	37
Figure 19: strains observed at top of sub-base post reinforcement.....	37
Figure 20: Main components of a Bias or Radial tire .....	39
Figure 21: Cross section profile of carcass plies for Bias.....	40
Figure 22: Cross section profile of carcass plies for Radial.....	40
Figure 23: Contact patch shape of Bias.....	41
Figure 24: Contact patch shape of Radial.....	41
Figure 25: Contact patch pressure distribution for Bias and Radial.....	42
Figure 26: Calculated contact patch pressure distribution for tire size 1400x530R23 40PR at 32% deflection.....	43
Figure 27: Rolling circumference of Bias tires.....	44
Figure 28: Rolling circumference of Radial tires .....	44
Figure 29: Instrumentation of section B .....	47
Figure 30: Surface layer rutting sensor .....	48
Figure 31: Horizontal strain gauges .....	49
Figure 32: Vertical strain gauges .....	49
Figure 33: Core equipped with temperature gauges .....	51
Figure 34: Acquisition Unit.....	51
Figure 35: The simulator.....	52
Figure 36: Dimensions of the simulator .....	53
Figure 37: Loading cases principle .....	53
Figure 38: Simulator trajectories during preloading phase .....	55
Figure 39: Consolidation phase procedure .....	56
Figure 40: Fatigue test procedure.....	59
Figure 41: Evolution of the cumulative traffic and the temperature in AC.....	60
Figure 42: Temperatures in AC during the tests .....	61
Figure 43: Typical strain-gauge signals at the bottom of the surface AC and the top of base AC layer. Structure B, load configurations C2 and C3, tire pressure 1.75 MPa (gauge measure in µstrain, negative sign for contraction).....	62
Figure 44: Typical strain-gauge signals at the bottom of the surface AC and the top of base AC layer. Structure B, load configurations C2 and C3, tire pressure 1.75 MPa (gauge measure in µstrain, negative sign for contraction).....	63

Figure 45: Typical strain-gauge signals at the bottom of the surface AC and the top of base AC layer. Structure B, load configurations C2 and C3, tire pressure 1.75 MPa (gauge measure in  $\mu$ strain, negative sign for contraction) .....64

Figure 46: Sensor repeatability tests. Signals measured by horizontal strain-gauges at the bottom of surface AC .....65

Figure 47: Sensor repeatability tests. Signals measured by horizontal strain-gauges at the top of the UGM subbase .....65

Figure 48: Evolution curve of rutting measured on section B, configuration M3 .....66

Figure 49: Evolution curve of rutting measured on section G, configuration M3.....67

Figure 50: Transversal rutting profiles measured on section B, profile P2, module M3, by means of the transverso-profilometer.....68

Figure 51: Transversal rutting profiles measured on section G, profile P2, module M3, by means of the transverso-profilometer.....68

Figure 52: Maximal rutting depth reached at 11,000 passes on section A to section F .....69

Figure 53: Maximal rutting depth reached at 10,500 and 11,000 passes on section G .....69

Figure 54: Side view of the simulator .....98

Figure 55: Bottom view of the simulator.....98

Figure 56: Top view of the simulator.....99

Figure 57: Bottom view of the simulator.....99

Figure 58: Picture of the Dynaplaque .....100

Figure 59: Picture of the Portancemetre .....101

Figure 60: Evolution curve of rutting measured on section A, configuration M1 .....102

Figure 61: Evolution curve of rutting measured on section A, configuration M2 .....102

Figure 62: Evolution curve of rutting measured on section A, configuration M3 .....103

Figure 63: Evolution curve of rutting measured on section A, configuration M4 .....103

Figure 64: Evolution curve of rutting measured on section B, configuration M1 .....104

Figure 65: Evolution curve of rutting measured on section B, configuration M2 .....104

Figure 66: Evolution curve of rutting measured on section B, configuration M3 .....105

Figure 67: Evolution curve of rutting measured on section B, configuration M4 .....105

Figure 68: Evolution curve of rutting measured on section C, configuration M1 .....106

Figure 69: Evolution curve of rutting measured on section C, configuration M2 .....106

Figure 70: Evolution curve of rutting measured on section C, configuration M3 .....107

Figure 71: Evolution curve of rutting measured on section C, configuration M4 .....107

Figure 72: Evolution curve of rutting measured on section D, configuration M1 .....108

Figure 73: Evolution curve of rutting measured on section D, configuration M2 .....108

Figure 74: Evolution curve of rutting measured on section D, configuration M3 .....109

Figure 75: Evolution curve of rutting measured on section D, configuration M4 .....109

Figure 76: Evolution curve of rutting measured on section E, configuration M1 .....110

Figure 77: Evolution curve of rutting measured on section E, configuration M2 .....110

Figure 78: Evolution curve of rutting measured on section E, configuration M3 .....111

Figure 79: Evolution curve of rutting measured on section E, configuration M4 .....111

Figure 80: Evolution curve of rutting measured on section F, configuration M1 .....112

Figure 81: Evolution curve of rutting measured on section F, configuration M2 .....112

Figure 82: Evolution curve of rutting measured on section F, configuration M3 .....113

Figure 83: Evolution curve of rutting measured on section F, configuration M4 .....113

Figure 84: Evolution curve of rutting measured on section G, configuration M1 .....114

Figure 85: Evolution curve of rutting measured on section G, configuration M2 .....114

Figure 86: Evolution curve of rutting measured on section G, configuration M3 .....115

Figure 87: Evolution curve of rutting measured on section G, configuration M4 .....115

## TABLE OF TABLES

Table 1: Initial tire pressure categories and associated limits as proposed by Boeing and FAA.....	8
Table 2: Properties of the 3 types of surface asphalt concrete.....	23
Table 3: Compared laboratory characteristics of Class 3 and Class 4 base asphalt concrete.....	24
Table 4: Surface layers compaction controls .....	30
Table 5: Theoretical water content profile.....	32
Table 6: Measured water content profile.....	32
Table 7: Asphalt material mechanic characteristics synthesis.....	35
Table 8: Surface layers compaction controls .....	36
Table 9: Final surface layer thickness.....	36
Table 10: Tire technologies abilities vs performance requested.....	45
Table 11: Depth of temperature gauges .....	50
Table 12: Configurations during consolidation phase before reinforcement.....	54
Table 13: Configuration C0 after pavement reinforcement.....	55
Table 14: Configuration C1'.....	57
Table 15: Configuration C1" .....	57
Table 16: Configuration C3.....	58
Table 17: Configuration C2.....	58
Table 18: Maximal rutting depth (in mm) reached at the end of the test and evaluation of tire pressure and wheel-load effects.....	70
Table 19: Dynaplaque specifications .....	100
Table 20: Portancemetre specifications.....	101



## 1 Introduction

### 1.1 AOSWG / Pavement subgroup task<sup>1</sup>

In 1978, ICAO initiated the adoption of a single means for airports to express the load capacity of airfield pavement, and at the same time, a means by which the aircraft manufacturers could indicate the pavement loading of their aircraft. The method is now used worldwide, and is referred to as the ACN/PCN System.

There are five attributes to the ACN/PCN system (the pavement type, the subgrade code, an allowable tire pressure and a description of the method by which the PCN was developed, as well as the numeric PCN - or ACN - value). From the advent of this system, the tire pressure element was, and remains, only loosely defined, having no ICAO proscribed methodology. Instead ICAO Document 9157 – AN/901, Aerodrome Design Manual Part 3 – Pavements (the ADM), refers the user to the methods that have been employed by two member states as examples. The dilemma facing both airports and aircraft manufacturers at this time when large commercial aircraft tire pressures have increased, is that no known pavement failures or other anomalies have been reported, which may indicate that tire pressure limits used in the ACN/PCN method ever since its inception, could possibly be increased without putting aircraft or pavements at risk.

#### 1.1.1 Composition

Over the past four years, the FAA with support of the Boeing Company, carried out a series of tests on a variety of typical flexible pavement test sections that were intended to exhibit whether the existing tire pressure limit code letter X (1.5 MPa or 15 bars) was a reasonable upper limit for X-rated pavements or not. Initial findings from the FAA test indicated that a 16.5 bar limit would make more sense in terms of the pavement reaction to applied tire pressure. Test results were well documented and subject of technical papers that were presented publicly, however the tests have been viewed as being too narrowly focused to justify an across-the-board change to the ICAO criteria. At that time, the French STAC in cooperation with Airbus SAS announced their intention to perform further and more detailed testing to increase data availability and knowledge of this phenomenon to a successful completion thereby allowing ICAO tire pressure limit codes to be formally and permanently changed to be more consistent with real world pavements performance.

#### 1.1.2 Task

Initial research into the tire pressure topic began with the original ACN Task (Task Number AGA-9301), and current tests in this area have been reported to the various working groups of the Aerodrome Panel (AOSWG/5 Report paragraph 2.6.1). Since the results of this work will potentially affect Annex 14 SARP's (Annex 14, paragraph 2.6.6.c) and the related guidance materials that appear in the ADM Part 3

---

<sup>1</sup> TERMS OF REFERENCE (TOR) FOR THE PAVEMENT SUB GROUP (PSG)  
Aerodrome Operations and Services Working Group (AOSWG)  
Aerodrome Panel (AP)

(paragraph 1.1.3.2.c, 3.3.4, 3.5.7, and 3.6.4.9.c), the PSG will require the approval of the AP to move forward with this task.

### 1.1.3 Procedures

The FAA tests were conducted on three sections of representative airfield pavement, built on a well compacted base and sub-base materials, and were supported by a low strength (CBR 4) subgrade. The three sections had surface courses of 2 inches, 4 inches and 6 inches (5, 10 and 15 centimeters) thickness. A single wheel module was used on the test sections loaded at 40,000 50,000 and 55,000 pound single wheel loads (18,144 – 22,680 – and 24,948 kg, respectively) and the each wheel load made between 250 and 2750 passes of the test sections. There were no discrepancies noted along the surface of the pavement after each 500 pass intervals, so the tire pressures were increased by 20 psi (0.14 MPa), and another 500 passes were carried out. This continued until the wheel loads and tire pressures reached the maximum conditions (55,000 pound single wheel load and 240 psi tire pressure – or 24,948 kg and 1.65 MPa). At test sequence completion, after more than 6000 passes, there were no cracks in the pavement surface (even along the thinnest – 2 inch [5 cm] section) and the measured ruts were just above the level considered as the serviceable limit for airfield pavement (0.6 inch, or 1.5 cm).

In ADM Part 3 – Pavement, the typical surface pavement requirements of the various agencies for asphalt surface course thicknesses is in the range of 4 to 6 inches (10 to 15 cm). The FAA tire pressure tests confirmed that, for relatively significant numbers of load cycles, higher tire pressures than those for which the flexible pavement is rated have no adverse effect.

Boeing and FAA’s tests results suggested that tire pressure categories currently used in ICAO PCN rating system could be modified to be more compatible with modern aircraft operating in current fleets by modifying the category limits. The proposed tire pressure limits based on the FAA tests, were as indicated in Table 1.

**Table 1: Initial tire pressure categories and associated limits as proposed by Boeing and FAA**

<b>Tire Pressure Category</b>	<b>Current ICAO Limit Psi (MPa)</b>	<b>Proposed ICAO Limit Psi (MPa)</b>
<b>W</b>	Unlimited	Unlimited
<b>X</b>	217 (1.50)	240 (1.65)
<b>Y</b>	145 (1.0)	181 (1.25)
<b>Z</b>	72 (.50)	72 (.50)

This proposal however was not considered to have been thoroughly investigated by some in the airport pavement arena, so a second series of tests are presented in this technical report on a test pavement in Toulouse, France. These tests have been run on seven test sections that have been designed to have representative base, sub-base and subgrade characteristics, but will isolate the surface asphalt as the key element of observation. Inflation pressures of 15 and 17.5 bars (218 psi and 254 psi respectively) are applied to the pavement by four dual wheels loading devices and utilizing radial (NZG) tires on surface course thicknesses varying from 6 to 12 cm (2.4 to 4.7 inches) including a grooved and a fiber-reinforced

surface section. The test pavement is fully instrumented, and the wheel loading is representative of the larger aircraft in the current fleet including an extrapolation of wheel loading in the next 20 years. The intent is to run the tests through to 10,000 passes (or more if the pavement condition and seasonal timing permits). The failure point was described as permanent rutting of 0.5 to 0.75 inches (1.3 to 1.9 cm) which is considered a medium severity rut, a level at which typical airports would initiate remedial action when found on runways or taxiways. Nevertheless, the need to extend process of pavement damage under heavy wheel loads, high temperature and high traffic level led to the decision of accepting higher rut deeper until traffic is no longer possible.

The final result of this work is contained in this report. It has been used to assemble professional articles written for and presented to well renowned airfield pavement seminars, conferences or journals (or combinations of all three), and will be collected into a proper Working Paper for the PSG to consider, then presented to the AOSWG. The final stage is the AP as required for adoption in Annex 14 including related guidance material.

## 1.2 Aircraft Classification Number / Pavement Classification Number system (ACN / PCN)

The intent is not to describe or discuss the ACN/PCN method which is well known and well documented either by the official International Civil Aviation Organization (ICAO) or in various papers, but to focus on the third code letter in a given Pavement Classification Number. This letter indicates the maximum tire pressure allowable for a given pavement type and subgrade strength category.

The ACN/PCN system introduced in 1983 is designated by the ICAO as the only approved standardized method for reporting aircraft weight-bearing capacity of airfield pavement. This system is an effective, simple and readily comprehensible method: An aircraft has an assigned ACN and the PCN number indicates the suitability of a pavement area for unrestricted operations by any aircraft that has an ACN and tire pressure not exceeding the limits reported in PCN format of stated pavement type and subgrade strength category.

- ACN is a number that expresses the relative structural effect of an aircraft on different pavement types for specified standard subgrade strengths in terms of standard single-wheel load. The ACN was developed for two types of pavements, flexible and rigid, and for four levels of subgrade strength. ACN values are provided by aircraft manufacturers at maximum and minimum operational gross weight, usually operating weight empty (OWE) and maximum ramp or taxi weight (MRW or MTW).
- PCN is a number that expresses the relative load-carrying capacity of a pavement in terms of a standard equivalent single wheel load (ESWL) at a standard tire pressure.
- The system is structured so that a pavement with a specific reported PCN value can support, without any weight restrictions, an aircraft that has an ACN value equal to, or less than, the pavement's PCN value.
- The PCN value is intended for reporting pavement strength only. It expresses the results of pavement evaluation in relative terms and cannot be used for pavement design or as a substitute for evaluation.

While type of pavement and subgrade strength category are well defined and clearly described, the allowable tire pressure categories are defined by engineering judgment and not substantiated by laboratory and/or full-scale tests.

ICAO, Airport Design Manual Part.3 – second edition – 1983 Doc 9157-AN/901 indicates that *“While tests of bituminous mixes and extracted cores for quality of the bituminous surfacing will be most helpful in selecting the tire pressure category, no specific relations have been developed between test behavior and acceptable tire pressure. It will usually be adequate, except where limitations are obvious, to establish category limits only when experience with high tire pressures indicates pavement distress”*.

Therefore our tests mainly focus on high tire pressure, greater than or equal to the current code X letter representing a tire pressure limitation of 15 bar (218 PSI).

### 1.3 Aircraft load trends

With the permanent air traffic increase (forecasters predict a threefold increase by 2025), aviation industry has made continuous strides in the past 50 years. As a result, load per wheel (and consequently internal tire pressure inflation) have significantly increased since the initial FAA policy, which was based on a DC-8 configuration at 158.757 tons (~ 18.8 tons wheel load). These improvements have been driven by the airlines demand to develop and design aircraft with high efficiency, maximum reliability and optimized performances. As a consequence, aircraft component are lighter and especially landing gear optimized to meet payload-range requirements. The only way to significantly improve pavement loading is to distribute aircraft weight over more wheels, which could have major impact on payload capability and block fuel. Such a trade-off may be acceptable if it allows an increase in payload-range capability e.g. very long range or stretch versions.

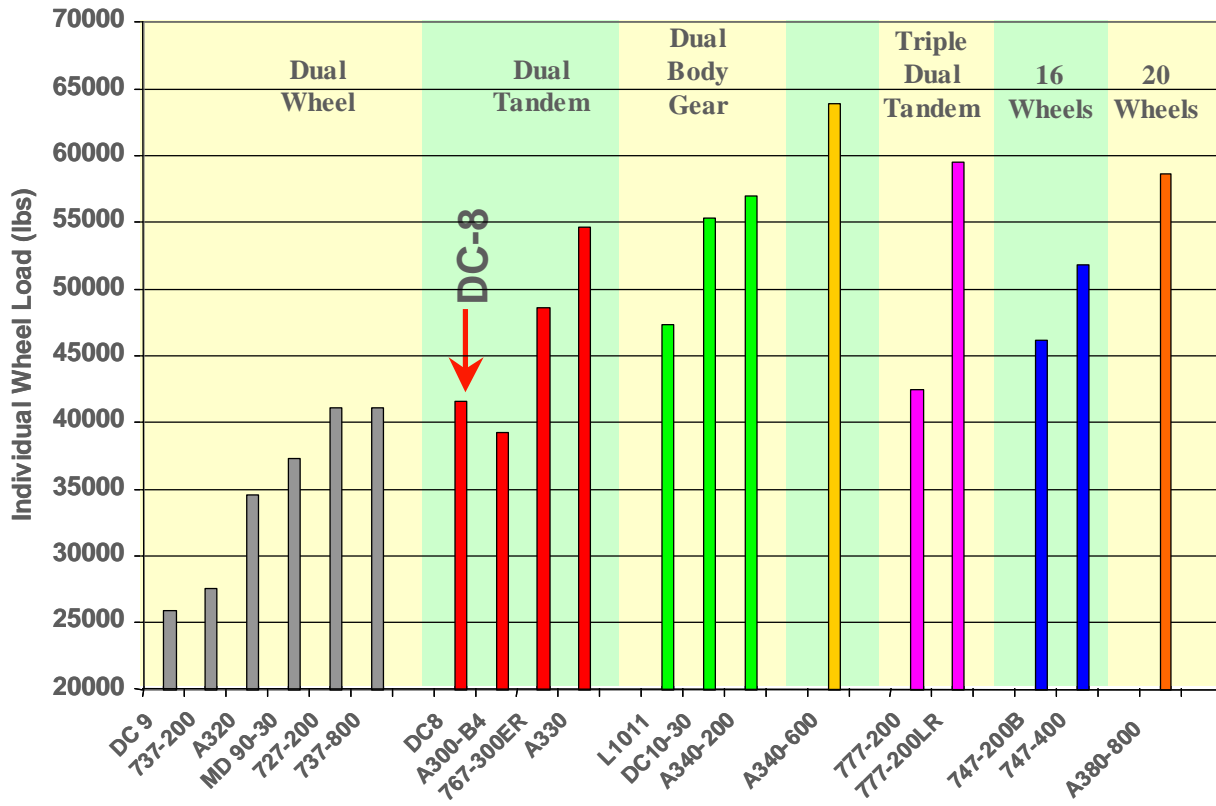


**Figure 1: Individual wheel load of various aircraft – History (FAA, R. Joel courtesy)**

The in-service tire pressure is directly derived from the worst aircraft static vertical load on the main landing gear (usually at maximum taxi weight and max. aft center of gravity (C.G) conditions). Therefore a relationship can be established between the aircraft gross weight, landing gear concept and the calculated internal tire pressure inflation. Figure 2 shows an overview of aircraft tire pressure.

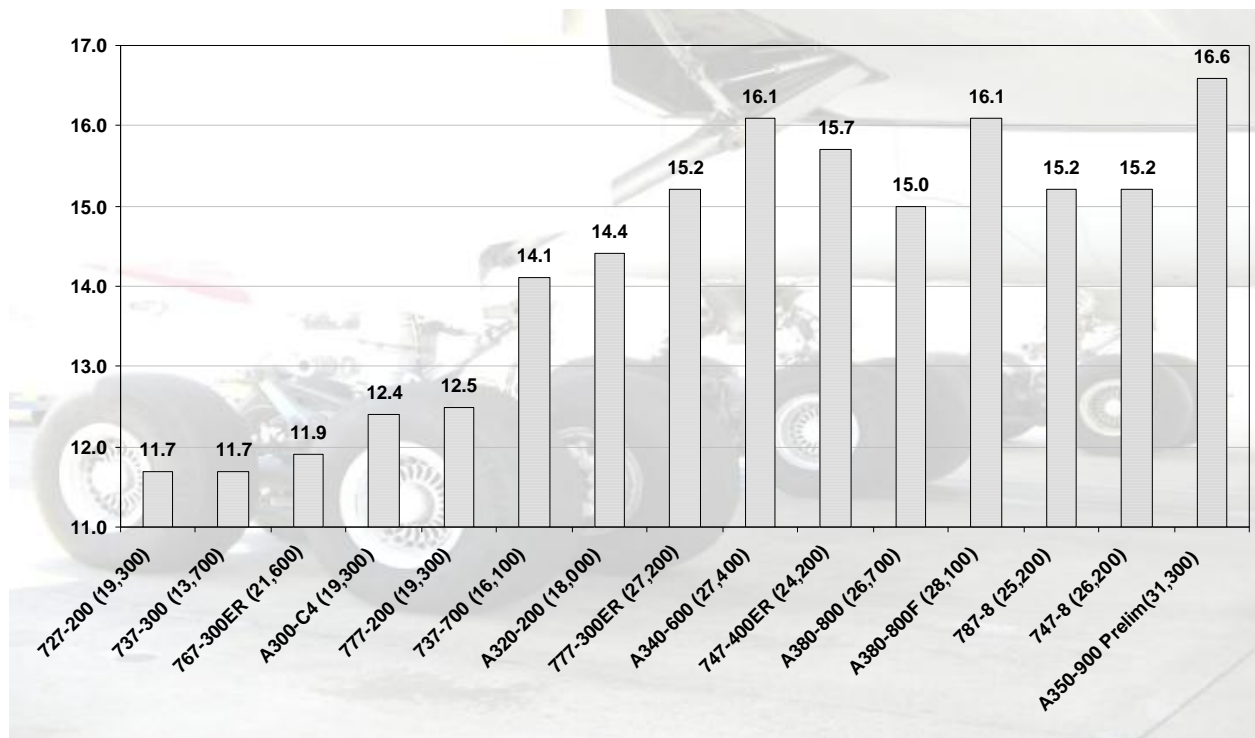


Figure 2: Aircraft internal tire pressure inflation trend

## 1.4 Consistency of current “allowable tire pressure” category?

For main landing gear tires, usual worst case is for static loads at max ramp weight and max. aft center of gravity conditions. For nose landing gear tires, usual worst case is for stabilized braking loads at max ramp weight and forward center of gravity conditions.

Worst-case load depends on aircraft landing gear concept e.g.: for multiple gear (A340, 747, A380) max static loads between flat & cambered runway condition. The internal tire pressure inflation is one of the parameters used for ACN calculation including wheel spacing and load per wheel. However, influence of tire pressure in ACN calculation is secondary to load and wheel spacing but tire pressure is heavily influenced by wheel load and tire specifications (ratings, size etc.).

As an example, an aircraft with a heavy wheel load will necessarily have a specific tire with compliant load capabilities, resulting in high tire pressure and a high ACN number due to the heavy wheel load. This is the dilemma of the double penalty: The aircraft is penalized due to its heavy wheel load, i.e. a high ACN, so the aircraft can only operate on runways with high PCN without tire pressure limitation (code W). However, many runways with a relatively high PCN are limited to 15 bar operations (code X) which means the aircraft operation is limited by tire pressure not PCN. For runways with a relatively low PCN and a 15 bar (or less) tire pressure limitation the tire pressure limitation is redundant because aircraft operations are already limited by their ACN exceeding the reported PCN.

## 1.5 How to manage tire pressure?

### 1.5.1 Tire characteristics

Each tire is assigned a load rating and a pressure rating. In-service tire pressure calculation is based on two sets of data, one from aircraft, and the other from tire characteristics. For each tire, the following points shall be recorded:

- Tire size and ply rating.
- Structure/technology (e.g. bias or radial and/or nylon or lightweight technology).
- Load Rating, as marked on the tyre.
- Rated pressure, as marked on the tire.
- Aircraft to which the tire is fitted.
- Corresponding aircraft rated load (usually max static load).
- Theoretical tire pressure for aircraft rated load for an optimum deflection per TRA guidelines (usually 32% for radial tire).

### 1.5.2 Definitions

Tire rating definition:

- PLY rating identifies the maximum static load carrying capacity of a given tire and corresponding inflation pressure in a specific type of service.
- Load rating is the maximum permissible static load. For main landing gear tire, FAR/JAR 25.733 specifies that for an aircraft with a MLG axle fitted with more than one wheel, the maximum load capability of a tire be at least 7% greater than the requirement of the aircraft for that wheel.

Calculated unloaded pressures are derived from worst-case loads for each landing gear multiplied by the ratio of rated load and pressure for the specified tire.

Calculated loaded pressures are derived from calculated unloaded pressures +4%. The calculated loaded pressure remains unchanged whatever irrespective of the operational aircraft gross weight.

### 1.5.3 Example of in-service tire pressure calculation

An aircraft has a maximum taxi/ramp weight of 250t and a maximum aft CG position (at MRW) representing 95% load on the MLG. The MLG configuration is two 4-wheel bogies (wing landing gears).

Required aircraft load =  $(250 \times 0.95) / 8 = 29.7\text{t}$  per wheel.

- Selected tire: 1400x530R23 36PR  
Tire ratings are 31,070 kg / 223 PSI (15.4 bar).  
Required aircraft wheel load  $\times 1.07 = 29.7 \times 1.07 = 31.8 \text{ t} >$  Tire load rating, i.e. the tire does not comply with the FAR/JAR 25.733 requirement.

- Selected tire: 1400x530R23 40PR  
Tire ratings are 33996 kg / 249 PSI (17.2 bar)  
Required aircraft wheel load  $\times 1.07 = 29.7 \times 1.07 = 31.8 \text{ t} <$  Tire load rating, i.e. tire compliance.  
Unloaded tire pressure =  $(29700 \times 17.2) / 33996 = 15.02 \text{ bar}$   
Loaded tire pressure =  $15.02 \times 1.04 = 15.6 \text{ bar}$ .

Tire manufacturer generally advise against reducing the tire inflation pressure. Under-inflation leads to an over-deflection. Endurance dyno tests show that the endurance vs. deflection relationship is exponential. For example, a tire developed and qualified for a 32% deflection application, and operated at 35% (over-deflection of 10%) leads to reduce endurance by 75%. Tests at deflection rates higher than recommended resulted in bulges in the bead area (see Figure 3).



**Figure 3: Bulges at bead area**

The conclusion is that tires should not exceed the maximum deflection rate recommended by the supplier. Therefore, for a given load, it is not recommended to reduce in-service tire pressure for long-range aircraft network.

A statistical study was made using the SITA database on airports used by current long-range aircraft (B767, B777, B747, A330, A340, MD-11 etc.), on scheduled flights to establish:

- Which airports do not use the ICAO recommended ACN/PCN system (the only pavement rating system with maximum permissible tire pressure)
- For those that do use the ACN/PCN system, the repartition between the code X (limited to 15 bar) and code W (No limitation).



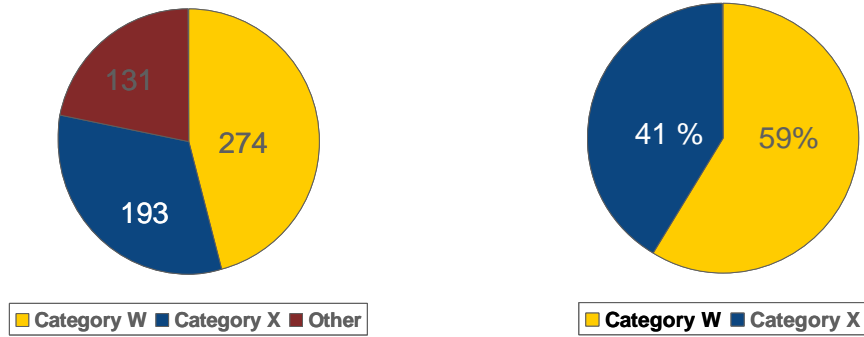


**Figure 4: Tire pressure category repartition for LR aircraft operations**

Figure 4 shows that if the ICAO rule was strictly applied, that would suggest that more than 40% of current scheduled long-range aircraft network could not be accommodated by aircraft with a tire pressure exceeding 15 bar. Airport owners need to decide either to accept such aircraft or refuse (revenue reduction).

## 2 Partnership

The high tire pressure tests are based on a partnership between Airbus S.A.S, the DGAC-STAC, the LCPC, the LRPC-T, Vancouver2 and Michelin.

DGAC-STAC: French civil aviation Technical Center, Bonneuil/Marne, France (Ministry of Transport & Infrastructure)

LCPC: Laboratoire des Ponts et Chaussées, Nantes, France

LRPC-T: Laboratoire régional des Ponts et Chaussées, Toulouse, France

VANCOUVER2: Toulouse based design office, Toulouse, France

MICHELIN: French Tire Manufacturer, Clermont-Ferrand, France

## 3 Test facilities

### 3.1 Design

The construction phase of the HTPT test facility was executed under the specifications defined by the STAC (French Technical Center for Civil Aviation) in two phases:

- Initial phase in 2008
- Update phase in 2009, in order to deal with in-situ conditions

The aim of the STAC was to provide the Airbus Engineers with a precise document (contractual document) containing the guidelines, cross-sections, material and testing requirements (included specified tolerances) conforming to French and European standards (up to 20 standards) related to materials and methods used in the construction of airports.

#### 3.1.1 Initial phase

##### 3.1.1.1 Site selection

The site selected for the full-scale HTPT experiment is an outdoor site within the Toulouse-Blagnac airport area, 2 km south of the commercial air terminal (as shown in Figure 5). This location was chosen in order to minimize the impact of the simulator radio-electric system on the runway equipment. The site was constructed at the location of an existing taxiway made of 6 cm of surface asphalt concrete, 25cm of concrete and 30cm of untreated graded aggregate.



Figure 5: HTPT site location

### 3.1.1.2 Specifications

#### 3.1.1.2.1 Structural design

The aim of the structural design is to provide adequate thickness above the subgrade to prevent detrimental shear deformation under traffic. The pavement distributes the imposed load to the subgrade over an area greater than that of the tire contact area.

The HTPT structure design was inspired by the PEP flexible design, based on the French CBR method. The reference structure of the HTPT site was designed in order to support 10 passes/day of a B747-400, during a 10 years lifetime, which is the conventional design life in the CBR-based conventional method. The B747-400 aircraft chosen as the reference aircraft in the design (see Figure 6) displays the following characteristics:

- MTOW of 398t
- Load per wheel: 23t
- Tire pressure: 1.38MPa

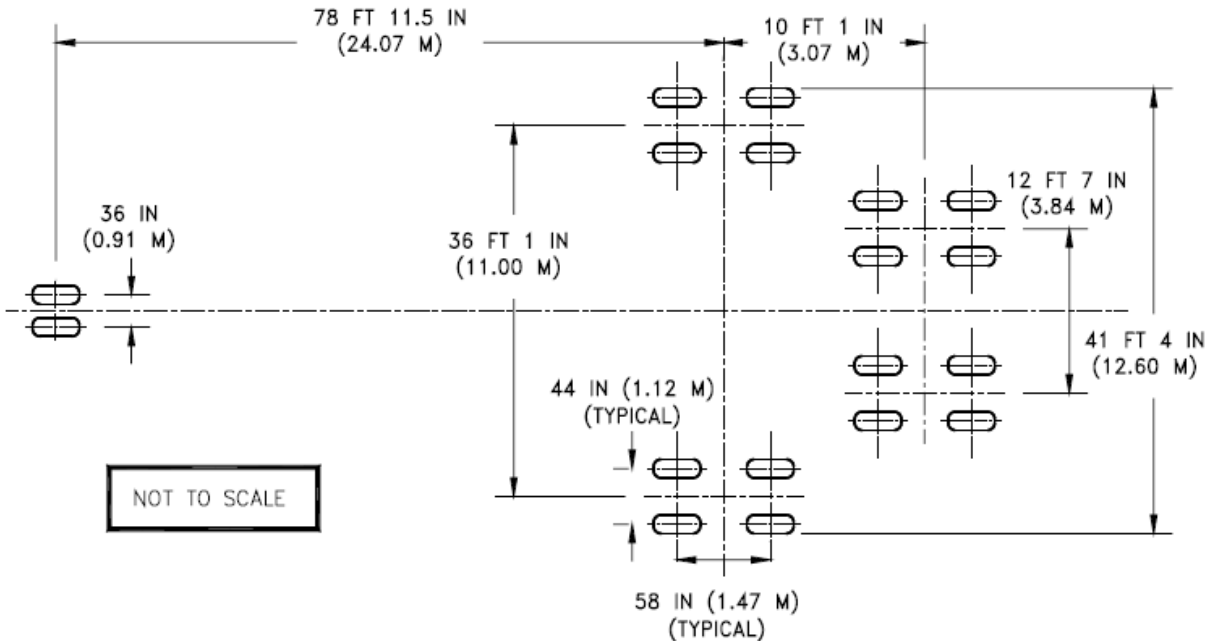


**Figure 6: B747-400 gear geometry**

The HTPT reference structure was chosen as intermediate between PEP structure B (CBR = 10) and C (CBR=6).

In the conventional design method, flexible pavements are predicted to fail by overstressing the subgrade. The design method consists in calculating first the  $L_0$  allowable load value, according to the Wöhler curve

(fatigue law of the subgrade). In the HTPT case, the  $L_0$  value (93t) is calculated from the maximum take-off weight of the B747-400 distributed on the four four-wheel bogies (398tx23.3%). As there is an equal load distribution between the wheels of a given bogie, the load per wheel of the 747-400 is 23t.

This  $L_0$  value is then entered in the design chart of the considered aircraft. With the example of the B747-400 (as represented in Figure 7), the process consists in entering the  $L_0$  value (93t) on the top horizontal axis of the chart, drawing downwards to the appropriate CBR value (CBR=8) and then reading horizontally across for the required pavement granular design thickness 't' on the left vertical axis (82 cm in the HTPT example).

From the chart of Figure 8, the required minimum thickness of bounded materials (base and surface) is then deduced (minimum of 36 cm) by considering the pavement granular design thickness 't' and the CBR value.

The thicknesses provided by the two charts (Figure 7 and Figure 8) do not correspond to real material thicknesses, but to the thicknesses of a reference material of well-known characteristics (untreated graded aggregate with a modulus of 500MPa). The relation between equivalent and real thicknesses is made by means of equivalency factors (from 0.5 for sandy material to 2.5 for high modulus surface asphalt concrete). The equivalency factor of the reference material (500MPa UGA) is 1. When applying these coefficients (2 for surface asphalt concrete (SAC) and 1.5 for base asphalt concrete (BAC)), the condition that must be checked is that  $SAC+BAC>36$  cm (chart of Figure 8). Consequently, sub-structure can be calculated:  $8\text{cm}_{SAC} \times 2 + 18\text{cm}_{BAC} \times 1.5 = 43\text{cm}$  (>36 cm) of equivalent granular thickness leading to  $8\text{cm}_{SAC} + 18\text{cm}_{BAC} = 26$  cm of real material thicknesses.

The next step is to subtract the thickness of surface and base from the total granular thickness to obtain the sub-base thickness ( $82-43=39$  cm of Untreated Graded Aggregates (UGA)).

The HTPT reference structure is then composed of 8 cm of surface materials, 18 cm of base surface materials and 40cm of sub-base materials.

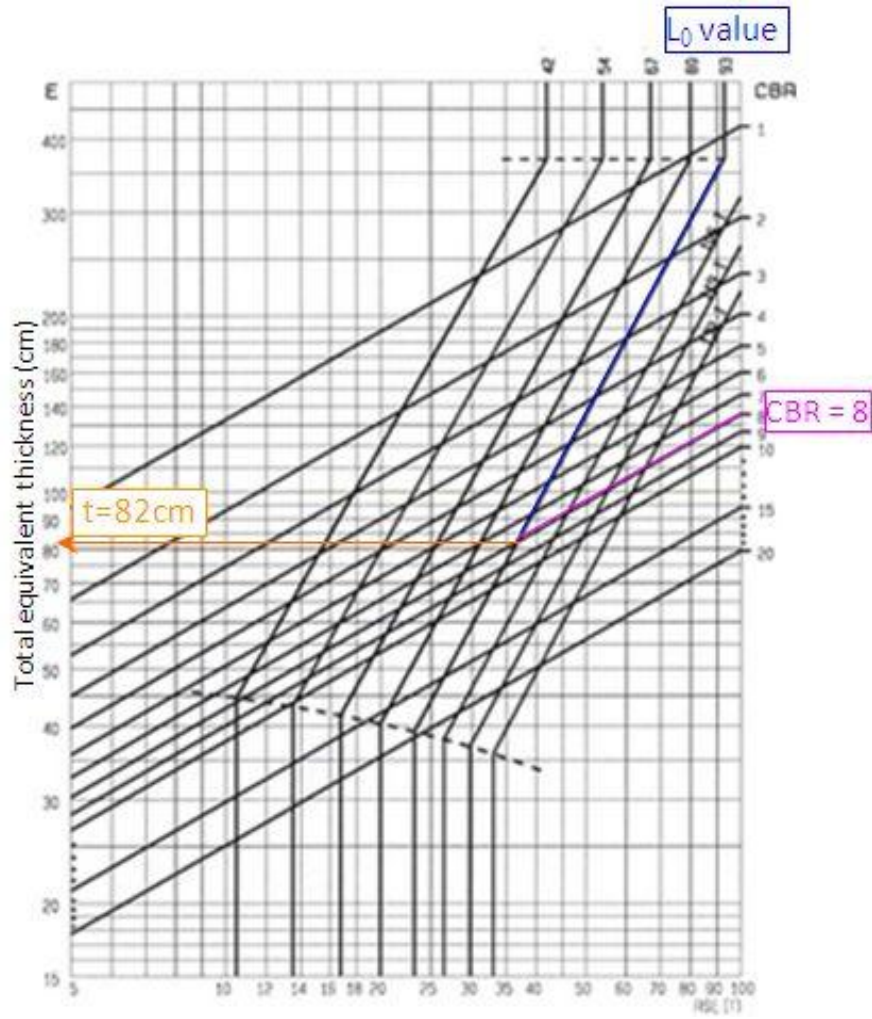
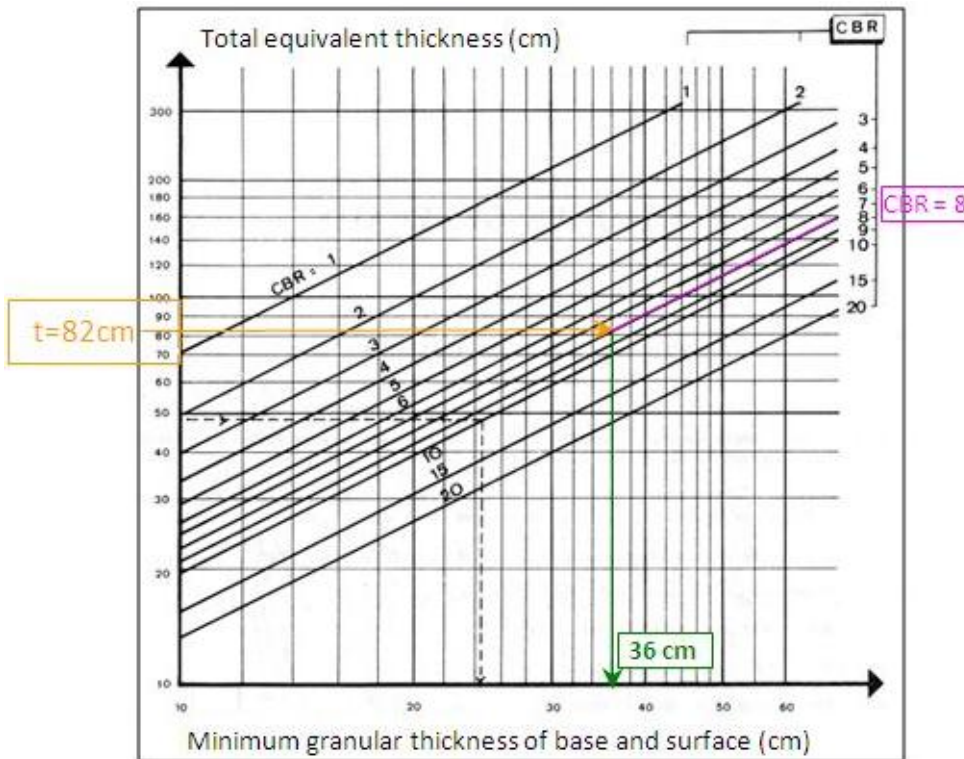


Figure 7: Design chart of the B747-400



**Figure 8: Chart for determining the minimum granular thickness of base and surface materials**

A CBR of 8 being required at the bottom of the pavement, a foundation course made of 70 cm of UGA was laid beneath the UGA sub-base.

A 70 m long and 25m large experimental area was defined, composed of 7 sections (referred as A to G), each one being 7 m wide and separated from the next one by a 3.5m wide transition zone. The selected surface and base asphalt concrete courses include seven different test sections, representative of current airfield flexible pavement. Variant parameters from one section to another are thickness of AC surface layer, its performance towards rutting and surface treatment as grooving.

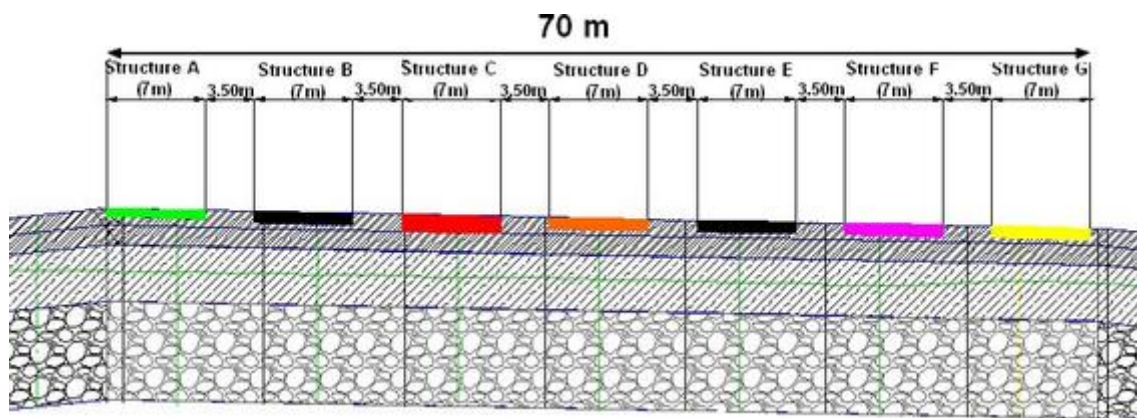


**Figure 9: Longitudinal typical cross-section showing the 7 tested sections**

### 3.1.1.2.2 Construction specifications

The experimental pavement longitudinal slope was fixed at a maximum of 0.2% to facilitate the simulator tracking.

The transverse slope of the pavement was fixed at 1% for drainage.

The HTPT test facility was constructed according to the building procedures described in European and French current standards. The following building steps were defined:

- Removal of existing pavement (asphalt concrete and concrete)
- Excavation work and drainage
- Finishing and protection of subgrade
- Stabilization with 1% lime
- Capping layer construction: 70 cm of Untreated Graded Aggregate
- Sub-base course construction: 40 cm of Untreated Graded Aggregate
- Application of bituminous prime coat (emulsified asphalt)
- Application of the base asphalt concrete over 26 cm (in two layers: 14 cm and 12 cm) till the final grade of the pavement
- Construction of 7 experimental sections by cold micro milling of the base asphalt concrete to a specified depth of cut depending on the final expected configuration (see Figure 9).
- Transversal application of the 3 types of surface asphalt concrete on the 7 experimental sections. The 3.5 m transition zone between each section was designed to facilitate the compaction of the surface course.

### 3.1.1.2.3 Material specifications

The aim of the material specifications is to provide adequate surface quality, base and sub-base materials in order to withstand the compressive and tensile strains generated by the experimental traffic. Material properties were determined in accordance with the European and French current standards.

- **Capping layer material**

The specified material was an Untreated Graded Aggregate 0/20 mm. The objective was to obtain on the finished surface an  $EV_2$  modulus  $>70$ MPa, a grade tolerance of  $\pm 3$  cm for 90% of the controlled points and a mean density  $>95\%$  OPM for 50% of the controlled points.

- **Sub-base course material**

The specified material was an Untreated Graded Aggregate 0/20mm. The objective was to obtain a mean density  $> 97.5\%$  OPM (for 50% of the control points), a grade tolerance of  $\pm 2$  cm (for 90% of the control points) and a finished surface with depressions less than 2 cm when measured by a 3 m straight-edge.



- **Base course material**

The specified material was continuous graded 0/14 mm base surface asphalt (EB14-GB). These specifications concerned the quality of manufacturing (control of job mix formula, grading and binder content, air void content, water sensitivity, rutting test, modulus) and the quality of application (minimum temperature of 130°C, grade tolerance of +/- 1cm, slope tolerance of +/- 1cm/m for more than 95% of control points, and surface depressions less than 0.3 cm with a 3m straight-edge for 100% of control points).

- **Surface course material**

The aim of the HTPT experiment is to test the influence of tire pressure on the characteristics of 3 types of surface asphalt concrete (SAC), when subjected to 10,000 passes of the AIRBUS simulator. The properties of SAC1, SAC2 and SAC3 are given in Table 2.

Surface asphalt concrete type 1 (EB14-BBA C class 3, according the European designation) is the material commonly used in airfield pavement with a required minimum modulus of 7000 MPa. Surface asphalt concrete type 2 (EB14-BB class 3, according the European designation) exhibits higher rutting performances than Surface asphalt concrete type 1. Surface asphalt concrete type 3 (EB14-BB, according the European designation) is sensitive to rutting.

**Table 2: Properties of the 3 types of surface asphalt concrete**

Abbreviation	Material	Grading	Specified Bitumen	Maximum rutting depth
SAC 1	EB14-BBA C Class 3 Surface	Continuous 0-14mm	35/50 or 50/70	comprised between 5 et 7.5% deep 10,000 cycles
SAC 2	EB14-BBME C Class 3 Surface	Continuous 0-14mm	50/70	comprised between 2 et 4% deep 30,000 cycles
SAC 3	EB14-BB C Surface	Continuous 0-14mm	Pure bitumen 50/70 or 70/100	comprised between 9 et 14% deep 10,000 cycles

As shown in Figure 10, SAC1 is tested on 4 structures (A, B, C and E), with distinct thickness values, evolving from 6 cm to 12 cm. This material is tested as a grooved surface on structure F.

The base asphalt concrete of the 7 sections consists of the material commonly used on civil platforms: EB14-GB class 3 (referred to as BAC) with a thickness fixed at 14cm on structure C, 18 cm on structures B, D, E, F and G and 20 cm on structure A.

The sub-base course, made of 40 cm of UGA and the foundation course and composed of 70 cm of UGA, is common to all the sections.

Structure A	Structure B	Structure C	Structure D	Structure E	Structure F	Structure G
0.06m SAC 1 0.20m BAC	0.08m SAC 1 0.18m BAC	0.12m SAC 1 0.14m BAC	0.08m SAC 2 0.18m BAC	0.08m SAC 1 0.18m BAC	0.08m SAC 1 gr. 0.18m BAC	0.08m SAC 3 0.18m BAC
0.40m U6A 0.70m foundation	0.40m U6A 0.70m foundation	0.40m U6A 0.70m foundation	0.40m U6A 0.70m foundation	0.40m U6A 0.70m foundation	0.40m U6A 0.70m foundation	0.40m U6A 0.70m foundation

**Figure 10: Pavement materials of the 7 test sections**

The contract specifications concerned the quality of manufacturing (control of job mix formula, grading and binder content, air void content, water sensitivity, rutting test, modulus) and the quality of application (minimal temperature of 125°C for SAC1 and 130°C for SAC2 and 3, air void content (Colin White test) mean value in the range 93-97% of the reference density (XP P 98 151), thickness tolerance of +/- 0.5cm for more than 95% of control points, slope tolerance of +/- 0.5cm/m for 100% of control points, surface depressions less than 0.3cm with a 3m straight-edge for 100% of control points).

### 3.1.2 Update phase: flexible overlay

The reinforcement phase (see paragraph 3.2.4.3 page 34) consisted in removing the superficial part of the existing pavement by cold micro milling. The specified depth to be removed was comprised between 2 and 5 mm. Using the Alizé software, it was calculated that an additional 21cm asphalt base (EB14-GB) had to be applied in 2 layers (9 cm at the bottom and 12 cm at top) on the overall surface. In that stage, EB14-GB class 4 replaced class 3 EB14-GB. Class 4 EB14-GB is higher resistant than class3 EB14-GB. Compared characteristics are given in Table 3.

**Table 3: Compared laboratory characteristics of Class 3 and Class 4 base asphalt concrete**

Abbreviation	Material	Maximal void content	Rutting at 60°C	Complex modulus at 15°C - 10 Hz
BAC	EB14-GB Class 3 Base	10% (120 gyrations)	comprised between 7 et 10% deep at 10,000 cycles	Minimum = 9,000MPa
	EB14-GB Class 4 Base	9% (120 gyrations)	comprised between 5 et 8% deep at 30,000 cycles	Minimum= 11,000MPa

## 3.2 Construction and acceptance

The test pavement is to be as representative as possible of existing airport pavement, and therefore usual methods and machines were used in its construction. No special machines were developed or used for this project.

As explained in paragraph 3.1 page 17, the pavement structure was designed to support 10,000 passes of a Boeing B747-400 loaded at 23.3 t per wheel.

All the construction works done for the construction of the test pavement were made in compliance with specifications presented in paragraph 3.1 page 17 based on general regulations used in French public works domain (including work methods, selection, specifications and material control).

### 3.2.1 Natural soil

#### 3.2.1.1 Construction

To obtain homogeneity in bearing capacity, the natural soil is stabilized with 1% lime on a 35 cm thick layer.

#### 3.2.1.2 Acceptance

Some EV2 modulus controls with LCPC plate were operated. Results are summarized in Figure 11.

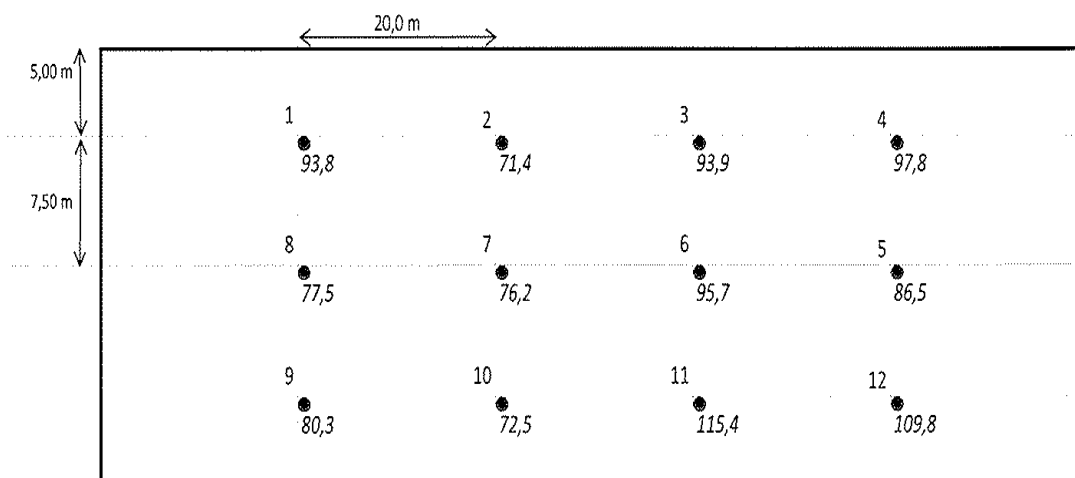


**Figure 11: EV2 modulus controls on stabilized sub-grade**

The objective was to reach 70 MPa at the top of capping layer. The measure at the top of the natural soil shows that the 70MPa was already attained.

### 3.2.2 Capping layer

#### 3.2.2.1 Construction

Two 35 cm layers (70cm) of 0/20 (mm) gravel were laid on this stabilized layer to reach an EV2 value of 70MPa.

#### 3.2.2.2 Acceptance

Bearing capacity controls were performed with local static tests, and both local and continuous dynamic tests.

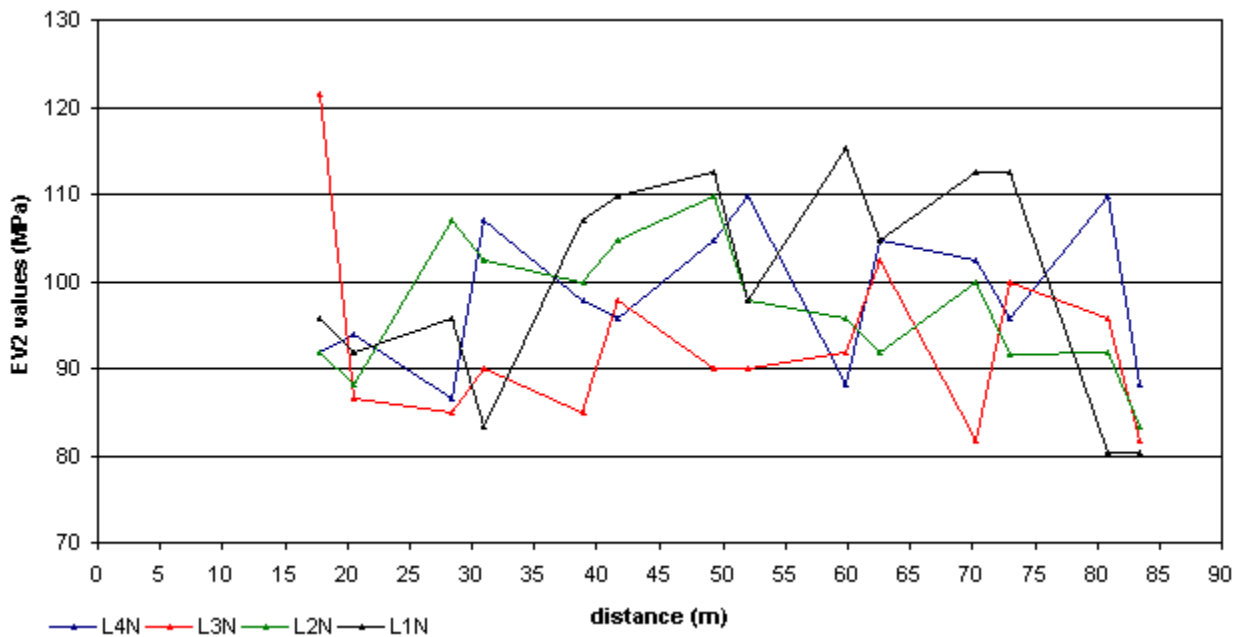
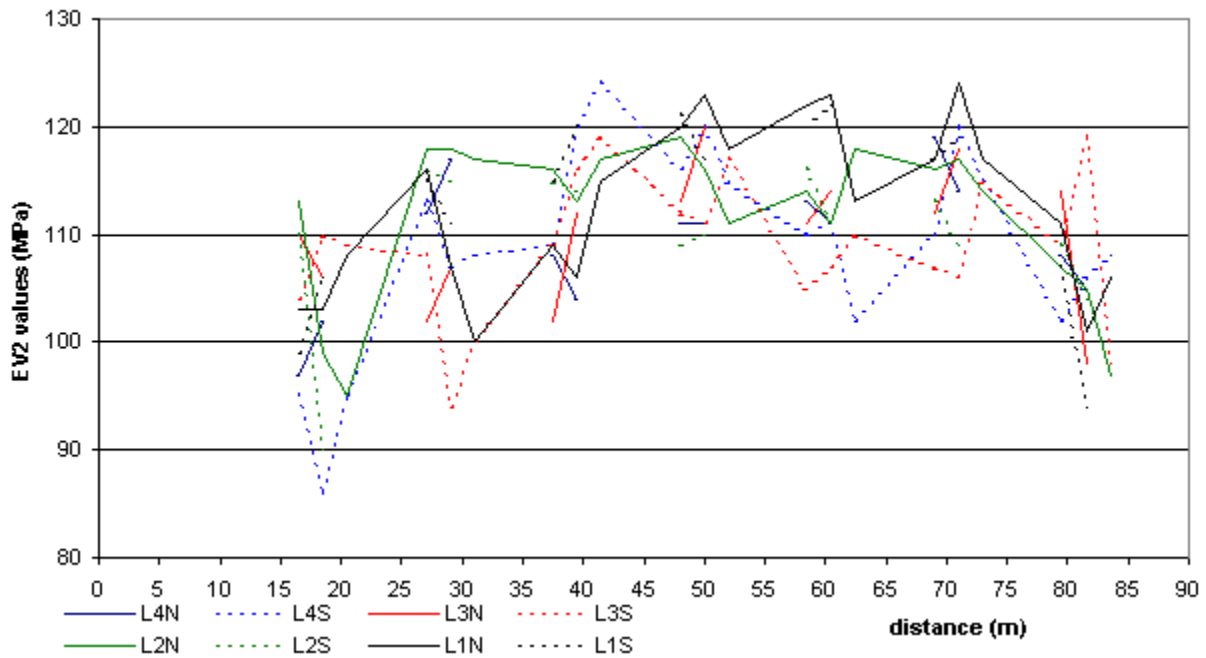


Figure 12: EV2 modulus controls on capping layer (LCPC’s plate)

Local static tests (using LCPC’s plate) give the average value of 97 MPa (see Figure 12) with a standard deviation of 10MPa. More information about EV2 modulus measurement is available in the NF P 94-117-1 standard.



**Figure 13: EV2 modulus controls on capping layer (LCPC's Dynaplaque)**

Local dynamic tests (done with the equipment called LCPC's Dynaplaque) give average value of 110 MPa with standard deviation of 7 MPa (see Figure 13). More information about LCPC's Dynaplaque is available in norm NF P 94-117-2 and in Appendix 14.

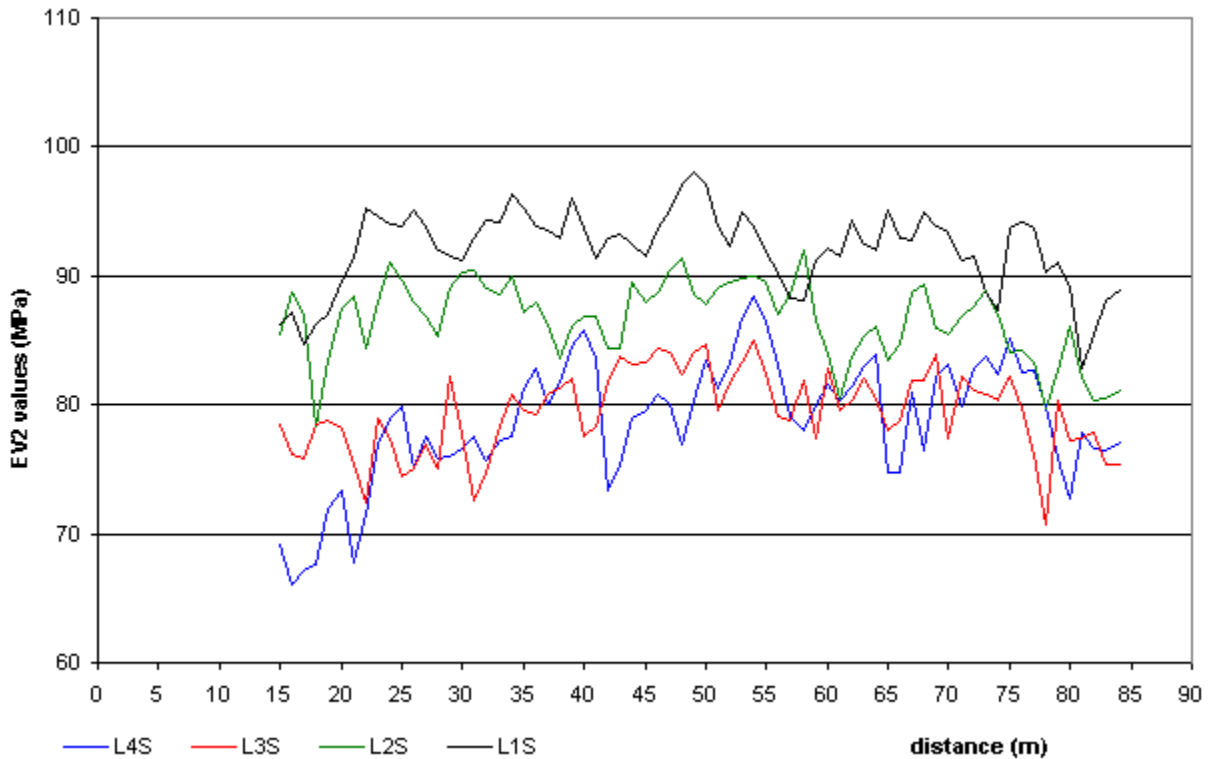


**Figure 14: EV2 modulus controls on capping layer (LCPC's Portancemètre)**

Continuous dynamic tests (done with the equipment called LCPC's Portancemètre) give an average value of 85 MPa (see Figure 14) with standard deviation of 6 MPa. More information about LCPC's Portancemètre is available in Appendix 15.

All tests give EV2 values higher than 70MPa on all points therefore producing a homogenous sub-grade bearing capacity of CBR 8 or greater.

### 3.2.3 Sub-base layer

#### 3.2.3.1 Construction

Two 20cm gravel layers (40cm) of 0/20 (mm) sub-base course were laid and compacted in two stages

#### 3.2.3.2 Acceptance

Material density was controlled at the end. The result of 98.7% compaction is higher than specification (97%).

### 3.2.4 AC material

#### 3.2.4.1 Construction

As explained in paragraph 3.1.1.2.2 page 22, the asphalt concrete material was laid to the following specifications:

- The 26 cm base asphalt course consists of 2 base asphalt layers (14 cm lower, 12 cm upper).
- Both base asphalt layers were built with specified joint distances to avoid joints superposition with simulator trajectories, and superposition of joints between two layers (top and bottom base asphalt concrete layer). Pass width is 3, 4 or 5 meters.
- The top base asphalt layer depth was adjusted transversally by means of a scraper to remove top surface so that the specified various surface layers thickness (6, 8 or 12 cm) can be laid
- Surface layers were laid down transversally without construction joints.
- Section C has the maximum surface layer thickness of 12 cm which could not be achieved in one layer so it has two layers of 6 cm each.
- Compaction was first performed transversally to consolidate the joints, then longitudinally to avoid a granular orientation perpendicular to simulator direction

### 3.2.4.2 Initial pavement acceptance

#### 3.2.4.2.1 Compaction

Final material grading, asphalt content and compaction (see Table 4) were controlled on each material and section. Compaction (94.7% on each layer) is in specification range s (93-97% all layers).

**Table 4: Surface layers compaction controls**

	Compaction (in %)	Specification Range (in %)
<b>Section A</b>	93.9	93-97
<b>Section B</b>	95.3	93-97
<b>Section C</b>	95.2	93-97
<b>Section D</b>	94.4	92-96
<b>Section E</b>	94.5	93-97
<b>Section F</b>	94.5	93-97
<b>Section G</b>	95.8	93-97

#### 3.2.4.2.2 Signal acquisition and interpretation

Values on strain gauges and vertical displacement sensors were compared to the Alizé model on the first simulator passes. On average, these values were two to three times higher than expected.

Figure 15 illustrates the base asphalt layer elongation against time and shows an amplitude of 360µdef when:

- The simulator passes on trajectory T7 (see paragraph 4.3.3 page 55),
- The surface temperature is 15°C,
- A load of 19.2t per wheel,
- Tire pressure of 0.87Mpa (all tires)



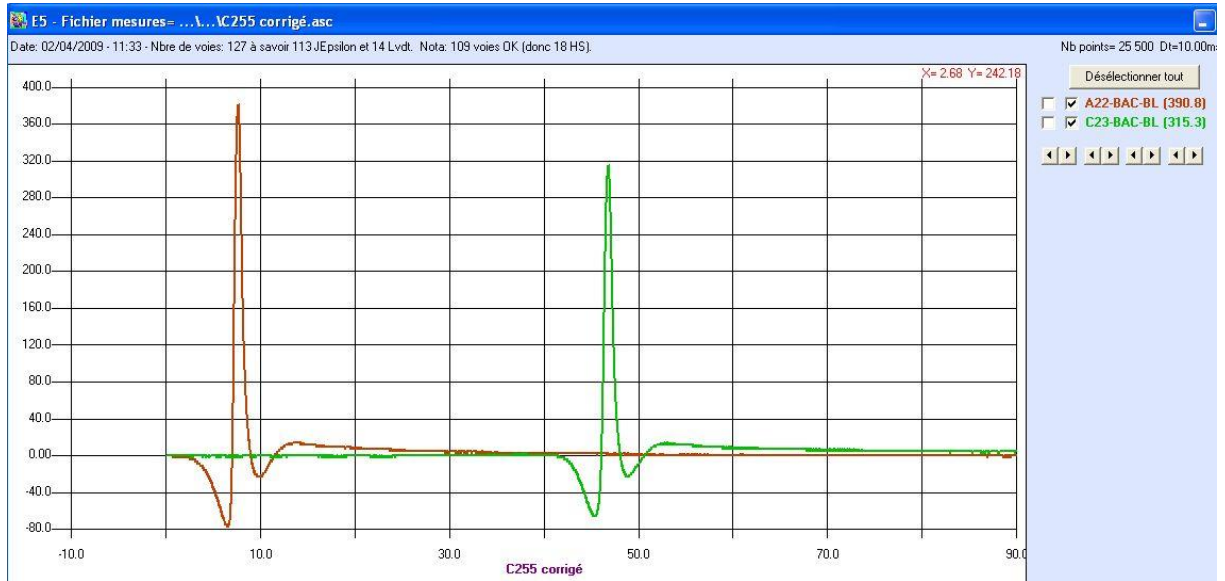


**Figure 15: Horizontal strains observed at bottom of base asphalt layer prior to reinforcement**

Under the same conditions, Figure 16 shows an elevated top sub-base compression of -2700  $\mu\text{def}$ .

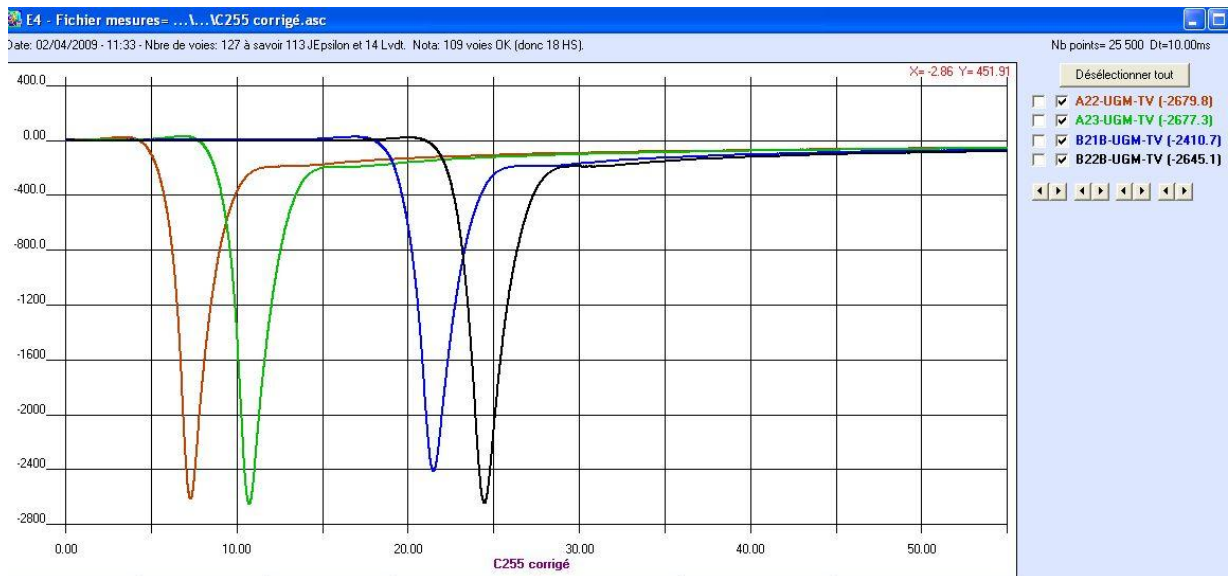


**Figure 16: Vertical strains observed at top of sub-base prior to reinforcement**

### 3.2.4.2.3 In situ investigation

Because these values do not compare with the Alizé model values (refer to paragraph 3.2.4.4 page 36), an investigation of a pavement's section was carried out.

During the investigation, an exploratory 1m x 1m50 excavation was dug from the section B pavement surface to the top of the natural soil. Then pavement samples of sub base and capping were analyzed in the LRPC's laboratory.

Table 5 shows the test results. In this table, 0 corresponds to the top of the sub-base. Differences appear compared to theoretical profile: top layers (to 75cm depth) were drier than initial conditions and bottom layers are wetter than initial conditions. However, the weighted average water content of the pavement matches the theoretical value of 5.2%.

**Table 5: Theoretical water content profile**

<b>Total thickness (in m)</b>	1.10
<b>Water content (in %)</b>	5.20

**Table 6: Measured water content profile**

	<b>Thickness (in m)</b>	<b>Measured water content of the sample (in %)</b>
<b>Layer 0/10cm</b>	0.10	3.50
<b>Layer 10/20cm</b>	0.10	3.20
<b>Layer 20/30cm</b>	0.10	4.09
<b>Layer 30/40cm</b>	0.10	4.21
<b>Layer 40/57.5cm</b>	0.18	4.10
<b>Layer 57.5/75cm</b>	0.18	4.25
<b>Layer 75/85cm</b>	0.10	5.53
<b>Layer 85/95cm</b>	0.10	7.54
<b>Layer 95/110cm</b>	0.15	9.96
<b>Total</b>	1.10	5.24

Visual observation of the excavation (see Figure 17) revealed water captured in the capping layer base. This unusually high amount of water is explained by insufficient drainage along the pavement.



**Figure 17 : Water contamination under the pavement**

It can be concluded that water contamination in the deepest layers could be one the causes of the high strains. Further, the insufficient drainage entailed a deformation mechanism.

### 3.2.4.3 Reinforcement

Experimental pavement was initially designed to support heavy loads representative of current aircraft fleet (and high tire pressure up to 17.5 bar) but it was initially considered as unnecessary to simulate high traffic level since rutting curve is expected to have a logarithmic progression therefore in respect of high tire pressure effect, only the first 2,000 or 3,000 passes need be considered.

However, during the High Tire Pressure Tests Workshop held in Toulouse, France, March 2009, worldwide recognized attendees requested:

1- To simulate high traffic (between 10,000 and 15,000 passes) to be representative of a 'normal' pavement design life, and to explore the full process of pavement surface damage. This simulation led to re-design the pavement test section accordingly so that premature structural damage could be avoided and test objectives maintained, although some could argue that passes above 3,000 passes is of less interest when considering high tire pressure effects.

As a result of the decision to test the pavement with high traffic level (under heavy loads and pressure, resp. 33.2 t and 17.5 bar), test pavement was re-built by removing the asphalt concrete (AC) surface layer and adding extra base AC course. The new asphalt concrete surface is identical to the previous one, with a new set of additional gauges. This 'base course overlay' is essential to avoid preliminary structural damages when testing pavement with high traffic level.

2- To emulate Australian runways, i.e to test pavement in high ambient temperatures. Tests will be stopped in July 2010, after a significant number of passes at high temperature (around 55 or 60°C) at pavement surface.

The reinforcement consisted of two phases: first to reduce the existing surface level by 1cm of for levelling reasons; then, a 21 cm thick EB14-GB4 (higher E modulus than EB14-GB3) base course was laid in two layers (lower 9 cm, upper 12 cm) using the same methodology as previously, to improve the pavement structural strength. Grading, asphalt content and compaction of final material were controlled.

During the reinforcement, the asphalt concrete material specifications as used in the different sections are given in Table 7.

**Table 7: Asphalt material mechanic characteristics synthesis**

	Sections A, B, C, E, F	Section D	Section G	Base layer	Base layer
<b>Material</b>	EB14-BBA C Class 3 Surface	EB14-BBME Class 3 surface	EB14-BBA C Surface rutting	EB14-GB Class 4 Base	EB14-GB Class 3 Base
<b>Grading</b>	0/14	0/14	0/14	0/14	0/14
<b>Hydrocarbon binder</b>	35/50 5.3%	20/30 5.3%	35/50 -	35/50 4.7%	35/50 4.5%
<b>Compaction %</b>	94.8	93.6	-	92	93.8
<b>Modulus MPa</b>	11,951 (1)	13,107 (2)	> 11,000 (2)	14,068 (2)	> 9,000 (2)
<b>Rutting parameter %</b>	6.4 (3)	4.2 (4)	13.07 (3)	-	4.4 (3)

(1) Complex modulus test

(2) Direct tensile test

(3) At 10,000 cycles

(4) At 30,000 cycles

### 3.2.4.4 Final pavement acceptance

#### 3.2.4.4.1 Compaction after reinforcement

The compaction (93.9% lower layer and 95.7% upper layer) matches the specifications (93-97%) in all layers and all sections, as shown in Table 8. Surface layers were laid using the same methodology as previously. Grading, asphalt content (see 0 to Appendix 12) and compaction of final material were controlled in all materials and each section.

**Table 8: Surface layers compaction controls**

	Compaction (in %)	Normalized Range (in %)
<b>Section A</b>	96.4	93-97
<b>Section B</b>	95.7	93-97
<b>Section C</b>	96.3	93-97
<b>Section D</b>	95.3	92-96
<b>Section E</b>	97.1	93-97
<b>Section F</b>	96.2	93-97
<b>Section G</b>	97.1	93-97

#### 3.2.4.4.2 Thickness after reinforcement

Final surface layer thickness was again controlled by a land surveyor who had also performed topographical surveys both prior to and after the building works. Table 9 shows the measured average thickness, which is in all cases superior to the theoretical thickness for each section.

**Table 9: Final surface layer thickness**

	SECTION	A	B	C	D	E	F	G
<b>Thickness</b>	<b>Theoretical (cm)</b>	6	8	12	8	8	8	8
	<b>Average (cm)</b>	6.45	8.83	12.39	8.41	7.88	8.20	8.76
	<b>Min (cm)</b>	5.8	7.7	11.8	7.7	6.5	7.6	8.0
	<b>Max (cm)</b>	7.1	9.7	13.3	9.6	8.7	8.9	9.5

### 3.2.4.4.3 Signal acquisition interpretation after reinforcement

Strain data acquisition was carried out after pavement reinforcement. Figure 18 shows a base asphalt layer amplitude of  $280\mu\text{def}$  (compared to  $360\mu\text{def}$  prior to reinforcement, as shown in Figure 15). Figure 19 shows a top sub-base deformation of  $-1900\mu\text{def}$  (compared to  $-2700\mu\text{def}$  prior to reinforcement, as shown in Figure 16). The external conditions are the same as those during the measurements prior to reinforcement, except surface temperature, which was  $19^\circ\text{C}$  instead of  $15^\circ\text{C}$ .

Post-reinforcement strains are lower than the ones measured prior to reinforcement, and their level corresponds to Alizé model predictions.



Figure 18: strains observed at bottom of base asphalt layer post reinforcement

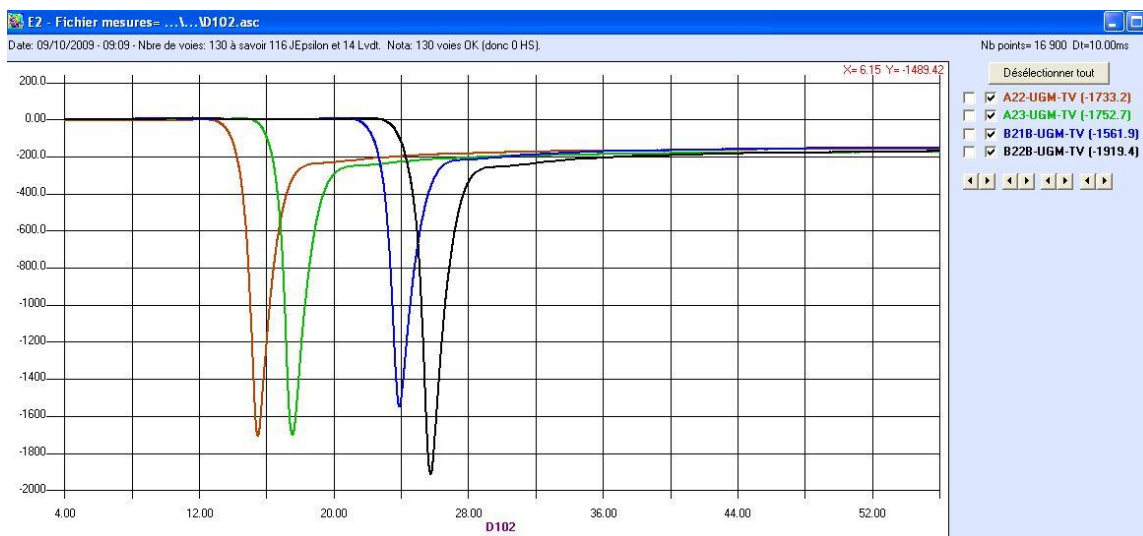


Figure 19: strains observed at top of sub-base post reinforcement

### 3.3 Simulator

The HTPT simulator is the same one as used for the PEP rigid campaign. Specifications and characteristics of the simulation vehicle are detailed in the P.E.P report.

### 3.4 Tires technology and specifications

#### 3.4.1 Specifications

##### 3.4.1.1 Test objectives

All performances can be measured either by units or test criteria except bead seat temperature resistance. To test the tire inflation pressures effect on pavement under high load by rolling tires in a straight line at very low speed for approximately 1,000 km in cycles (back and forth, one pass in each direction) simultaneously testing and using:

- Two inflation pressure levels referenced on P=15b
- Load levels

##### 3.4.1.2 Tire Specifications

The tests consist in rolling tires in a straight line at very low speed.

- **Load Capacity**
  - The tire size and PR allow high loads > 30,000 daN.
- **Pressure Capacity**
  - The tire PR will allow inflation pressure > 17,5 bar.
- **Geometrical Stability**
  - The tire technology will have the most stable geometry for maintaining mechanical properties throughout the tests.
- **Wear Resistance**
  - To allow > 1,000km
  - To avoid excessive wear difference between the 4 test configurations
  - To minimize change of contact patch characteristics throughout the test
  - To avoid tire changes throughout the test.
- **Tire Technology**
  - To choose the tire technology that best isolates inflation pressure effect on the pavement



### 3.4.2 Element of tire mechanic

#### 3.4.2.1 Tire components

The main components of a tire are shown in Figure 20. Each figure represents basic functions in tire construction, to be managed to reach expected performances (and selection of tire for optimal performance in the test objective).

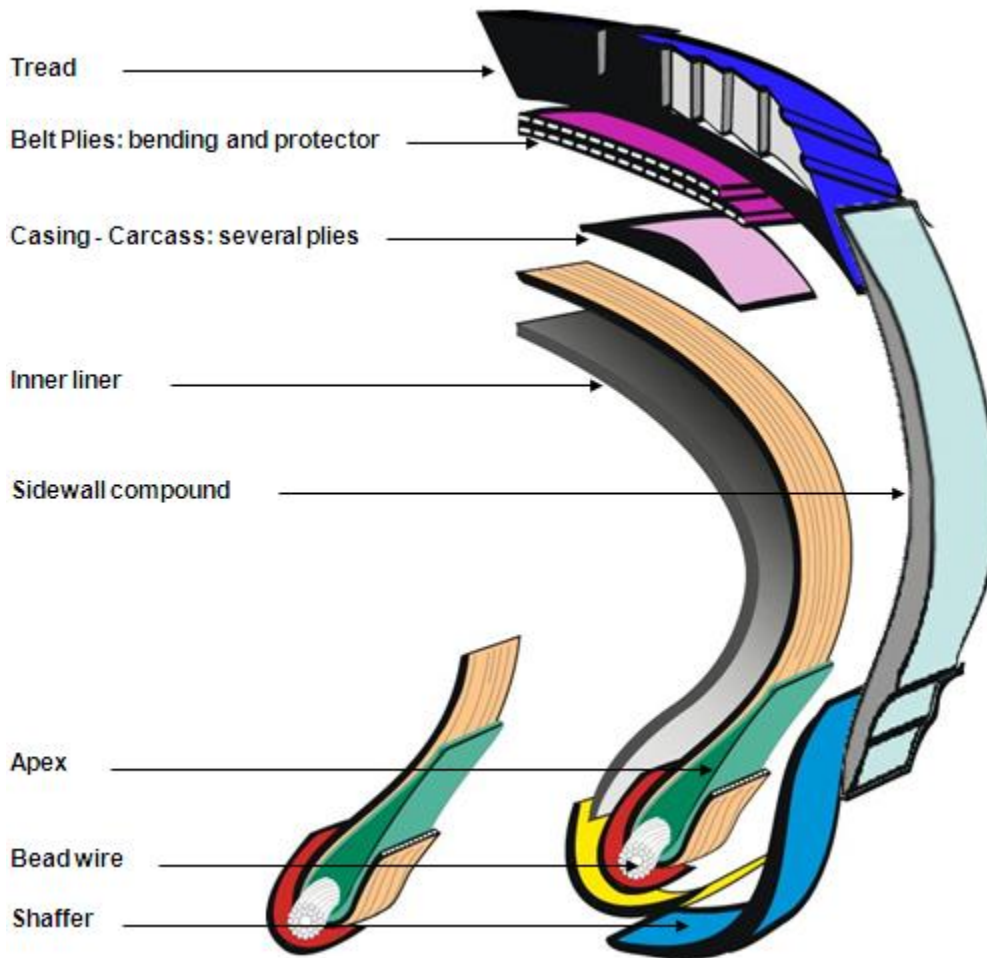
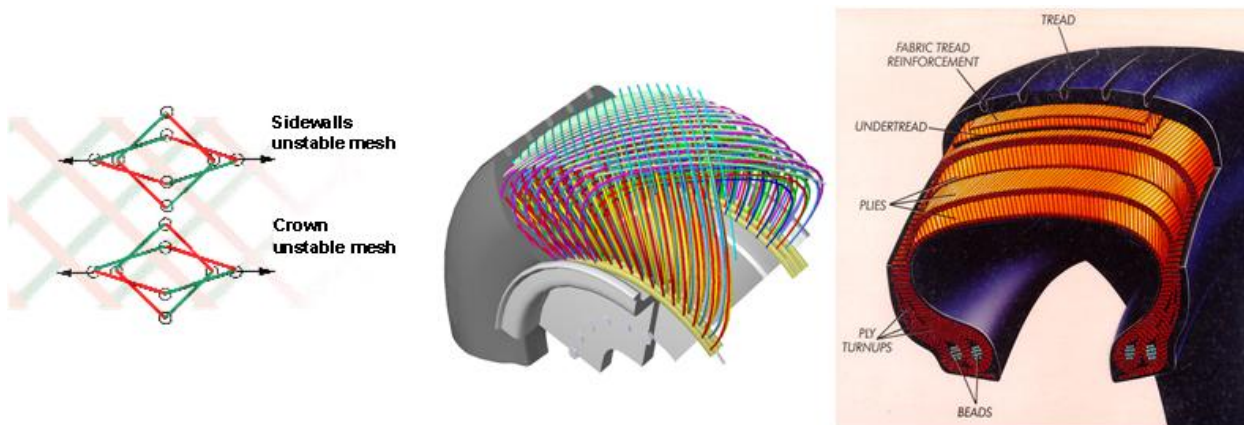


Figure 20: Main components of a Bias or Radial tire

**3.4.2.2 Bias and Radial definition**

Figure 21 and Figure 22 show the difference of geometrical organization principle of casing and carcass, and of belt plies between Bias and Radial technology. Bias is managed by carcass plies angle; it is constituted by crossed carcass plies. Radial is managed by belt plies; it is constituted by parallel carcass plies.



**Figure 21: Cross section profile of carcass plies for Bias**

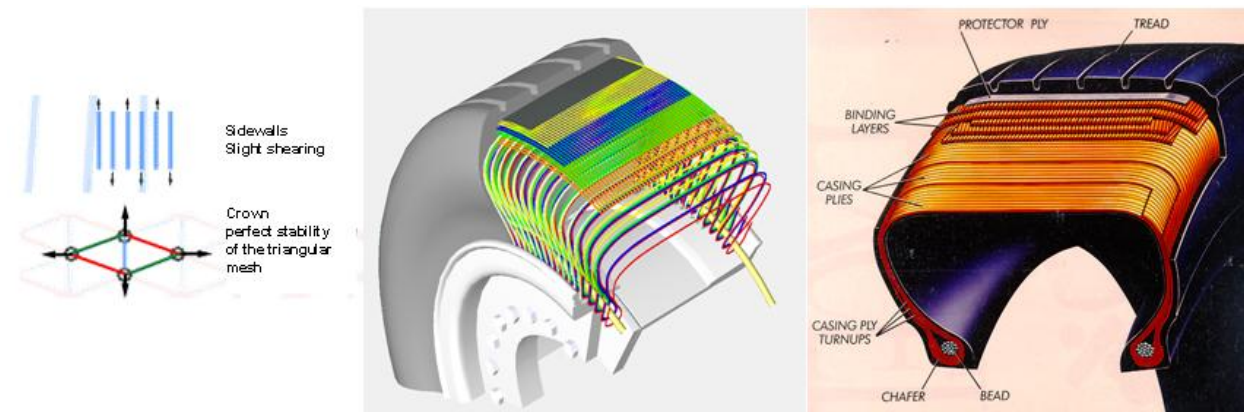


**Figure 22: Cross section profile of carcass plies for Radial**

### 3.4.2.3 Bias vs. Radial technologies, contact patch shape and evolution vs. deflection

The main difference of the Bias and Radial constructions is the contact patch shape and its evolution vs. deflection.

For Bias construction, as represented in Figure 23, contact width and length change with deflection. The contact patch is generally oval in shape, and mechanical balance changes with the longitudinal and transversal elements.

For Radial construction, as represented in Figure 24, contact patch width is stable, only the length changes, remains cylindrical in shape, which helps to keep the same mechanical balance.

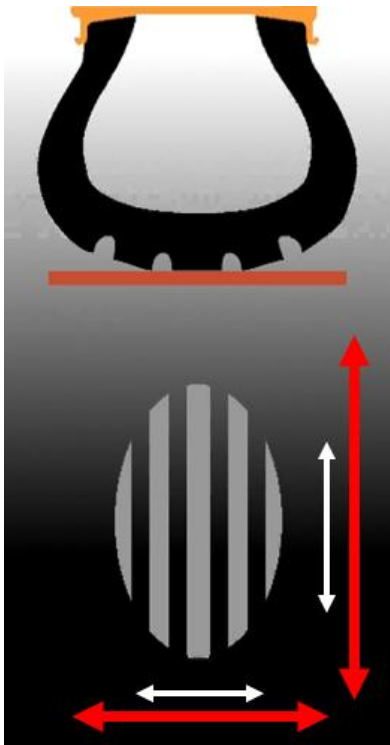


Figure 23: Contact patch shape of Bias

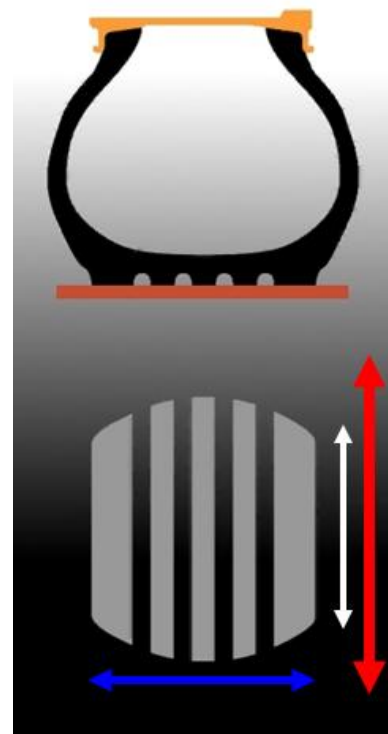
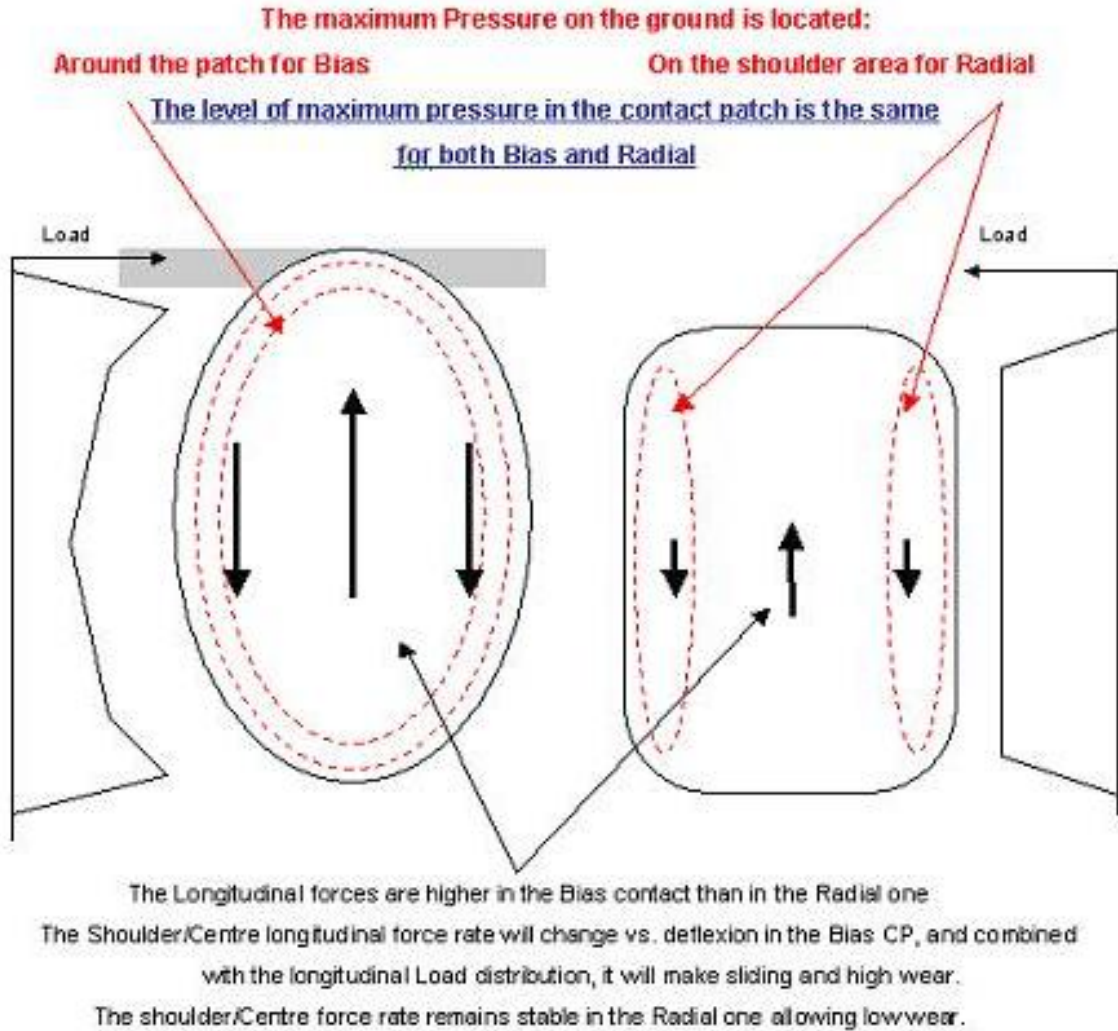


Figure 24: Contact patch shape of Radial

**3.4.2.4 Contact patch, pressure spectrum**



**Figure 25: Contact patch pressure distribution for Bias and Radial**

### 3.4.2.5 Contact patch, pressure level

Figure 26 shows contact patch pressure distribution calculated for tire size 1400 x 530 R23 40PR at about 32% deflection.

The evolution of the maximum pressure is more correlated with the load level than with the inflation pressure, in this case, around this deflection point it is about:  $(P_{max 2} / P_{max 1} \%) \sim \frac{1}{2} (L2 / L1 \%)$

The maximum pressure in the contact patch is close to 2 times the inflation pressure

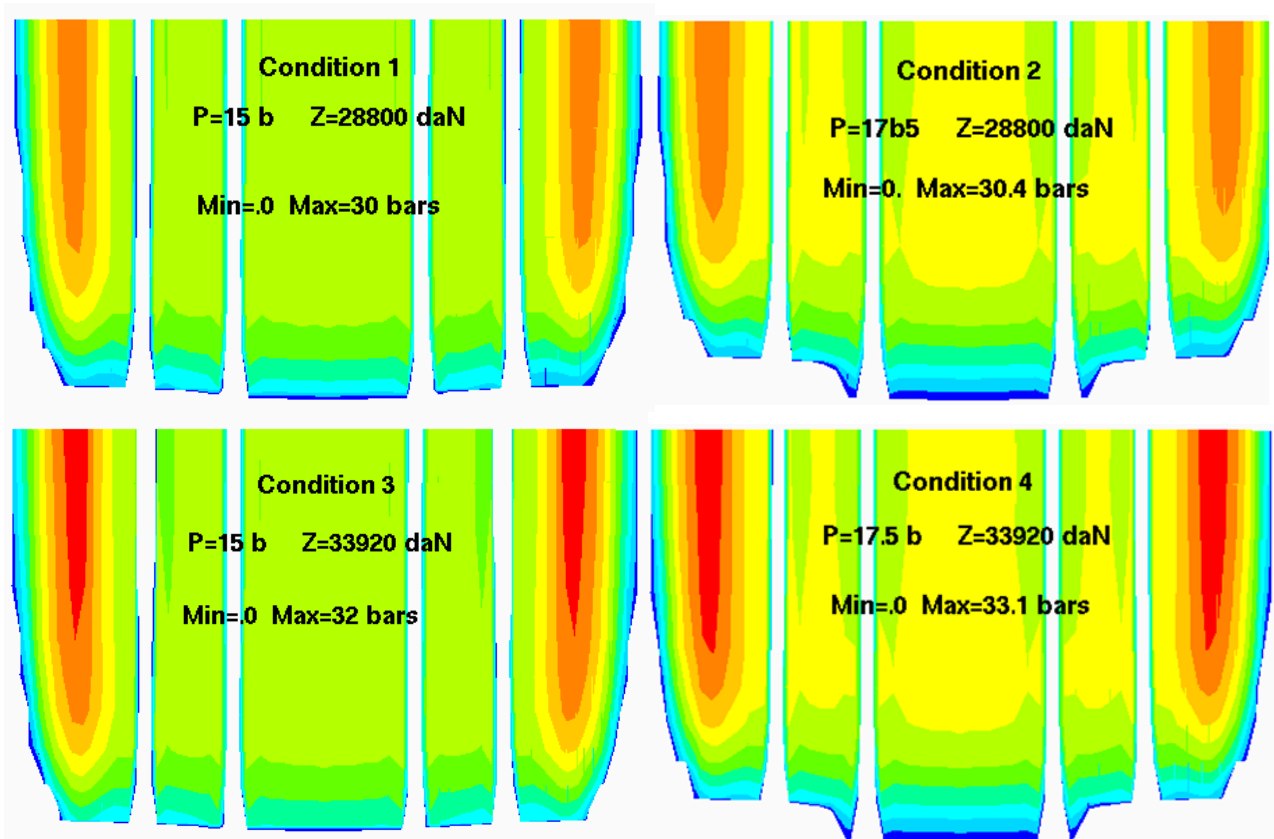


Figure 26: Calculated contact patch pressure distribution for tire size 1400x530R23 40PR at 32% deflection

### 3.4.2.6 Local rolling circumference and Wear

The most important difference between Bias and Radial technology is management of the Rolling Circumference (RC) of each rib, represented in Figure 27 and Figure 28.

The consequence of the Bias round cross shape is a large RC variation between pattern centre and shoulders which generates a large longitudinal force rate as shown in paragraph 3.4.2.4 page 42, and increases the pattern wear speed. Also energy generated there will not be available for tire adherence.

The Radial structure works almost like a cylinder allowing low RC differences between pattern centre and shoulder.

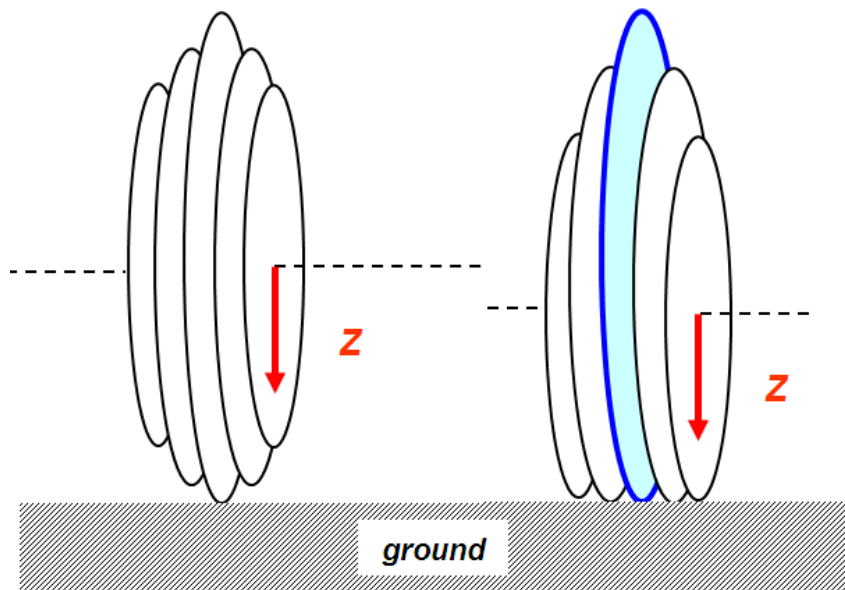


Figure 27: Rolling circumference of Bias tires

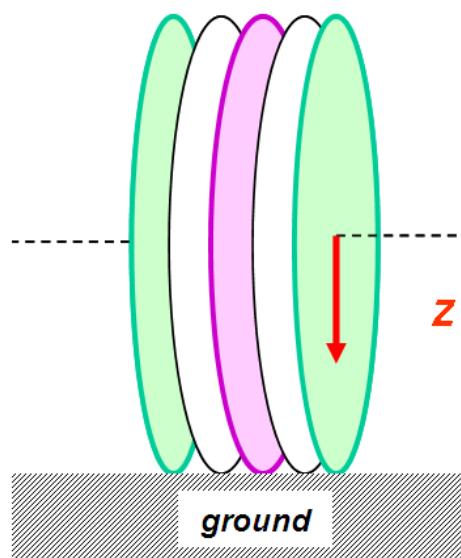


Figure 28: Rolling circumference of Radial tires

### 3.4.3 Specifications and tire technology

Table 10 summarizes the tire technologies abilities satisfying the requested performances for the HTPT.

**Table 10: Tire technologies abilities vs performance requested**

Performance Requested	Bias	Radial Nylon	NZG
<b>Tire size allowing the load capacity &gt; 30 000 daN</b>	54x21 – 23 36PR (not available)	1400x530 R23 36PR	1400x530 R23 40PR
<b>Pressure capacity</b>	36PR Loaded pressure<16bar	36PR Loaded pressure<16bar	40PR Loaded pressure<17,9bar
<b>Geometrical stability</b>	---	-	0
<b>Wear indicator (km)</b>	100 (1800 km)	200 (3200 km)	250 (4000 km)
<b>To test inflation pressure effect all along the test</b>	---	-	+

As a conclusion, only the NZG technology used in the tire size 1400 x 530 R23 40PR verifies the high pressure study specification.

### 3.5 Instrumentation and data acquisition

The main objective of the instrumentation is to obtain a comprehensive description of the pavement behavior during tests.

This includes:

- Permanent component of vertical displacement of surface layers (surface layer rutting sensors)
- Horizontal resilient strains in the different asphalt layers of the structure (strain gauges)
- Vertical resilient strains in unbounded layers (strain gauges)
- Permanent component of the vertical displacement of whole pavement structure (anchored deflectometer)
- Temperature profiles in asphalt material

This aim was to provide:

- Information on the origin of rutting observed at the pavement surface
- Comparative data between configurations at 15 bar and 17.5 bar
- Absolute data for the assessment of theoretical models
- Information on temperature gradient (asphalt being sensitive to high temperature)

Section B is the reference section because EB14-BBA C thickness (8cm) is the conventional average thickness. Therefore it is the most instrumented section (see section B instrumentation plan in Figure 29).

Instrumentation is positioned along lines corresponding to wheels axle of the simulator (see paragraph 4.4.3 page 59). L2S line is the reference trajectory (15 bar modulus trajectory) and therefore the most instrumented line. L3N is the reference trajectory to 17.5 bar modulus and surface layer rutting sensors were installed to compare pressure effect.

For redundancy 3 profiles are instrumented in asphalt material and granular layer on section B and L2S line. These profiles are used to follow surface rutting evolution during tests.

L2S trajectory on sections A and C are instrumented to get comparison between two thicknesses with the same material thickness effect.

L2S trajectory on sections D and B are instrumented to get comparison between two materials with same thickness.



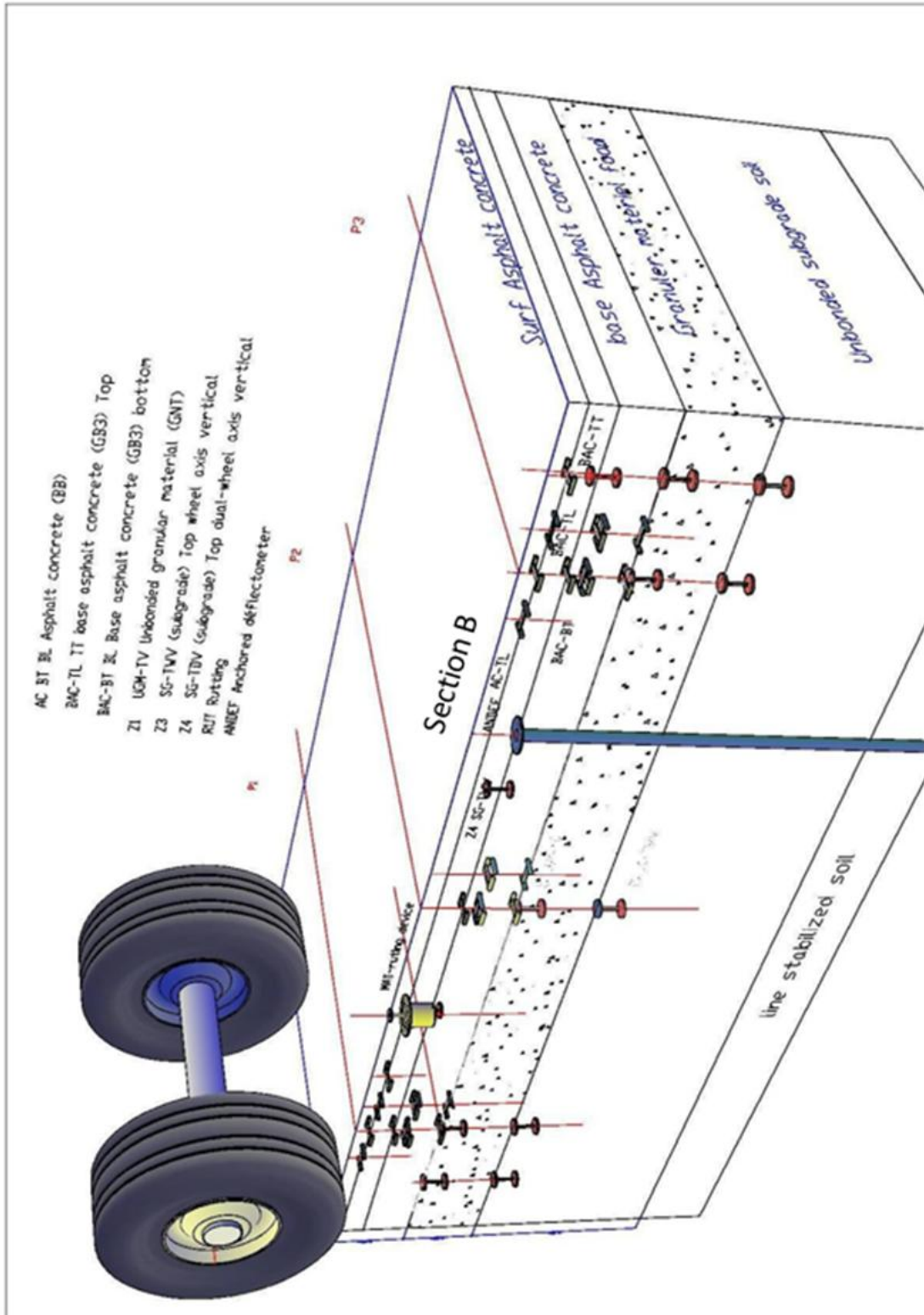


**Figure 29: Instrumentation of section B**

Figure 29 shows the location of the instrumentation in section B, the reference section, composed of standard materials and fully instrumented. All instruments are detailed in this chapter.

### 3.5.1 Surface layer rutting sensors

The aim is to measure permanent vertical displacement in surface asphalt layers on section A, B, C, and D. Each section is instrumented on two lines to compare effect of the two pressures (15 and 17.5bar).

System developed by LCPC and LRPC is equipped with LVDT sensors. LVDT sensor measures vertical displacement of a plate fixed at the pavement surface. Amplitude of sensors is +/- 25mm, average sensitivity is 625  $\mu\text{m}/\text{mV}$ .

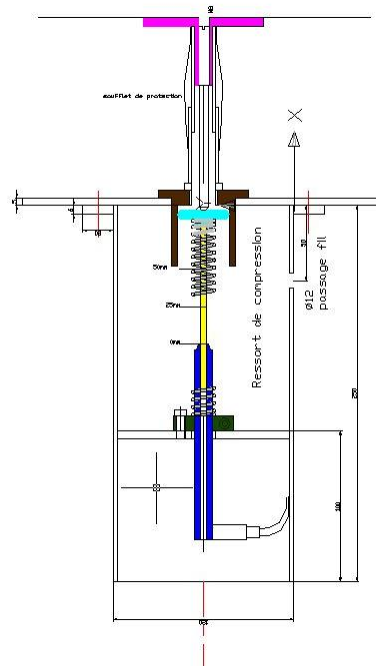


Figure 30: Surface layer rutting sensor

### 3.5.2 Horizontal strain gauges

These strain gauges allowing the measurements of the reversible strains are located at different pavement depth on different sections:

- at the base of surface layers (longitudinal and transversal measurements)
- at the base of GB4 base layers (transversal measurements)
- at the base of BB base layers (longitudinal and transversal measurements)
- at the top of GB3 base layers (longitudinal and transversal measurements)
- at the base of GB3 base layers (longitudinal and transversal measurements)

Strain sensors are manufactured by LRPC using KYOWA strain gauges, the installation uses the  $\frac{1}{2}$  bridge principle. The average gauge factor is 2285  $\mu\text{strain}/\text{mV}$ .



Figure 31: Horizontal strain gauges

### 3.5.3 Vertical strain gauges

These gauges measure resilient vertical strains and are located:

- at the top of unbounded foundation material
- at the top of unbounded capping layer

These two groups are installed either in wheel axle or in dual-wheel axle in order to get information on wheel interaction due to the stress diffusion pattern and the load superposition in the deepest layers.

Sections A, B, C and D are equipped with vertical resilient strain gauges.

Strain sensors are manufactured by LRPC using KYOWA strain gauges, the installation used the  $\frac{1}{2}$  bridge principle. The average gauge factor is 2285  $\mu\text{strain/mV}$ .



Figure 32: Vertical strain gauges

### 3.5.4 Absolute vertical displacement

These sensors anchored in fixed bedrock allowed measurement of absolute displacement of whole initial pavement (top of surface asphalt concrete course).

Sections A, B, C, D, E, are instrumented with anchored deflectometer. This system developed by LCPC and LRPC is equipped with LVDT sensors. LVDT sensor measures vertical displacement of a plate fixed at the top of surface asphalt concrete course. Amplitude of sensors is +/- 25mm, average sensitivity is 625  $\mu\text{m}/\text{mV}$ .

### 3.5.5 Temperature profiles

Many gauges are installed to monitor pavement profile temperatures. The temperature gauges are Pt 100 ohm.

Two profiles are installed for redundancy. The profile was reconstructed in an asphalt material core sample then sealed with mortar in a test runway core drilling.

Depth of gauges on two profiles is shown in Table 11.

**Table 11: Depth of temperature gauges**

Core sample 1	Core sample 2
0	0
-2	-2
-4	-4
-6	-6
-8	-8
-12	-12
-18	-18
-26	-26
-36	NA
-46	NA

In complement, air T°C, moisture and black body T°C are measured.

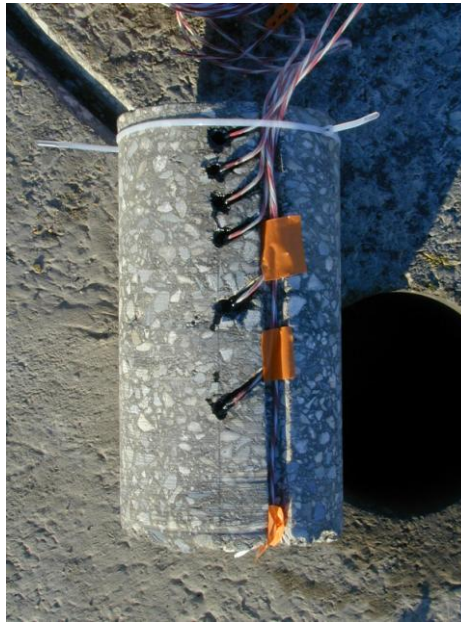


**Figure 33: Core equipped with temperature gauges**

### 3.5.6 Acquisition unit

Instrumentation is managed by a single acquisition unit (except for temperature data) to facilitate analysis and to have simultaneous data acquisition from all sensors and gauges.

Various hardware are used:

- 1 MGCPlus unit with a maximum capacity of 128 channels (16x8 channel cards) connected to the acquisition PC by an Ethernet link. 96 strains gauges and 14 LVDT sensors are connected
- Spiders with a capacity of 8 channels maximum. 20 strains gauges are connected.

The acquisition unit is controlled by Catman soft. The files are saved in ASCII format for direct use with dedicated LCPC software.

Temperatures are monitored by a Datalogger unit connected to a standalone PC. These are recorded 24 hours-a day, every 15 min.



**Figure 34: Acquisition Unit**

## 4 Tests

### 4.1 Objectives

The test campaign consists in running a simulation vehicle on the experimental pavement. Its aim is to collect data from the network of sensors at pavement depth. This data is then sorted and analyzed (see chapter 5 page 60) to isolate the effects of tire pressure on the pavement from all other parameters. The simulator configuration used for the tests is designed to comply with these objectives, and is presented in this section.

The test campaign is divided into a consolidation phase and a fatigue phase. For each phase, different configurations of the simulator, i.e. a given wheel-load a given tire pressure have been selected, and specific procedures applied.

This section details the principles, configurations and procedures of the two phases.

### 4.2 Test principles

#### 4.2.1 General simulator specification



**Figure 35: The simulator**

The simulation vehicle has a speed of around 5km/h. Schematics of the simulator are represented in Appendix 13. This paragraph presents its general geometric specifications.

The simulator is equipped with four dual wheel modules. The distance between the two wheels of a given module, and the distance between two different modules is as large as possible so that the wheels and gears interaction are minimized in the deepest layer of the pavement. This is done in order to study the influence of each module and each wheel on the pavement independently. As a result, the wheel track is 1550 mm, and the axle-to-axle distance between two neighboring modules is 5000 mm, as shown in Figure 36.

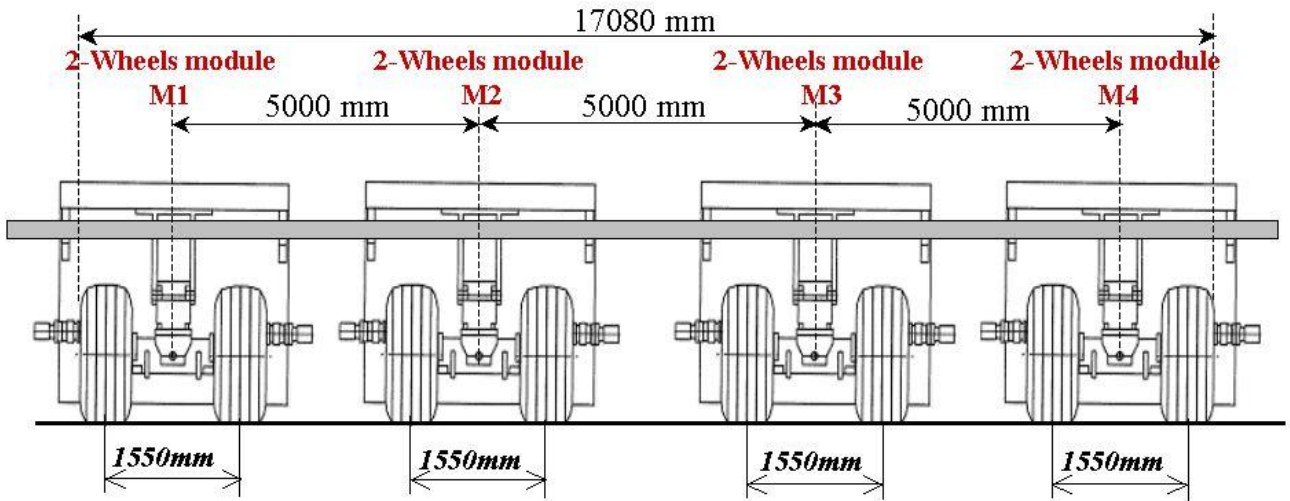


**Figure 36: Dimensions of the simulator**

Tires used are Michelin 1400x530R23 40PR as fitted to the A340-500, A340-600, and A380-800 and are the only existing tires capable of supporting the heavy loads applied at the highest configuration (see paragraph 4.4.2.2 page 58).

## 4.2.2 Loading cases principle

The modular configuration of the simulator allows simulation of two different loads and two different tire pressures simultaneously, i.e. in the same meteorological and thermal conditions. The loading cases principle is represented in Figure 37. As shown in this figure, the modules M1 and M4, and M2 and M3 are identically loaded but differ in tire pressures, allowing analysis of pressure effects on the pavement. Such load repartition respects the symmetry of the simulator thus ensuring its stability. Modules M1 and M3, and M2 and M4, present identical internal tire inflation, with different loads, allowing observation and analysis of the load effect.

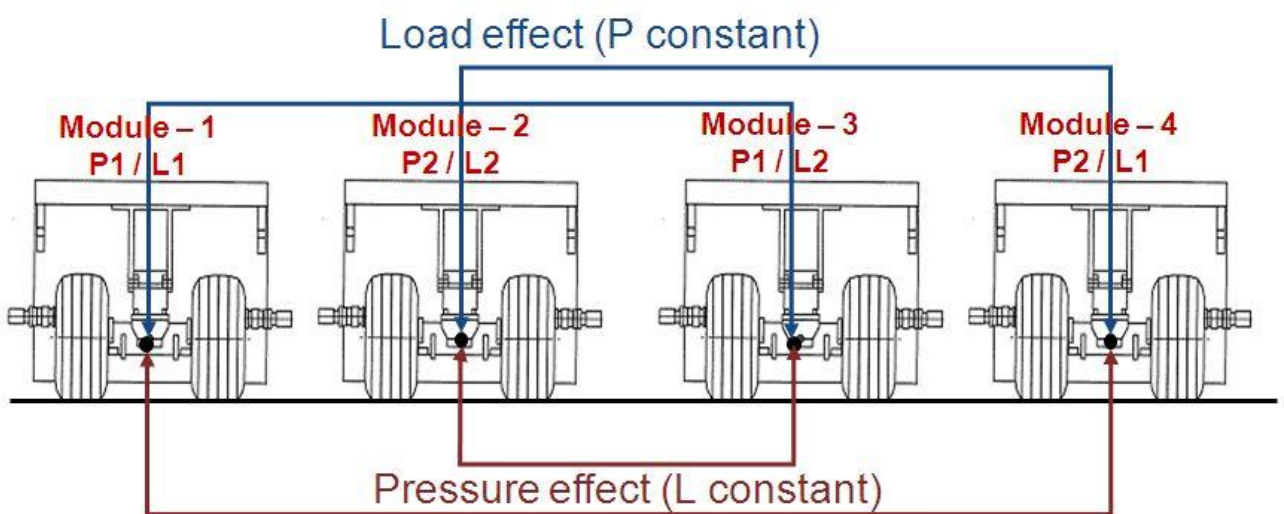


**Figure 37: Loading cases principle**

## 4.3 Consolidation phase: C0

### 4.3.1 Objectives

A first phase of consolidation (C0) is carried out for the runway to reach its stabilized initial geometry and characteristics. Also, it aims to homogenize the pavement for objective comparison between the tested loading cases. Pavement status after consolidation is then used as a reference for measuring the geometric and mechanical data during the fatigue phase.

### 4.3.2 Simulator's configuration

As the aim of the consolidation phase is to pass with the simulator equally all over the pavement's surface, the load per wheel and tire pressure must be the same for all the modules. The empty weight of modules M1 and M2 is 19.2 tons per wheel, which is higher than modules M3's and M4's empty weight, respectively equal to 15.0 tons per wheel and 12.8 tons per wheel. As a result, 19.2 tons per wheel is the minimum reachable load to obtain identical loads on every module.

#### 4.3.2.1 Before pavement reinforcement

Four different configurations were selected during consolidation phase before reinforcement for a total of 698 passes. Table 12 details these configurations.

To consolidate the pavement, the first configuration selected was a heavy one (28t/wheel, tire pressure 15bar). Deformation levels in the different layers of the pavement, especially in the UGA and the asphalt concrete base course, were abnormally high compared to the model predictions (Alizé). Also, signals showed a structural deformation mechanism at constant volume, revealing insufficient drainage of the pavement, which is incompatible with the consolidation process.

To avoid permanent pavement damage due to this constant volume mechanism, it was decided to decrease the load on each module and the tire pressure, for configurations commencing passage number 131. Consolidation phase was carried on because a drainage and consolidation was expected to start, but the number of passes necessary to initiate it was unknown.

The consolidation phase was stopped after 698 passes since the expected drainage did not begin.

**Table 12: Configurations during consolidation phase before reinforcement**

Module	Pnz		Load per wheel		Deflection mm	Gross contact area cm <sup>2</sup>	Passes number
	Bar	PSI	Tons	Lbs			
All	15.0	218	28.0	61,700			1 - 130
All	8.7	126	19.2	42,300	123	2165	131 - 584
All	12.0	174	19.2	42,300			585 - 658
All	8.7	126	19.2	42,300	123	2165	659 - 698



### 4.3.2.2 After pavement reinforcement

Reasons for reinforcement and ways to achieve it are explained in paragraph 3.2.4.3 page 34. After the reinforcement, a new consolidation phase of 380 passes was applied. To consolidate without premature pavement structural damage, the configuration selected is the minimum possible load (19.2t/wheel) and a low tire pressure (8.7bar). Table 13 provides the details of configuration C0 (after reinforcement).

**Table 13: Configuration C0 after pavement reinforcement**

Module	Pnz		Load per wheel		Deflection mm	Gross contact area cm <sup>2</sup>	Passes number
	Bar	PSI	Tons	Lbs			
All	8.7	126	19.2	42,300	123	2165	1 - 380

### 4.3.3 Procedure

The purpose of the consolidation phase is to cover equally the whole pavement’s surface with the simulator’s wheels. To reach this objective, 13 different trajectories have been defined (T1 to T13) and are represented in Figure 38. One trajectory corresponds to two passes (one in each direction) of the simulator on a given lateral position on the pavement. The lateral wandering between two consecutive trajectories is 400mm. One cycle is constituted by 26 trajectories, from T1 to T13, then from T13 to T1, each being passed on twice by the simulator (once in each direction), as shown in Figure 39. A cycle corresponds then to 52 passes of the simulator.

A longitudinal area of 1.62m width on each side of the pavement is never covered by the simulator’s wheels. The 18.56m wide central area is covered 8 times by the simulator’s wheels during one cycle. Between these two areas, a longitudinal area of 1.6m width on each side of the pavement is covered 4 times during one cycle.

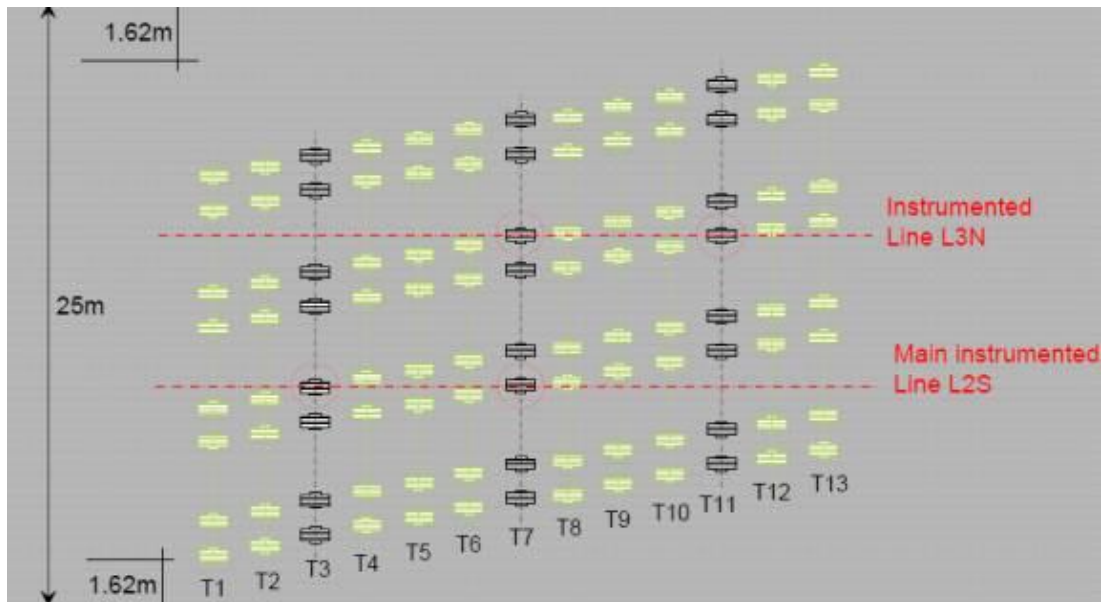


**Figure 38: Simulator trajectories during preloading phase**

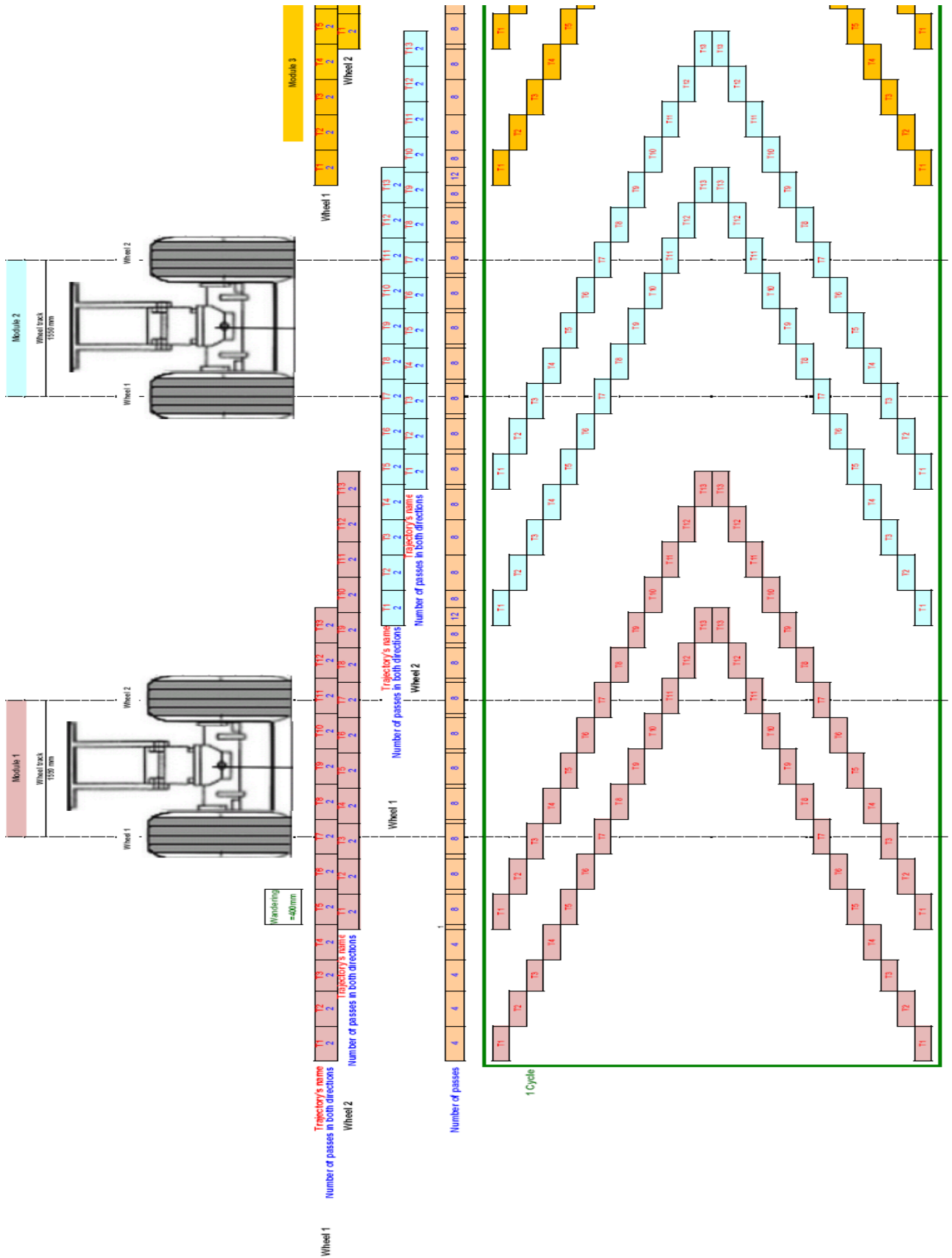


Figure 39: Consolidation phase procedure

## 4.4 Fatigue tests

### 4.4.1 Objectives

During fatigue tests, continuous data acquisition and regular topographic measurements are performed to obtain relevant data on pavement response to the wheel-loads and tire pressures applied.

Fatigue tests are divided into three phases, namely C1 (constituted by C1' and C1''), C2 and C3, each corresponding to a given configuration. To ensure the structural pavement integrity until the end of the test campaign, the load of the modules is progressively increased from one configuration to the next. The procedure (lateral wandering and cycles) for fatigue tests is specified in this section, as well as simulator's configurations for each phase.

### 4.4.2 Simulator's configuration

#### 4.4.2.1 Lowest configuration: C1' and C1''

Configuration C1, used for the first 1000 passes, and divided into two sub-configurations C1' and C1'', aims at verifying the sensors' response, while applying a low load on the pavement. As a result, configuration C1' is the same as configuration C0, but the wandering procedure is the one applied for all fatigue test configurations. This configuration, presented in Table 14, is used for the first 100 passes.

**Table 14: Configuration C1'**

Module	Pnz		Load per wheel		Deflection mm	Gross contact area cm <sup>2</sup>	Passes number
	Bar	PSI	Tons	Lbs			
M1	8.7	126	19.2	42,300	123	2165	from 1 to 100
M2	8.7	126	19.2	42,300	123	2165	
M3	8.7	126	19.2	42,300	123	2165	
M4	8.7	126	19.2	42,300	123	2165	

For configuration C1'', and for the following configurations, the process presented in paragraph 4.2.2 page 53 is applied. Also, tire pressures P1 and P2 are defined as P1=17.5bar and P2=15.0bar, which remains unchanged until the end of the tests. Loads applied on central modules M2 & M3, which correspond to the instrumented lines, are higher than those on external modules (L2>L1). L2 is determined using the criterion of iso-deflection of the tire (in mm) between P2=15bar and L1=19.2t onM4, and P1=17.5bar and L2 on M3 (L2 is the load for which tire deflection is the same as for tire loaded at L1 and inflated at 15 bar). Configurations of modules M1 and M2 correspond respectively to P1/L1 and P2/L2, for the comparison iso-load and iso-pressure. Results of these calculations are presented in Table 15. 900 passes have been performed in configuration C1''.

**Table 15: Configuration C1''**

Module	Pnz		Load per wheel		Deflection mm	Gross contact area cm <sup>2</sup>	Passes number
	Bar	PSI	Tons	Lbs			
M1	17.5	254	19.2	42,300	72	1076	from 101 to 1000
M2	15.0	218	22.0	48,500	85	1478	
M3	17.5	254	22.0	48,500	80	1267	
M4	15.0	218	19.2	42,300	80	1256	

#### 4.4.2.2 Highest configuration: C3

The load to apply on the lightest module of configuration C3 (P2=15.0bar and L1) is derived from the tire ratings given by Michelin, namely P=17.2bar and L=34.0t at a deflection of 32%. Using the tire ratings to maintain the design operating conditions (Static Load Radius) of the tire (as recommended by Michelin) at a tire pressure of 15bar, the figures obtained are P2=15bar and L1=28.7t. L2 is then determined by using the criterion of tire's iso-deflection (in mm) between P2=15bar and L1=28.7t on M4, and P1=17.5bar and L2 on M3. Configurations of modules M1 and M2 correspond respectively to P1/L1 and P2/L2. Results of these calculations are presented in Table 16.

**Table 16: Configuration C3**

Module	Pnz		Load per wheel		Deflection mm	Gross contact area cm <sup>2</sup>	Passes number
	Bar	PSI	Tons	Lbs			
M1	17.5	254	28.7	63,270	99	1608	from 2001
M2	15.0	218	33.2	73,200	125	2171	
M3	17.5	254	33.2	73,200	112	1861	
M4	15.0	218	28.7	63,270	112	1877	

#### 4.4.2.3 Intermediate configuration: C2

The aim of the intermediate configuration is to progressively reach the maximum load for which the tests are performed.

The mean of L1 values of configurations C1" and C3 gives L1 value for configuration C2, i.e. L1=24.0t. L2 is determined by using the criterion of the tire's iso-deflection (in mm) between P2=15bar and L1=24.0t on M4, and P1=17.5bar and L2 on M3. L2=27.7t obtained with the iso-deflection criterion also corresponds to the mean of L2 values of configurations C1" and C3.

Configurations of modules M1 and M2 are derived from these results and correspond respectively to P1/L1 and P2/L2. This configuration, presented in Table 17, is used for 1000 passes.

**Table 17: Configuration C2**

Module	Pnz		Load per wheel		Deflection mm	Gross contact area cm <sup>2</sup>	Passes number
	Bar	PSI	Tons	Lbs			
M1	17.5	254	24.0	52,900	84	1345	from 1001 to 2000
M2	15.0	218	27.7	61,100	107	1812	
M3	17.5	254	27.7	61,100	97	1553	
M4	15.0	218	24.0	52,900	97	1570	

### 4.4.3 Procedure

Figure 40 shows the wandering procedure selected during fatigue tests, and represents the trajectories followed by each module of the simulator. The lateral wandering between two following trajectories is 400mm. This lateral wandering aims at avoiding the creation of gutters, which would have appeared if the simulator had passed solely on trajectory “0” (i.e. the central trajectory).

Four reference lines (L1 to L4) have been defined as the trajectories followed by the axle of each module when the simulator passes on the central trajectory. For example, L1 represents the trajectory followed by the axle of module M1 when on central trajectory.

When the simulator follows trajectory “0”, the external wheel of module M3 is on the instrumented line L3N, and the external wheel of module M2 is on the instrumented line L2S, as it was for the consolidation phase trajectory T7. For that reason, this central trajectory is repeated two times.

One complete cycle described 20 passes of the simulator (10 in each direction).

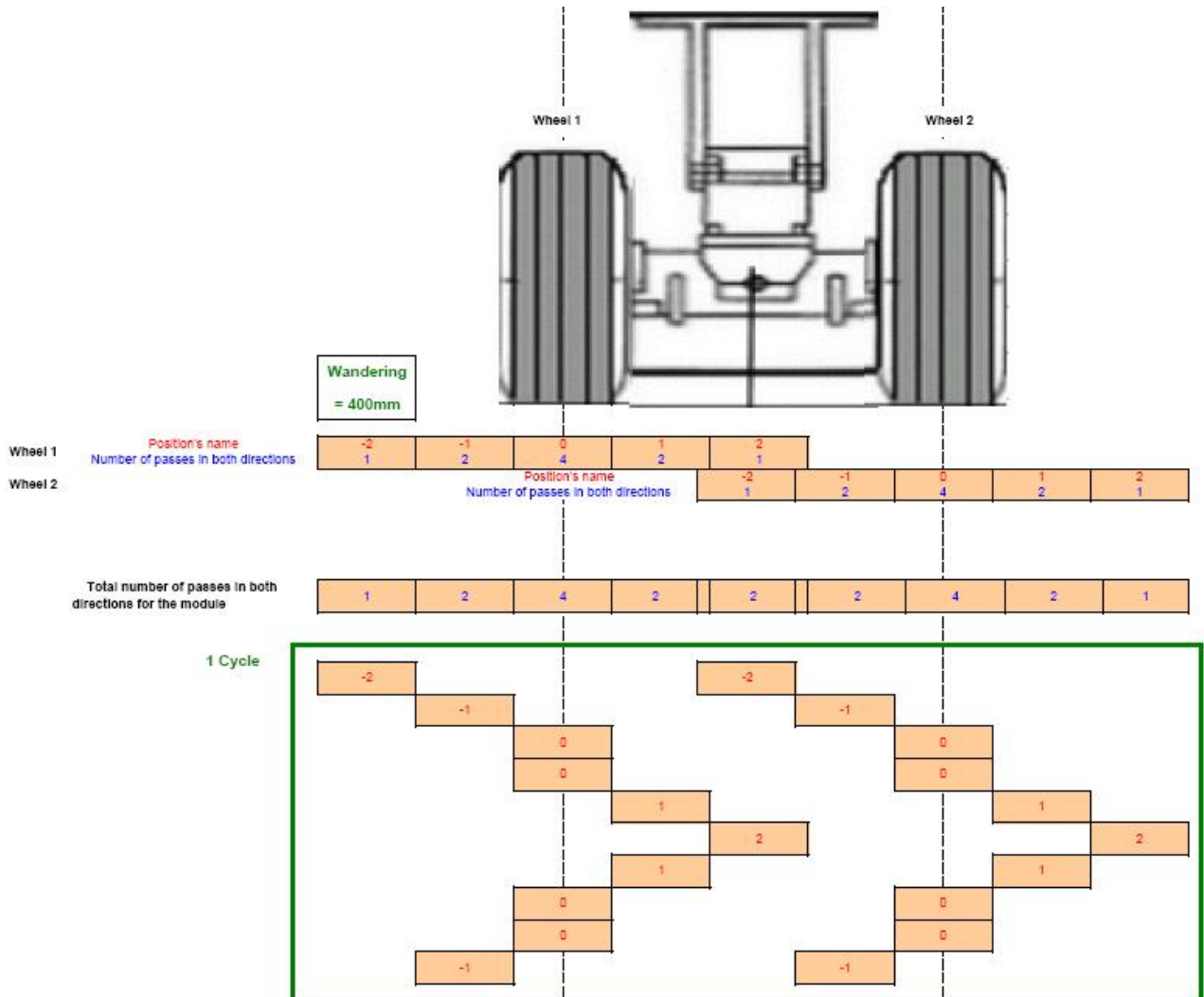


Figure 40: Fatigue test procedure

## 5 Data analysis

### 5.1 Introduction

Started on October 22, 2009 the test was completed on August 08, 2010 as cumulative traffic of the simulator reached 11,000 passes. However it should be pointed out that the simulator tests running on section G were completed at 10,500 passes on July 27, as pavement deformation from 32 to 45 mm had been achieved and simulator maneuverability became no longer possible on this test section.

As rutting deformation is the main failure mode with regard to tire pressure effect, this chapter focuses only on the main pavement rutting results of the tests.

Moreover, the pavement survey during the 10 months of the HTPT test includes a comprehensive monitoring of the resilient displacements and strains developed in the pavement by the dynamic loads. It is based on the pavement instrumentation by LVDT sensors and strain gauges in bituminous and untreated materials.

### 5.2 Thermal conditions of the tests

Figure 41 shows the evolution against time of the cumulative traffic and the temperature in surface AC. The temperature considered is the mean temperature over the 8 cm AC at the top of the section B of the pavement. It should be noted that AC temperature greater than 30°C were not reached before mid April 2010, when the cumulative traffic was 6,900 passes.

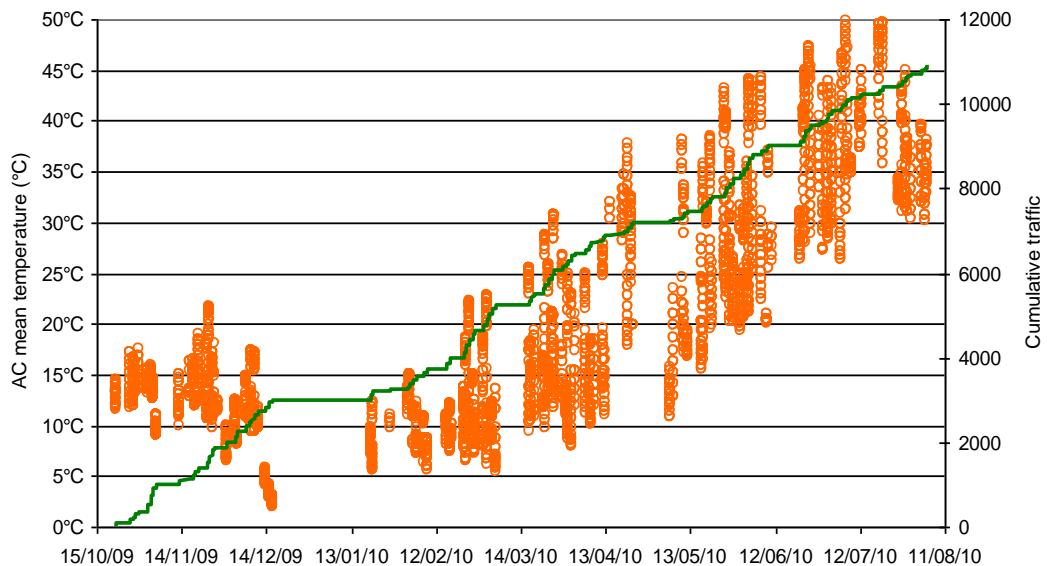


**Figure 41: Evolution of the cumulative traffic and the temperature in AC**

The AC temperature vs. traffic histograms during the 11,000 load applications are shown in Figure 42. The temperatures considered in these 3 histograms are still the mean temperatures over the 8 cm of surface AC. The temperatures during the test for configurations C1 and C2 are representative of common thermal condition in Southwest France from October to December. The very low level of rutting during these two first phases can be explained by the low AC temperatures, which never exceeded 21°C.

Higher temperatures in asphalt concrete are monitored during the C3 phase. 4.3% of the cumulative traffic (i.e. 237 passes out of 11,000) are applied when AC temperature exceeds 30°C and 2.3% (ie. 124 passes) when AC temperature exceeds 40°C. The maximum temperature 50-52°C was reached for 37 simulator passes. Surface temperature is obviously higher in all cases compared to the considered mean temperature and can exceed 60°C for max. mean temperature or 45/50°C for mean temperature equal to or less than 40°C.

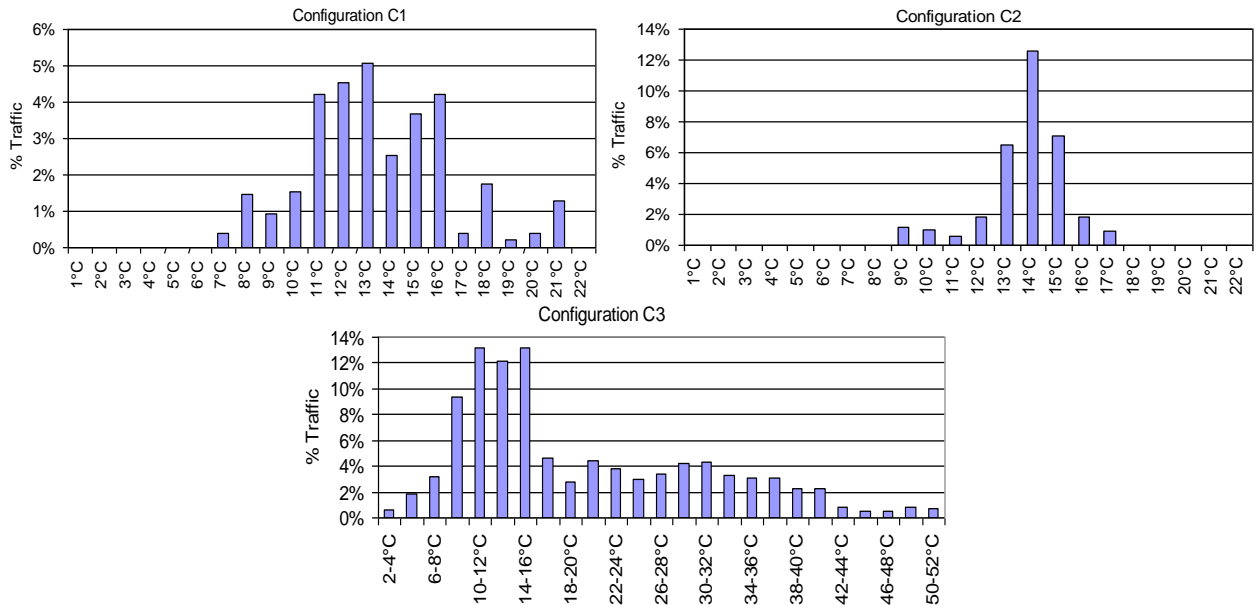


Figure 42: Temperatures in AC during the tests

### 5.3 Strain-gauge signals

From the start of testing to 1,000 loadings, a complete sensor acquisition including the recording of 116 stain-gauges and 14 LVDT sensors (130 channels valid today) is recorded at each simulator run. A detailed presentation of the instrumentation is presented in paragraph 3.5 page 46. From 500 loadings to 3,000 passes, 1,230 further data acquisitions were recorded.

These measurements constitute a database including 2,230 data acquisition at the present time, stored in 1,115 ASCII measurement files (one file for one simulator pass-and-back). Pavement temperature survey is also performed continuously (acquisition period = 15 minutes) since test initiation.

This database allows a complete description of the dynamic response of the experimental pavement trafficked by heavy loads at low speed under variable thermal conditions. However, it should be observed that the pavement instrumentation was initially conceived for a typical and new airport runway without anticipating subsequent reinforcement (see paragraph 3.2.4.3 page 34). Therefore it could be concluded that an appreciable part of the instrumentation objectives will not be fully obtained by the end of the tests, mainly concerning data for the French rational design method for new airfield pavement assessment and the calibration. However full instrumentation installed in the pavement part sensitive to tire pressure was entirely reproduced so that tire pressure effect on surface and base asphalt concrete can be accurately assessed.

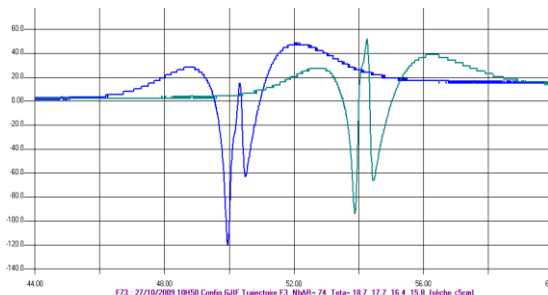
### 5.3.1 Wearing course-base AC interface

The quality and durability of the bonding between the different pavement layers highly affect the structural resistance of the pavement. As heavy load induced very high shear stresses in the upper pavement layers, interface un-bonding of the wearing course must be considered as a possible degradation mode of the pavement, which significantly reduces its service life by developing premature cracks and accelerating subsequent deterioration.

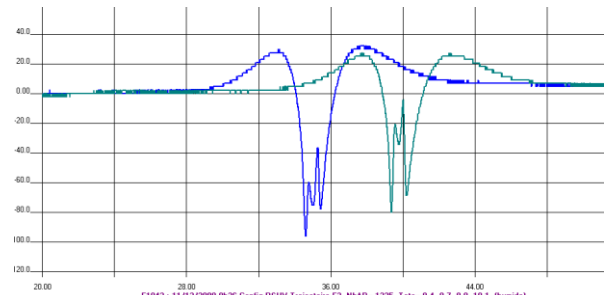
Information concerning the bonding condition between the AC wearing course and the base AC layer may be deduced from the strain gauge response at the bottom and the top of these two layers.

### 5.3.2 Vertical strains gauges and vertical displacement sensors

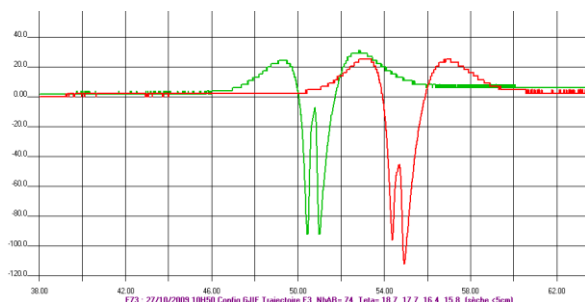
Figure 43 shows typical signals measured for the load conditions C2 and C3. Contraction strains are expressed with negative sign. Flexural strains created by the load at the bottom of the AC surface and the top of the base AC layers are both contraction strains. Furthermore, the maximal contraction strain values on both sides of the interface are very close. It clearly reveals the flexural strain vertical continuity in the structure and consequently good bonding condition between the two layers, in spite of the very high loads and tire pressure applied to the pavement.



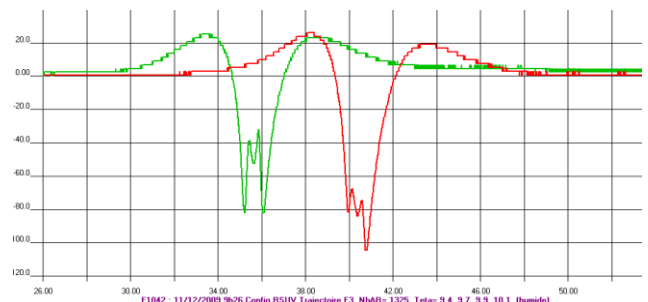
Configuration C2, Temp=17.2°C  
Longitudinal strain gauge at the bottom of the surface AC:  
Typical signal  $\epsilon_{\text{long}} = f(\text{time})$



Configuration C3, Temp=9.8°C  
Longitudinal strain gauge at the bottom of the surface AC:  
Typical signal  $\epsilon_{\text{long}} = f(\text{time})$



Configuration C2, Temp=17.2°C  
Longitudinal strain gauge at the top of the base AC:  
Typical signal  $\epsilon_{\text{long}} = f(\text{time})$

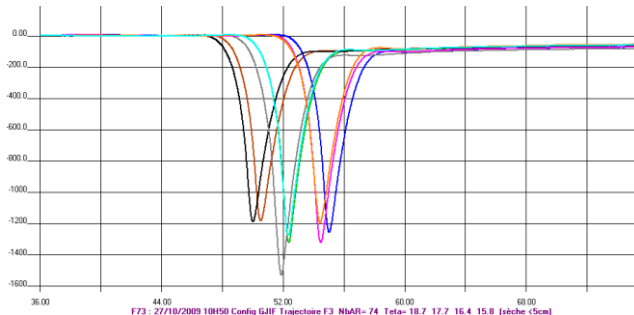


Configuration C3, Temp=9.8°C  
Longitudinal strain gauge at the top of the base AC:  
Typical signal  $\epsilon_{\text{long}} = f(\text{time})$

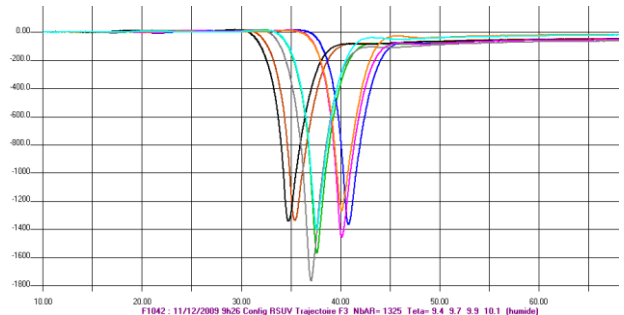
**Figure 43: Typical strain-gauge signals at the bottom of the surface AC and the top of base AC layer. Structure B, load configurations C2 and C3, tire pressure 1.75 MPa (gauge measure in  $\mu\text{strain}$ , negative sign for contraction)**



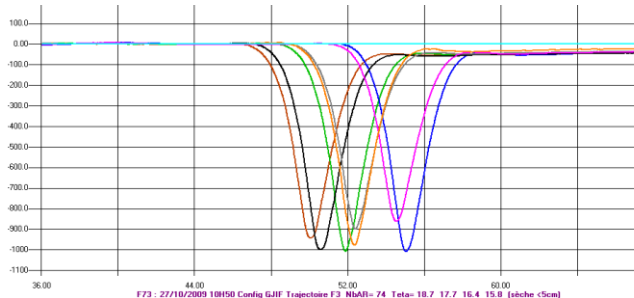
Typical signals measured by the vertical strain gauges at the top of the UGM subbase and capping layer are presented in Figure 44.



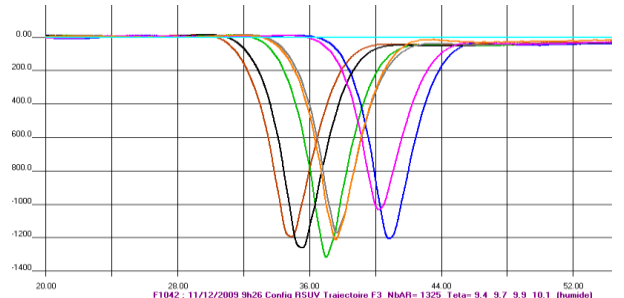
Configuration C2, Temp=17.2°C  
Vertical stain gauge at the top the UGM subbase  
Typical signal  $\epsilon_{vert} = f(\text{time})$



Configuration C3, Temp=9.8°C  
Vertical stain gauge at the top the UGM subbase  
Typical signal  $\epsilon_{vert} = f(\text{time})$



Configuration C2, Temp=17.2°C  
Vertical stain gauge at the top the UGM capping layer  
signal  $\epsilon_{vert} = f(\text{time})$



Configuration C3, Temp=9.8°C  
Vertical stain gauge at the top the UGM capping layer  
signal  $\epsilon_{vert} = f(\text{time})$

**Figure 44: Typical strain-gauge signals at the bottom of the surface AC and the top of base AC layer. Structure B, load configurations C2 and C3, tire pressure 1.75 MPa (gauge measure in  $\mu\text{strain}$ , negative sign for contraction)**

Typical signals measured by the anchored deflectometer and surface layer rutting sensors are presented in Figure 45.

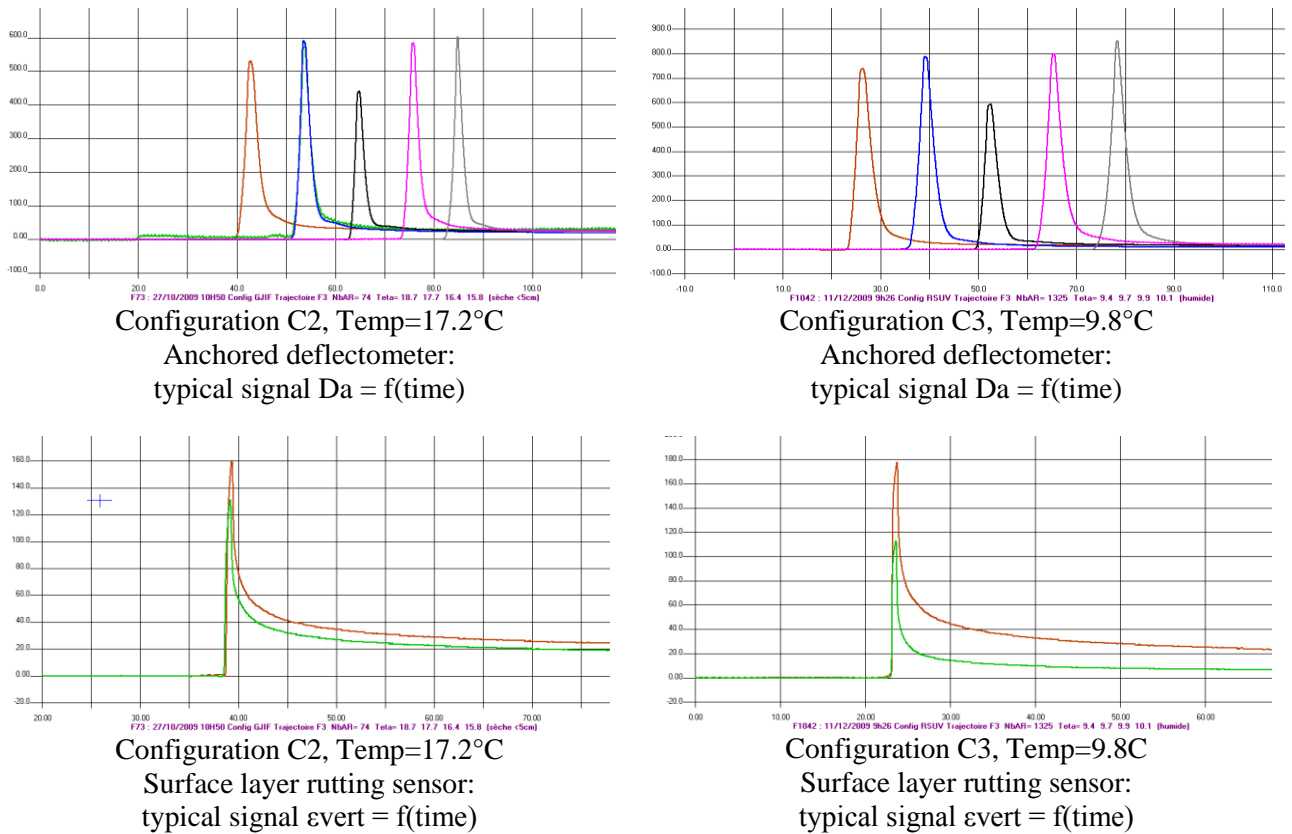


**Figure 45: Typical strain-gauge signals at the bottom of the surface AC and the top of base AC layer. Structure B, load configurations C2 and C3, tire pressure 1.75 MPa (gauge measure in  $\mu$ strain, negative sign for contraction)**

Strain and displacement signals as those shown in Figure 43, Figure 44, and Figure 45 will be analysed in a later task of the HTPT project, according to the improvement of the structural modelling of pavement under heavy load objective:

As this objective is widely based on comparisons between the sensor responses under different loads and/or tire pressures, it is important to evaluate the accuracy and the reproducibility of the various sensors, and their sensitivity to other external factors.

To evaluate if the sensors return more or less identical measures under the same loading conditions (i.e. sensor repeatability), special runs of the simulator were performed. They consist in ten successive simulator back and forth along exactly the same median trajectory (T3). The signals measured by horizontal strain gauges at the bottom of surface AC and the top of the UGM subbase are presented in Figure 46 and Figure 47 respectively. It is observed that the mean repeatability range is about 5% (common value for this type of pavement instrumentation). This leads to the conclusion that the effects of tire pressure on the pavement structural behavior must not focus on the analysis of local and individual gauge responses. But it is essential to integrate a statistical approach taking into account the response fluctuations of the different sensors between them, and their one reproducibility characteristics.

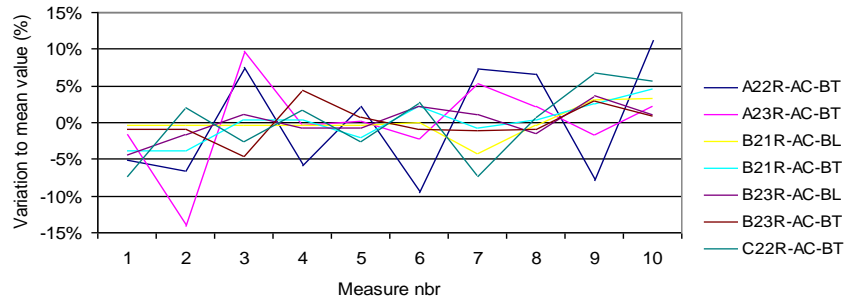


**Figure 46: Sensor repeatability tests. Signals measured by horizontal strain-gauges at the bottom of surface AC**

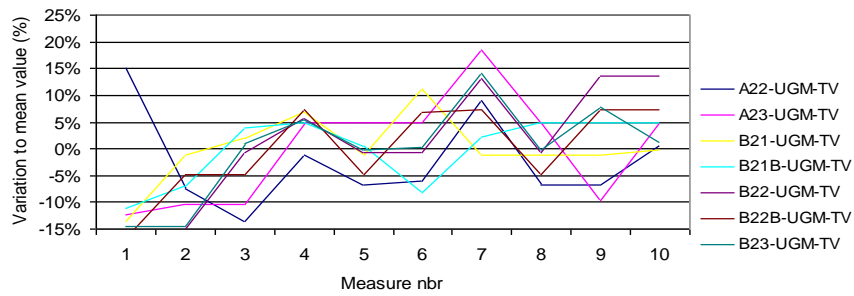


**Figure 47: Sensor repeatability tests. Signals measured by horizontal strain-gauges at the top of the UGM subbase**

## 5.4 Rutting deformation

### 5.4.1 Rutting measurement and evolution curves with traffic

Each rutting survey operation consists of 84 transversal profiles monitors by mean of the LRT numerical transverso-profilometer, distributed over the 7 structures and 4 twin-wheel modules (3 transversal profiles P1, P2 and P3 for each structure-module set, as detailed before in §3.5). Periodicity of rutting measurements was every thousand simulator passes, but complementary measurements were also performed at specific times, for instance load at configuration changing, thermal regime alteration,

The evolution curves of the final rutting depth measured along the 3 transversal profiles P1, P2 and P3, on each section A to G and for each load configuration M1 to M4, are presented in Appendix 16. Figure 48 and Figure 49 are extracted from this appendix as examples. Each rutting survey operation consists of 84 transversal profiles monitors, distributed over the 7 structures and 4 twin-wheel modules (3 profiles for each of the 28 structure-module sets).

For sections A to F, rutting depth at 7000 passes (mid April 2010) remains very low, less than 2 mm, due to the AC temperature remaining very moderate up to this date (see Figure 41). On section G (low rutting performance AC), rutting depth up to mid April also remains low, less than 4 mm. The evolution curves in Appendix 16 clearly exhibit a change in the slope after this date, as a more and more significant percentage of the traffic is applied at AC temperatures greater than 30°C.

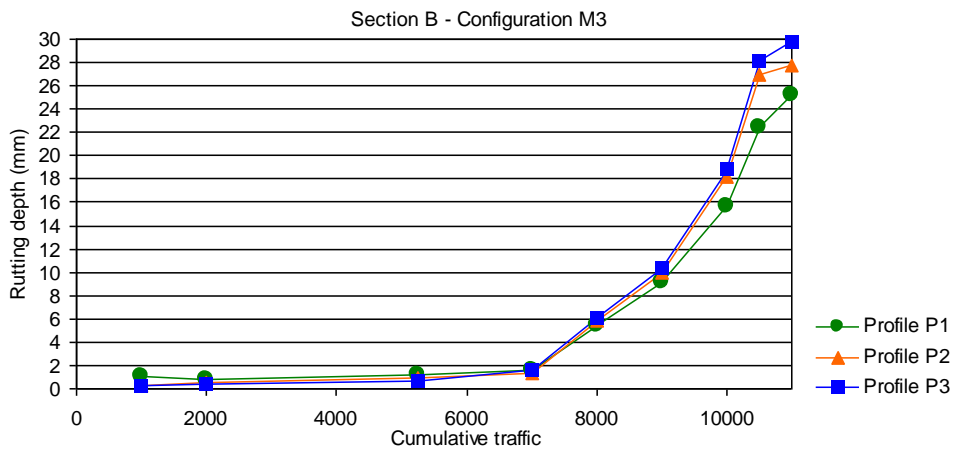


**Figure 48: Evolution curve of rutting measured on section B, configuration M3**

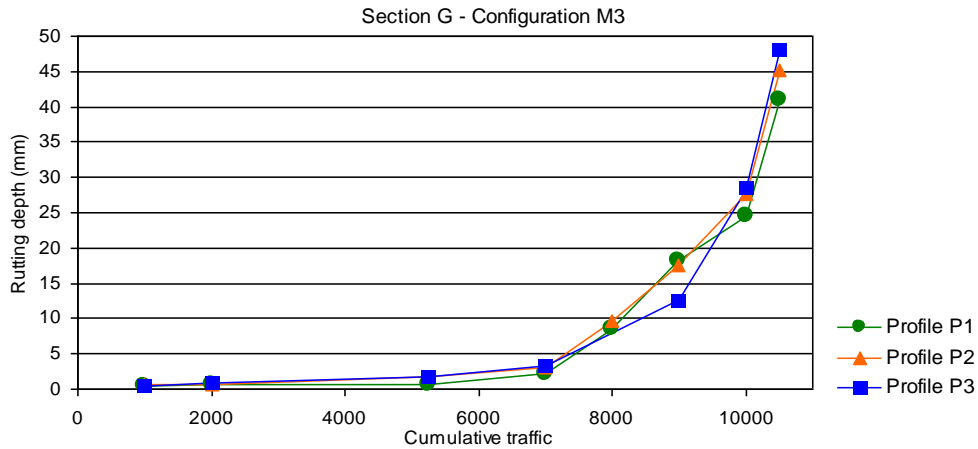


**Figure 49: Evolution curve of rutting measured on section G, configuration M3**

Figure 50 and Figure 51 show examples of transversal rutting profiles measured on sections B and G along profile P2 at various dates from 1,000 to 11,000 passes, by means of the LRPC-T transverso-profilometer (accuracy is about +/- 1mm). For a given configuration, it is generally observed that the transversal rutting curve is asymmetrical, which may suggest that the weight and/or tire pressure of the two wheels of the dual-wheel gear are not identical. However, differences in wheel load never exceeded 250 kg per wheel which is negligible in comparison of the 33200 kg of the heaviest wheel load; therefore this asymmetrical shape would be more related to lateral slope of the experimental pavement as described in the runway specification.

It is also observed that the permanent upward deformation (upheaval) on the lateral sides of the wheel-path remains negligible or very low in comparison with the downward deformation (rutting depth), apart from section G at the end of the test. This suggests that the rutting mechanism is largely due to the post-compaction of the pavement material by traffic (bituminous material and also untreated materials as discussed below). The visco-thermoplastic creeping of AC layer which induced lateral upward deformation due to constant volume strain-path should also be present, but not as much as the post-compaction which did not induce upward permanent strains. This first analysis concurs with the first Gamma bank tests performed on AC samples measured in section B at the end of the tests.

This observation does not apply to the section G, constituted with low rutting performance surface, which exhibits significant upward permanent deformation at the end of the test.

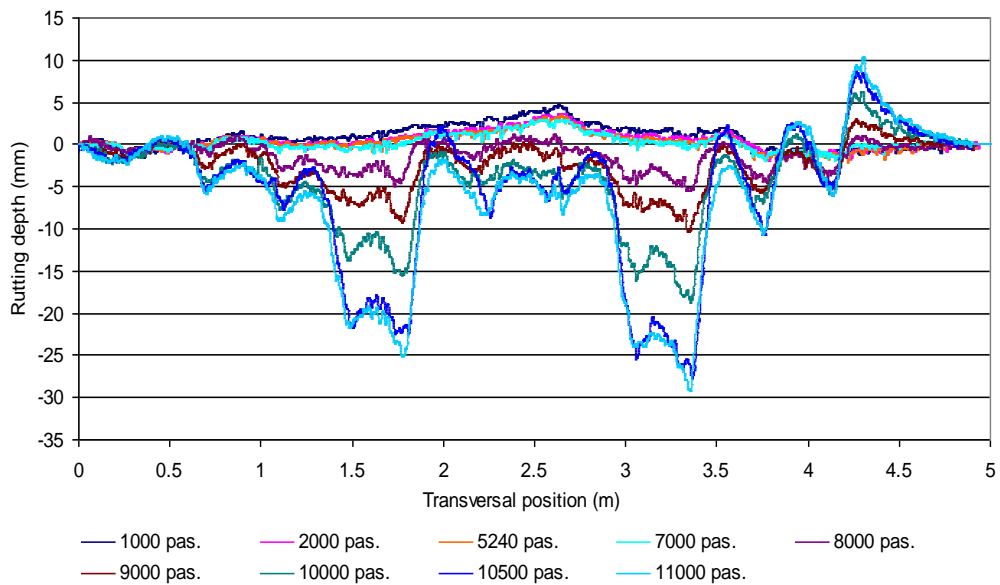


**Figure 50: Transversal rutting profiles measured on section B, profile P2, module M3, by means of the transverso-profilometer**

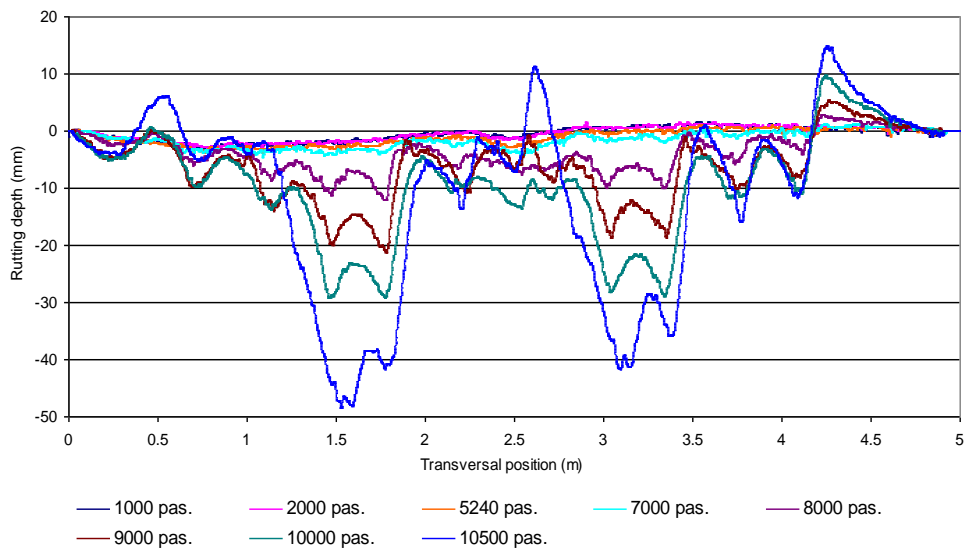


**Figure 51: Transversal rutting profiles measured on section G, profile P2, module M3, by means of the transverso-profilometer**

For the synthesis of the Appendix 16 evolution curves, divergent or spurious measurements among profiles P1 to P3 were ignored, and average validated values were used. Moreover a single curve has been set for sections B and E, as section E duplicate section B. This Figure 52 synthesis presents the maximal rutting depth reached at 11,000 passes on section A to section F, for the 4 load configurations.

For section G, this synthesis shown in Figure 53 was performed at 10,000 passes (maximum rutting 27 mm for configuration M3), and at the end of the simulator running (10,500 passes, maximal rutting 45 mm for configuration M3). For this section G, the magnitude of rutting, combined with its evolution curve with

traffic and development of cracking visible at the AC surface, suggest that the structural failure of the pavement is certainly initiated between 10,000 and 10,500 passes. Consequently only the rutting values at 10,000 passes will be considered for the further analysis. Moreover, it should be noted that rutting level higher than 25-30mm is not representative of real airfield pavement use, as maintenance works should certainly be done at a lower rutting depth level.

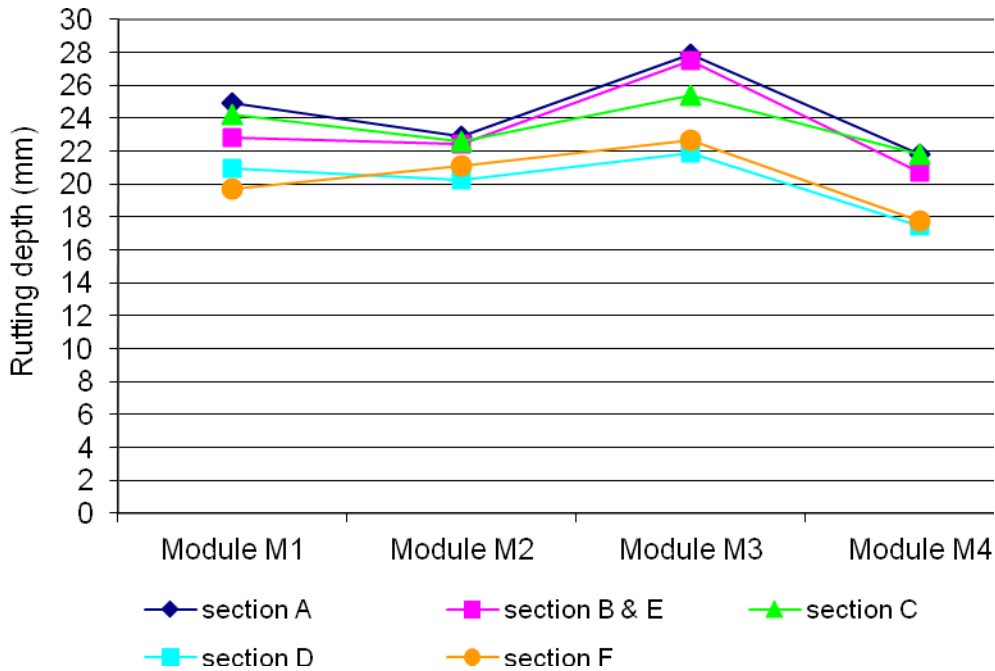


**Figure 52: Maximal rutting depth reached at 11,000 passes on section A to section F**

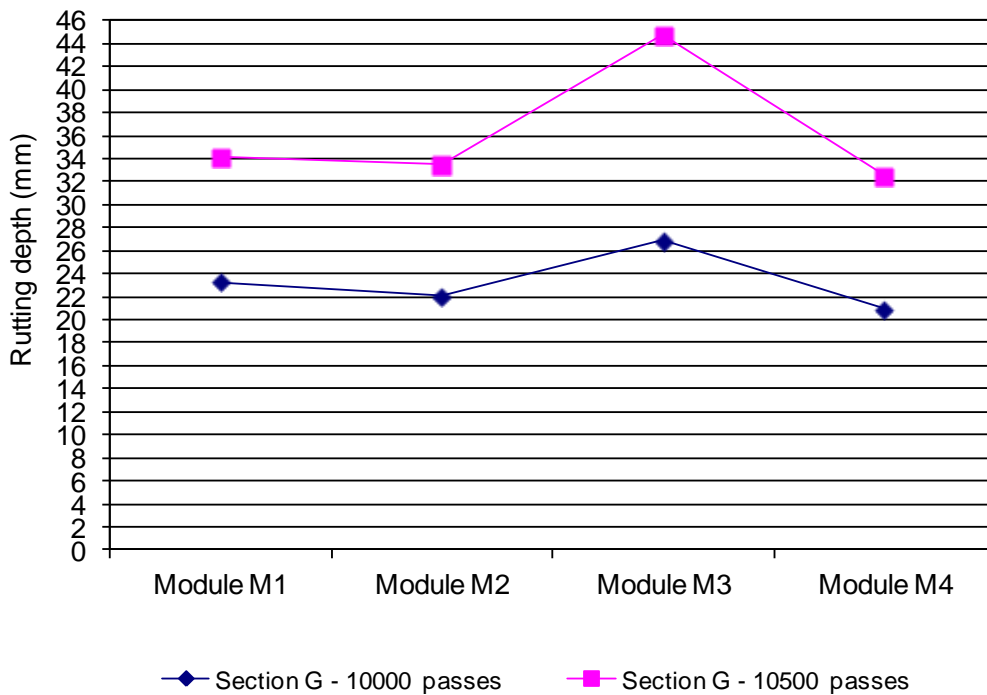


**Figure 53: Maximal rutting depth reached at 10,500 and 11,000 passes on section G**

The rutting depth synthesis is again presented in Table 18, which gives an evaluation of tire pressure and wheel-load effects on rutting.

**Table 18: Maximal rutting depth (in mm) reached at the end of the test and evaluation of tire pressure and wheel-load effects**

Section	Module	Module	Module	Module	Pressure effect		Wheel-load effect	
	M1 (mm)	M2 (mm)	M3 (mm)	M4 (mm)	M3 vs M2 @33.2t (Δ in mm)	M1 vs M4 @28.7t (Δ in mm)	M3 vs M1 @17.5bar (Δ in mm)	M2 vs M4 @15bar (Δ in mm)
<b>A</b>	24.9	22.9	27.9	21.8	5.0	3.1	3.0	1.1
<b>B - E</b>	22.9	22.4	27.5	20.7	5.1	2.2	4.6	1.7
<b>C</b>	24.2	22.6	25.4	21.8	2.8	2.4	1.2	0.8
<b>D</b>	20.9	20.2	21.9	17.5	1.7	3.5	1.0	2.7
<b>F</b>	19.7	21.1	22.6	17.8	1.5	1.9	2.9	3.3
<b>G at 10,000 passes</b>	23.2	22.0	26.9	20.9	4.9	2.3	3.7	1.1
<b>G at 10,500 passes</b>	34.1	33.5	44.7	32.5	11.2	1.6	10.6	1.0

Wheel-load effect is addressed by considering the differences in rut depth for both tire pressure of 15 and 17.5 bar at the two wheel-loads of 28.7t and 33.2t.

For a range of wheel-load from 28.7t to 33.2t, the wheel-load effect can be also determined by considering the difference between tire pressure effect at the higher wheel-load of 33.2t and tire pressure effect at the lowest wheel-load of 28.7t. In that case, wheel-load effect on rut depth from 28.7t to 33.2t for section A (6cm AC) is 1.9mm (i.e. 5.0mm-3.1mm). For section B-E (8cm AC), wheel-load effect is 2.9mm and 0.4mm for section C (12cm AC). These results can be also found by considering the differences between wheel-load effect at the highest tire pressure of 17.5 bar and the lowest tire pressure of 15 bar. These results remain valid for a range of wheel-loads from 28.7t to 33.2t and a tire pressure ranging from 15 to 17.5 bar. The change of wheel-load (greater than 33.2t or lower than 28.7t) with both tire pressure of 15 bar and 17.5 bar remaining unchanged will give different rut depth values, which corroborates that tire pressure effect must be considered with an associated wheel-load, both parameters being closely linked and cannot be described as isolated parameter but contribution of each parameter to rut depth development can be evaluated separately.

For section D (modified AC), tire pressure effect is lower for the highest wheel-load configuration, but the difference is close to the device measurement accuracy, and material behavior with regard to rutting is noticeably better and tends to reduce wheel-load and tire pressure effect compared to the other test sections.

Section F also appears to have performed better than section A, B, C and E but as opposed to section D, for which the result was expected and considering that section F is similar to section B and E with the exception of surface groove characteristics, this result is quite surprising. The grooving appears to improve the rutting behavior as per for the modified AC. As this finding is the opposite of the expected result, it will be investigated at a later stage.

As expected, rut depth on section G is higher compared to the other test sections; In that case, visco-plastic creeping at constant volume strain-path is more significant than other test sections.



## 5.4.2 Observation on sample caught from the section B and G

Before drawing the main conclusions from the rutting results presented in Figure 52, Figure 53 and Table 18, we present the observations made on samples taken from the bituminous layers of section B and G combined with the permanent vertical displacements measured by surface layer rutting sensors and anchored deflectometers.

At the end of the tests on August 16 and 17, 2010 core samples of 150 mm diameter were taken from sections B and G for a direct measurement of bituminous materials' thickness, to obtain information on the bonding quality of the interface between layers, and to perform Gamma bank tests in laboratory. For each load configuration, samples on structure B and G were taken in the wheel path giving the maximum rutting depth, and also on not-trafficked areas representing the initial thicknesses prior to traffic application. Other core samples were taken to survey the permanent deformation obtained with the surface layer rutting sensors, and two additional cores were made on section C

Resulting thickness data from these samples are crossed-checked with:

- Topographical level measurements made during the construction, which give the initial thickness of the different layers,
- Thickness variations between trafficked and not-trafficked paths, deduced from the compaction index given by the Gamma bank tests,
- Rutting depth of the surface AC layer measured by the surface layer rutting sensors (see paragraph 3.5.1 page 48),
- Total vertical displacements measured by total displacement anchored devices (see paragraph 3.5.4 page 50).

At the present date, neither the Gamma bank test nor the thickness measurement on core samples (which necessitates the interface un-bonding by means of oven heating at 100°C) have not been completely achieved. The next section shows these results for section B and for the section G, for M3 load configuration (33.2 tons at 17.5 MPa). The evaluation of the respective rutting of the different layers deduced from the combination of the topological, core sample and pavement instrumentation leads to the following trends:

### 5.4.2.1 Section B (standard surface AC 8cm on 12 cm base AC), load configuration M3 (33.3tons at 17.5 MPa):

- Total rutting depth : 28 mm
- Surface AC total rutting: 5 mm (initial thickness 8cm)
- Base AC total rutting : 8 mm (initial thickness 4+8 = 12 cm)
- Total AC concrete rutting 13 mm (initial thickness 20cm) resulting from post-compaction of 10 mm and visco-plastic creep of 3 mm.
- Unbound materials and soil total rutting : 15 mm

### 5.4.2.2 Section G (low performance rutting surface AC 8cm on 12 cm base AC), load configuration M3 (33.3tons at 17.5 MPa):

- Total rutting depth : 45 mm
- Surface AC total rutting: 8 mm (initial thickness 8cm)
- Base AC total rutting : 12 mm (initial thickness 4+8 = 12 cm)
- Total AC concrete rutting 20 mm (initial thickness 20cm)
- Unbound materials and soil total rutting : 25 mm

It should be pointed out that this first evaluation of the rutting distribution between the different layers still needs to be confirmed by continuing test and field post-survey investigations.

### 5.4.3 Main results drawn from rutting measurement and core samples

The main following observations are drawn from Figure 52, Figure 53 and Table 18:

The main test results are summarized as follows:

#### Rutting mechanism:

Development of permanent deformations increased with high AC temperatures. The tests confirmed that the speed of the rutting evolution significantly increased as the AC temperature exceeds the range 30-35°C, irrespective of the load configuration. Neither high tire pressure 1.75 MPa nor high wheel-load 33.2 tons changed this threshold value of rutting release.

From both the shape of the measured transversal rutting profiles and the compaction values of AC measured by Gamma bank tests at the end of the tests, we have deduced that the rutting mechanism is largely due to the post-compaction of the pavement material by traffic (bituminous material and untreated materials). There is an element of visco-thermoplastic creeping of AC layer characterized by constant volume strain-paths but not as much as the post-compaction.

Also it has been found that this permanent deformation not only affects the surface AC layer as anticipated, but also the whole thickness of the surface and base AC. In addition, rutting of the unbounded granular layer has been also observed. This permanent deformation of the unbounded materials is about the same as the rutting of surface and base AC material.

The interpretation of these results has still to be performed by means of numerical simulations of the test taking into account the real – and complex - pressure distribution applied by tire at the surface of the pavement, and also the visco-elastic behavior of the bituminous material. But it should be already considered that the permanent deformation of unbounded material is the consequence of the very low moving speed of the load. Rutting of these unbounded materials would certainly not have occurred with such amplitude in real taxiway trafficked with loads moving at usual taxiing speeds (more than about 30 km/h). In the present test at very low load speed, the rutting of UGA in fact largely resembles to the rutting mechanism of parking/apron more than runways or taxiways. It has been identified as follows: due to the visco-elastic behavior of AC, its resilient rigidity is considerably reduced by low frequency and high temperature situations, leading to high vertical stress in unbounded layer inducing significant rutting in this material.

### Wheel-load effect

The effect of wheel-load on rutting development is assessed by comparing modules M1 (28.7 tons) and M3 (33.3 tons) both inflated at 1.75 MPa, and modules M2 (33.3 tons) and M4 (28.7 tons) both inflated at 1.5 MPa.

Note: As test section G at 10500 passes has initiated structural failure, this section is only considered at 10 000 passes

At 1.75 MPa inflation pressure, weight increase from 28.7 tons to 33.3 tons leads to a growth in rutting between 5 % (+1 mm) and 20% (+4.6 mm).

At 1.5 MPa inflation pressure, weight increase from 28.7 tons to 33.3 tons leads to a growth in rutting between 4 % (+1 mm) and 19% (+3.3 mm).

As a first result, it should be noted that the impact of wheel weight on rutting depth remains relatively moderate. It completely invalidates the evaluation of permanent deformation by mean of a relationship which considers the weight value ratio to the exponent of 4.5 to 5, which would lead in the present case to a unrealistic growth in rating of +200%.

### Tire pressure effect

The effect of the tire pressure on the development of rutting is assessed by comparing modules M1 (1.75 MPa) and M4 (1.5 MPa) both loaded at 28.7 tons per wheel, and the modules M2 (1.5 MPa) and M3 (1.75 MPa) both loaded at 33.3 tons per wheel.

At a wheel-load of 33.3 tons, the tire pressure increase from 1.5 to 1.75 MPa leads to a growth in rutting between 7% (+2 mm) and 23% (+5 mm).

At a wheel-load of 28.7 tons, the tire pressure increase from 1.5 to 1.75 MPa leads to a growth in rutting between 10% (+2.2 mm) and 20% (+3 mm).

Similarly to weight effect, the impact of tire pressure on rutting can be considered as moderate. The results invalidates the evaluation of permanent deformation which considers the tire pressure ratio to the exponent of 4.5 to 5, which would also lead to a unrealistic growth in rating of +200%.

### Pavement material and structure characteristics influence on rutting

Rutting depths of section G using low rutting performance surface AC are obviously higher than the other six sections. On sections A to F, using standard or high performance Surface AC, rutting depths are closer: The difference in rutting varies only from 2.7mm (module M2) to 6 mm (module M3).

### Surface thickness effect of AC

The same standard surface AC in three different thicknesses (6 cm, 8 cm and 12 cm) is used in structures A, B, C and E. However, their rutting behaviour is quite similar, varying between 1 mm and 2 mm. This similarity may be explained by the fact that the rutting measured at the surface of the pavement is due not only by the permanent deformation of the surface AC, but also to the permanent deformations of AC base course and unbounded granular subbase. These layers and materials are identical in sections A, B, C and E.

### Effect of AC rutting performance and surface grooving

In comparison with the behaviour of sections A, B, C and E using standard Surface AC, the section D using high rutting performance surface AC (with modified bitumen) shows significantly lower rutting at the end of the test. The decrease in rutting varies from -2 mm (-10%) to -5 mm (-23%) according to the load moving path. The better performance is qualitatively in accordance with the prediction of the LPC laboratory rutting test. It is expected that further field and laboratory investigations will indicate whether this gain is only due the resistance of the modified surface AC, and/or lower permanent deformation of the other layers.

It is surprising that the behaviour of the grooved section F is so close to the section D, although it uses standard surface AC 8 cm thick as per sections B and E. Difference in rutting between these two sections is maximum 1mm. This gain in rutting performance for grooved AC is of interest for further investigations and/or airport survey since this technique is widely used on worldwide airfield pavement either on runway threshold or on the whole runway/taxiway length. (Note: grooving is initially used for lateral drainage improvement)

## 6 General conclusions and recommendations

### General conclusions:

High Tire Pressure Tests was performed to support the change of the limits used for the reporting of the maximum allowable tire pressure at an aerodrome (Annex 14 – *Aerodromes*, Volume I – *Aerodrome Design and Operations*, paragraph 2.6.6. c)

This new series of test was performed in addition of both the previous FAA/Boeing tests achieved in 2006, that already highlighted the need to review the current maximum allowable tire pressure and the FAA/Boeing high tire pressure test campaign performed in 2010.

The test consisted in the application of four dual wheel configurations on seven test sections representative of current airfield pavement by using the Airbus heavy traffic simulator. The seven pavement sections differed in their surface AC with regards to thickness (6, 8 and 12 cm) and their quality towards rutting (low, standard and high performance). The tested load configurations were a combination of two wheel-loads (28.7t and 33.2t) and two internal tire pressure inflation (1.5MPa and 1.75MPa). The test campaign was performed from October 2009 with test completion in August 2010. Total number of passes at completion was 11000.

### Representativeness of the HTPT programme:

The initial objectives of the HTPT program have been achieved, since significant rutting depths greater than 20-25 mm are observed after 11,000 loadings, without pavement structural failure. Test conditions, pavement structures and materials, building procedures and temperature were representative of actual in-service airfield pavement. It must be reminded that wheel-load and tire pressure have been selected to comply with current and future aircraft so that extrapolation will not be necessary in a foreseeable future as anticipated data are already considered in this study.

The primary objective of this full-scale test campaign was to exhibit whether the new proposed tire pressure limit for code letter X (1.75MPa) was a reasonable upper limit for typical pavements. This objective was successfully achieved and the experiment allowed additional lessons which could be of interest for further investigation on this topic.

The test results described and analyzed in Chapter 5 lead to the following conclusions:

- On Wheel-load and tire pressure effect: For a given wheel-load applied on pavement at a very low speed, the full-scale test campaign showed that rut depth differences ranged from 1.9mm (for the lowest wheel-load of 28.7t) to 5.1mm (for the heaviest wheel-load of 33.2t), showing that the contribution of the tire pressure (that is isolated from wheel-load effect) to rutting can be considered as very low. These results indicate clearly that an increase of tire pressure from 1.5MPa to 1.75MPa will not affect adversely neither surface and base AC layers, nor the structural capacity of the typical airfield pavement structure. Therefore pavement life duration will not be decreased as a consequence of increasing tire pressure. Wheel-load effect was identified as insignificant on surface and base AC, but more confined in unbounded material, therefore more related to the structural behavior of airfield pavement which is already considered in the ACN and the pavement thickness design method.
- On rutting mechanism: Rutting initiation is more related to mean AC temperature than traffic level or load parameters (wheel-load and internal tire pressure inflation). Indeed, the rutting appeared at the same time any considered wheel-load or tire pressure, and rut depth variation increased simultaneously with temperature independently of tire pressure. The prevailing rutting mechanism is the post compaction of the pavement material by traffic on both surface and base AC. The visco thermoplastic creeping of AC material is secondary to the post compaction with the exception of the

low rutting performance AC material which combines both failure modes on the same proportions. The core sampling performed after test completion showed that approximately half of the total rut depth is found on the unbounded materials. This unbounded material rutting is more sensitive to the higher wheel-loads confirming the prevailing wheel load effect on the deepest layers and therefore the relative low tire pressure effect on AC material. This experimental result will be subject of an additional study at a later stage by the mean of numerical modeling with detailed non-uniform tire footprint cartography to improve the rutting prediction modeling tool.

- On surface AC thickness effect: The test results showed no evidence on AC thickness effect. Rut depth appeared to be similar on the three different thicknesses (6, 8 and 12cm). Therefore surface AC thickness does not appear as a factor sensitive to tire pressure.
- On AC surface treatment surface: The rut depth on grooved section appeared to perform better than similar test sections without grooves. Its performances are close to those obtained with the modified bitumen section. This result is of interest for further investigation as it is the opposite of what was expected.
- On AC performance with regard to rutting behavior: The three different AC material specifications gave expected results. The modified AC performed better compared to the weakest AC material (sensitive to rutting). Post compaction is the prevailing rutting mode for modified and standard AC material whereas visco-thermoplastic creeping deformation has a more significant role in the weakest test sections which was designed with very high sensitivity to rutting.

#### Recommendations:

In light of the High Tire Pressure Test campaign, it has been established and substantiated that an increase of tire pressure from the current X category limit of 1.5MPa to an upper limit of 1.75MPa will not affect adversely neither surface and base AC materials nor the structural capacity of typical airfield pavement. Therefore such change could be ratified without putting aircraft or pavement at risk and would allow for the ICAO tire pressure limit codes to be formally and permanently changed to be more consistent with both the performance of real world pavement and the new aircraft generation.

The test outputs suggest that the observed rutting mechanism is closed to the A380 Pavement Experimental Programme (A380 PEP) findings. The prevailing post-compaction phenomenon on AC material so observed would lead to further considerations aiming at the optimization of mixing and compaction works. It is also recommended to further address the improvement of the post-compaction phenomenon in view of increasing the pavement life duration.

## Glossary

<b>French</b>	<b>English</b>
Alluvionnaire	Alluvial material
Bitume	Bitumen
Courbe theorique	Theoretical curve
Classe granulaire	Granular class
Compacité	Compactness
Compacteur à pneumatiques	Compactor with wheels
Compacteur vibrant	Vibrating roller
Concassé	Crushed material
Coupure	Gradation cut-off
Cycles	Cycles
Déformation	Deformation
Ecart absolu	Difference with theoretical value
Ecart type	Standard deviation
Enrobés bitumineux	Asphalt material
Epaisseur	Thickness
Essai de fatigue	Flex fatigue test ou fatigue test with alternate bending
Essai de traction directe	Direct tensile test
Essai d'orniérage	Rutting test
Essai duriez	Duriez test
Essai module complexe	Determination of the dynamic bending modulus test
Essai pcg	Compaction with gyratory shear press test
Filler calcaire	Limestone filler
Formule	Formula
Girations	Gyration
Liant hydrocarboné	Binder
Maximum	Maximum value

Minimum	Minimum value
Module	Modulus
Module de richesse	Richness modulus
Moyenne	Average value
Moyenne	Average value
Mva	Bulk density
Mvre	Real density of asphalt material
Mvrg	Real density of aggregates in paraffin test
Passants	Passing fraction
Pourcentage	Percentage
Rc à l'eau	Bulk compressive strength
Rc à sec	Dry compressive strength
Siliceux	Siliceous material
Surface spécifique	Specific surface area
Tamis	Screen, sieve
Temperature à la livraison	Delivery temperature

Unit conversion:

15 bar = 1.5 MPa = 218 PSI


17.5 bar = 1.75 MPa = 254 PSI

28.7t = 63.3 KLbs

33.2t = 73.2 KLbs



**Appendix 1. Untreated gravel material (sub-base and capping layer) specification**



**SABLIERES MALET**  
27, Avenue de Palarin  
31120 PORTET sur GARONNE

**Fiche Technique**  
**- SEPT 2008 / 01**  
Engagement du 24/09/2008 au 23/03/2009

Page 1/1

---

**GRAVE 0/20 C - Code 41 SMP**

---

**Péetrographie :** Alluvionnaire - Siliceux  
**Elaboration :** Concassé  
**Site de production :** PORTET SUR GARONNE  
**MARQUAGE CE :** NIVEAU 2 / N° CERTIFICATION 0333 / CFD 941006

**ATTENTION !** Ce document est la propriété du producteur et ne peut être reproduit sans son autorisation.

---

**Partie normative**  
*Valeurs spécifiées sur lesquelles le producteur s'engage*

**Classe granulaire**

0	20
---	----

**Norme**

XPP 18-545 Art 7 - EN 12242 - Chaussées - Couches de fondation, base et liaison

**Spécification**

CODE Ba Ang 3

---

	Partie normative													MB	LA	LA+MDE	MDE
	0.063	0.125	0.25	0.5	1	2	4	6.3	10	20	28	40					
Incertitude U	1								3	2	1	0	0.5	3	3	3	
V.S.S. +U	9.0								81	100	100	100	2.50	23.00	38.0		
V.S.S.	8.0								78	99	100	100	2.00	20.00	35.0		
V.S.I.	2.0								58	85	98	100					
V.S.I.-U	1.0								55	83	97	100					
Ecart-type max									6.06								

---

**Partie informative**  
**Résultats de production**

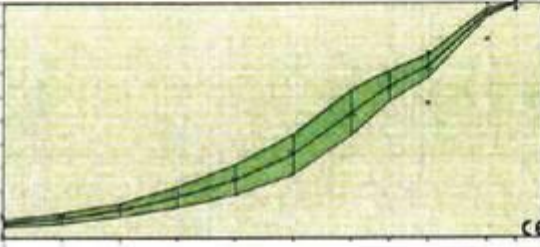
du 01/10/07 au 22/08/08

	0.063	0.125	0.25	0.5	1	2	4	6.3	10	20	28	40	MB	LA	LA+MDE	MDE
Maximum	8.0	12	17	24	33	45	66	74	78	98	100	100	0.75			
Moyenne XI	7.6	10	15	22	31	44	63	71	78	96	100	100	0.70			
Moyenne XI	6.1	8	12	17	25	35	53	65	73	95	100	100	0.54	20.00	31.0	11.00
Minimum	4.6	6	9	13	18	27	44	58	68	94	100	100	0.38			
Minimum	3.2	5	7	10	13	20	37	55	64	93	100	100	0.25			
Ecart-type	1.20	1.7	2.3	3.5	5.1	6.9	7.8	5.3	3.9	1.4	0.0	0.0	0.130			
Nombre de résultats	27	27	27	27	27	27	27	27	27	27	27	27	27	1	1	1

du 05/03/08 au 05/03/08

	0.063	0.125	0.25	0.5	1	2	4	6.3	10	20	28	40	MB	LA	LA+MDE	MDE
Maximum	8.0	12	17	24	33	45	66	74	78	98	100	100	0.75			
Moyenne XI	7.6	10	15	22	31	44	63	71	78	96	100	100	0.70			
Moyenne XI	6.1	8	12	17	25	35	53	65	73	95	100	100	0.54	20.00	31.0	11.00
Minimum	4.6	6	9	13	18	27	44	58	68	94	100	100	0.38			
Minimum	3.2	5	7	10	13	20	37	55	64	93	100	100	0.25			
Ecart-type	1.20	1.7	2.3	3.5	5.1	6.9	7.8	5.3	3.9	1.4	0.0	0.0	0.130			
Nombre de résultats	27	27	27	27	27	27	27	27	27	27	27	27	27	1	1	1

---



Norme : EN 12242  
 Type : C402  
 Niveau : N° 2  
 Matière : 2.210 g/cm³  
 Matière : Max 40%  
 Matière : Min 1%

© AIRBUS S.A.S. 2009. ALL RIGHTS RESERVED. CONFIDENTIAL AND PROPRIETARY DOCUMENT.

Page 79 of 115

**Appendix 2. Untreated gravel material control by sieving**

D\_Labo - 00-00-56 / 03

<p><b>GRAVES NON TRAITÉES</b> <b>NF EN 13285</b> <b>Analyse granulométrique par tamisage</b> <b>NF EN 933-1</b> <b>Rapport d'essai</b></p>		<p><b>CHANTIER</b> PISTE EXPERIMENTALE AIRBUS N° Chantier 1040612</p>																																																																													
<p><b>ENTREPRISE MALET</b> <b>LABORATOIRE</b> 30, Avenue de Larrieu-31081 TOULOUSE Cedex Tél. : 05.34.60.82.00 Fax: 05.34.60.82.01</p>		<p>DEMANDEUR / AGENCE Malet Toulouse sud-Mr FOIN. Date du prélèvement 22-janv.-09</p>																																																																													
<p>Provenance MALET Portet-sur-Garonne Date d'essais 22-janv.-09</p>		<p>PROVENANCE MALET Portet-sur-Garonne Date d'essais 22-janv.-09</p>																																																																													
<p>Fuseau de spécification</p>		<p>GRANULARITE TYPE DE GNT 0 / 20 B</p>																																																																													
<p>Analyse granulométrique</p>		<p>Analyse granulométrique NF EN 933-1</p>																																																																													
		<table border="1"> <thead> <tr> <th>Tamis</th> <th>Mini</th> <th>Maxi</th> <th>%passants</th> </tr> </thead> <tbody> <tr><td>125</td><td></td><td></td><td>100</td></tr> <tr><td>90</td><td></td><td></td><td>100</td></tr> <tr><td>80</td><td></td><td></td><td>100</td></tr> <tr><td>63</td><td></td><td></td><td>100</td></tr> <tr><td>56</td><td></td><td></td><td>100</td></tr> <tr><td>45</td><td></td><td></td><td>100</td></tr> <tr><td>40</td><td></td><td></td><td>100</td></tr> <tr><td>31,5</td><td></td><td></td><td>100</td></tr> <tr><td>20</td><td>85</td><td>99</td><td>96</td></tr> <tr><td>16</td><td></td><td></td><td>89</td></tr> <tr><td>10</td><td>55</td><td>85</td><td>66</td></tr> <tr><td>8</td><td></td><td></td><td>60</td></tr> <tr><td>6,3</td><td></td><td></td><td>57</td></tr> <tr><td>4</td><td>35</td><td>65</td><td>54</td></tr> <tr><td>2</td><td>22</td><td>50</td><td>34</td></tr> <tr><td>1</td><td>15</td><td>40</td><td>24</td></tr> <tr><td>0,500</td><td>10</td><td>35</td><td>17</td></tr> <tr><td>0,063</td><td>4</td><td>9</td><td>6,9</td></tr> </tbody> </table>		Tamis	Mini	Maxi	%passants	125			100	90			100	80			100	63			100	56			100	45			100	40			100	31,5			100	20	85	99	96	16			89	10	55	85	66	8			60	6,3			57	4	35	65	54	2	22	50	34	1	15	40	24	0,500	10	35	17	0,063	4	9	6,9
Tamis	Mini	Maxi	%passants																																																																												
125			100																																																																												
90			100																																																																												
80			100																																																																												
63			100																																																																												
56			100																																																																												
45			100																																																																												
40			100																																																																												
31,5			100																																																																												
20	85	99	96																																																																												
16			89																																																																												
10	55	85	66																																																																												
8			60																																																																												
6,3			57																																																																												
4	35	65	54																																																																												
2	22	50	34																																																																												
1	15	40	24																																																																												
0,500	10	35	17																																																																												
0,063	4	9	6,9																																																																												
<p>Numéro d'échantillon 70/1040612/01/09</p>		<p>Catégorie NF EN 13242</p>																																																																													
<p>SE NF EN 933-8 60</p>		<p>MB NF EN 933-9 0,8</p>																																																																													
<p>MB XP P 18-545 0,26</p>		<p>MB NF EN 933-1 6,9</p>																																																																													
<p>Spécifications Le technicien. CAPERAN C.</p>		<p>W%EXT. NF EN 1097-5 4,1%</p>																																																																													
<p>Le responsable. CAUBET J.</p>		<p>Commentaires CONFORME</p>																																																																													

## Appendix 3. EB14-GB Class 3 Base product specifications



ENROBÉS-TOULOUSE

3842

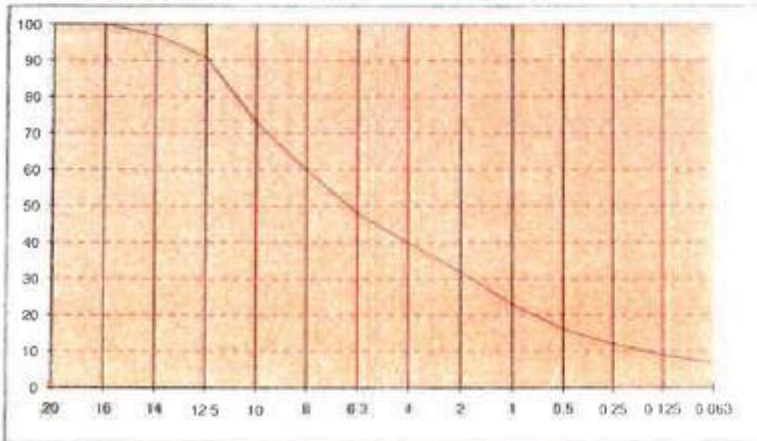
### FICHE DE SYNTHESE

#### POSTES NORD & SUD

Formule n°53 EB 14 assise 35/50 (GBE 0/14 c13) NF EN 13108-1

DATE DE L'ETUDE : 29/11/2006

COUPURES	FORMULE	PROVENANCES	CARACTERISTIQUES DE LA FORMULE	
0/21 alluvion. Code a Ang 1	28.7%	GARONNE/ARIEGE	M.V.R.g. (kg/m <sup>3</sup> )	2680
2/6 cl alluvion. Code BIII Ang 1	15.3%	GARONNE/ARIEGE	M.V.R.E. (kg/m <sup>3</sup> )	2500
6/10 cl alluvion. Code BIII Ang 1	22.0%	GARONNE	Surface Spécifique (m <sup>2</sup> /kg)	12.12
10/14 cl alluvion. Code BIII Ang 1	26.7%	GARONNE	Module de richesse K	2.92
Filler Calcaire	2.8%	La Provençale	*pourcentages indicatifs qui pourront être modifiés pour respecter la courbe granulométrique de l'étude	
Liant hydrocarboné	4.50%	Bitume 35/50		



# Tamis	% Passants
20	100
16	100
14	97.0
12.5	91.0
10	73.0
8	60.0
6.3	48.0
4	40.0
2	32.0
1	23.0
0.5	16.0
0.25	12.0
0.125	9.0
0.063	6.7

#### CARACTERISTIQUES MECANQUES DE L'ENROBE

ESSAI DURIEZ		Spécif	ESSAI P.C.G.		Spécif	ESSAI D'ORNIERAGE		Spécif
M.V.A. (kg/m <sup>3</sup> )	2344		10 girations	14.4	> 14	1000 cycles	2.8	
Compacité (%)	93.8		25 girations	10.8		3000 cycles	3.6	
Rc à sec (Mpa)	11.4		40 girations	9.0		10000 cycles	4.4	≤ 10
rc à l'eau (Mpa)	10.4		80 girations	6.5		30000 cycles	5.3	
rc/Rc	0.91	≥ 0.70	200 girations	3.7		% vides	8.5	

ESSAI MODULE COMPLEXE	Spécif	ESSAI TRACTION DIRECTE	Spécif	ESSAI DE FATIGUE	Spécif
Module à 15°C		Module à 15°C	≥ 9000 Mpa	Déformation	

#### OBSERVATIONS

Cette formule peut contenir jusqu'à 10% d'agrégats d'enrobés de classe c.

#### UTILISATION

<b>Domaine d'emploi:</b>	Couches d'assises, de base sous tous trafics. Peut servir PROVISoireMENT de couche de roulement.		
<b>Etat du support:</b>	Température mini de 5°C		
<b>Mise en œuvre:</b>	Epaisseur 10 à 15 cm	Température à la livraison 150°C	Observations
<b>Compactage:</b>	Compacteur à pneumatiques	Compacteur vibrant	

## Appendix 4. EB14-GB Class 3 Base control



**PROCES VERBAL D'ESSAIS SUR ENROBES BITUMINEUX**

N° AFFAIRE:  N° DE PV: **Fab 001**

ITINERAIRE CONCERNE: Planche expérimentale A350 SECTEUR:  
POLE:

DEMANDEUR: AIRBUS

Essais réalisés: Extraction de liant et détermination du module de richesse  
(Méthode asphaltanalyator:IEH 08)

Type de mélange hydrocarboné: **EB 14 assise 35/50** Norme de référence:

Centrale d'enrobage: ENROBES TOULOUSE Poste nord  
Entreprise de mise en œuvre: MALET

FORMULATION DE L'ENROBE: 53

CONSTITUANTS	PRODUCTEUR	POURCENTAGE(%)			
		Fétude*	Fa	Fb	Fc
.0 / 2	Garonne/Ariege	28,70%			
.2 / 6	Garonne/Ariege	15,30%			
.6 / 10	GARONNE	22,00%			
.10/14	GARONNE	26,70%			
Filler d'apport	LA Provencale	2,80%			
Bitume	35/50	4,50%			

\* Formulation définie au moment de l'étude(Fa,Fb,Fc:formules ajustées en cours de chantier)

COUCHE DE:

MVRE(T/m3)	2,500
MVRG(T/m3)	2,680
Module de richesse(K) Ext	
Module de richesse(K) Int	2,92

ECHANTILLONS PRELEVES SUR CHANTIER					
	N°1	N°2	N°3	N°4	N°5
MODE DE PRELEVEMENT: P:poche C:carotte	P	P	P	P	P
OPERATEUR:	Dega	Dega	Lavergne	Lavergne	Lavergne
ITINERAIRE					
PR OU PK					
DAIES	04-févr.	04-févr.	05-févr.	05-févr.	06-févr.
HEURES	9h30	14h00	11h15	14h00	9h40
T° DU PRELEVEMENT:	154°C	150°C	170°C	156°C	150°C
CONDITIONS METEOROLOGIQUES: NC:non conforme C:conforme	C	C	C	C	C
OBSERVATIONS					

Centre d'Études  
Techniques  
de l'Équipement  
du Sud-Ouest



Laboratoire  
Regional  
des Ponts  
et Chaussées  
de Toulouse

Unité LNEC



Complexe Scientifique  
de Rangueil  
1 avenue de Colonel Roche  
31400 Toulouse  
téléphone :  
05 62 25 97 92  
télécopie :  
05 62 25 97 98  
mail : dl.cete-so  
@equipement.gouv.fr

Unité Technique L.N.E.C. - Contrôles Chaudières

## MELANGES HYDROCARBONES

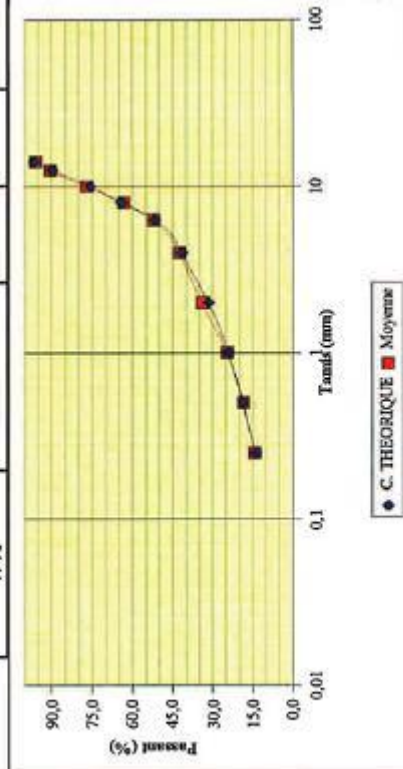
Résultats d'essais (Code : IEH08 )

N° Procès Verbal : **Fab 001**  
 N° Affaire : **0**  
 TYPE D'ENROBES : **EB 14 assise 35/50**  
 Couches de : **Base**

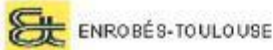
Tamis (mm)	Numéro d'échantillon										Ecart Absolu	Conformité	
	N°1	N°2	N°3	N°4	N°5	Moyenne	Specifications Min.	Specifications Max.					
16													
14	95,1	96,5	97,8	94,9	95,7	96,0	-0,51						
12,5	89,5	90,0	93,5	90,2	89,6	90,6	0,75						
10	74,6	76,9	79,5	78,6	74,7	76,8	1,03						
8	59,6	64,5	64,2	65,7	61,5	63,1	-0,99						
6,3	49,6	53,3	52,9	53,8	51,1	52,1	0,55						
4	40,6	43,7	42,8	43,7	41,8	42,5	0,92						
2	33,0	34,6	34,0	34,8	33,4	34,0	2,46						
1	24,6	24,4	24,6	24,8	24,3	24,5	0,44						
0,5	18,8	17,9	18,5	18,6	18,5	18,5	-0,27						
0,250	13,9	13,6	13,9	14,2	14,2	14,2	0,28						
0,063	6,9	8,0	8,3	8,6	8,2	8,6	1,66						
% Bitume Int	<b>3,94%</b>	<b>4,87%</b>	<b>4,42%</b>	<b>4,70%</b>	<b>4,44%</b>	<b>4,48%</b>	<b>0,00</b>						
K ( Int )	2,29	2,92	2,63	2,78	2,65	2,65	-0,27						
W%													

Observations sur la fabrication

Toulouse le,



## Appendix 5. EB14-GB Class 4 Base product specifications



42/42

### FICHE DE SYNTHÈSE

#### POSTES NORD & SUD

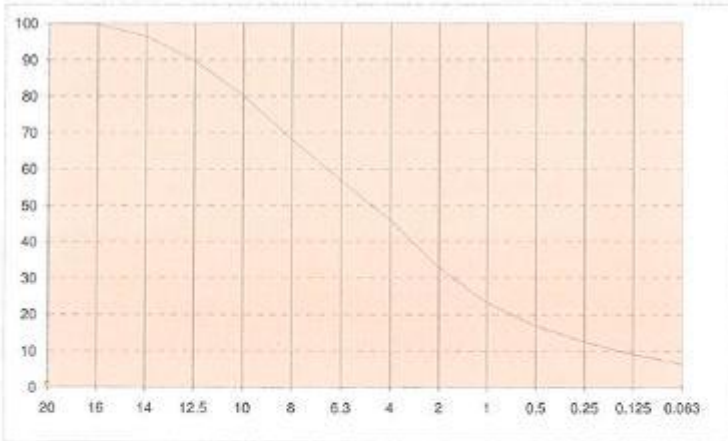
Formule n° 59 EB 14 assise 35/50 (GBE 0/14 cl4) NF EN 13108-1

DATE DE L'ETUDE : 26/10/2006

COUPURES	FORMULE	PROVENANCES
0/2f alluvion. Code a Ang1	30.5%	GARONNE/ARIEGE
2/6 cl alluvion. Code BIII Ang 1	22.9%	GARONNE/ARIEGE
6/10 cl alluvion. Code BIII Ang 1	20.0%	GARONNE
10/14 cl alluvion. Code BIII Ang 1	20.0%	GARONNE
Filler Calcaire	1.9%	La Provençale
Liant hydrocarboné	4.70%	Bitume 35/50

CARACTERISTIQUES DE LA FORMULE	
M.V.R.g. (kg/m <sup>3</sup> )	2695
M.V.R.E. (kg/m <sup>3</sup> )	2506
Surface Spécifique (m <sup>2</sup> /kg)	11.73
Module de richesse K	3.05

\* pourcentages indicatifs qui pourront être modifiés pour respecter la courbe granulométrique de référence.



# Tamis	% Passants
20	100
16	99.7
14	96.4
12.5	89.8
10	80.1
8	68.0
6.3	56.8
4	45.9
2	32.9
1	23.2
0.5	16.9
0.25	12.5
0.125	9.0
0.063	6.4

#### CARACTERISTIQUES MECANQUES DE L'ENROBE

ESSAI DURIEZ	Spécif	ESSAI P.C.G.	Spécif	ESSAI D'ORNIERAGE	Spécif
M.V.A. (kg/m <sup>3</sup> )	2305	10 girations	14.2	1000 cycles	1.6
Compacité (%)	92.0	25 girations	10.9	3000 cycles	1.7
Rc à sec (Mpa)	7.3	40 girations	9.2	10000 cycles	2.1
rc à l'eau (Mpa)	5.7	80 girations	6.9	30000 cycles	2.4
rc/Rc	0.78	200 girations	4.2	% vides	8.0

ESSAI MODULE COMPLEXE	Spécif	ESSAI TRACTION DIRECTE	Spécif	ESSAI DE FATIGUE	Spécif
Module à 15°C		Module à 15°C	14068	≥ 11000 Mpa	Déformation

#### OBSERVATIONS

Cette formule peut contenir jusqu'à 10% d'agrégats d'enrobés de classe c.

#### UTILISATION

<b>Domaine d'emploi:</b>	Couches d'assises, de base sous tous trafics. Peut servir PROVISOIREMENT de couche de roulement.		
<b>Etat du support:</b>	Température mini de 5°C		
<b>Mise en œuvre:</b>	Epaisseur	Température à la livraison	Observations
	8 à 15 cm	150°C	
<b>Compactage:</b>	Compacteur à pneumatiques	Compacteur vibrant	

		41/42
Année d'apposition du marquage : 08 N° identification de l'organisme notifié : 0333 N° certificat : 0333-CPD-420100		
<b>EN 13108-1</b>		
<b>Enrobés bitumineux pour routes et autres zones de circulation</b>		
<b>ENROBES-TOULOUSE</b>		
3 CHEMIN DE COTE GOUBARD - 31270 VILLENEUVE-TOLOSANE Tél : 05.61.72.05.08 Fax : 05.61.72.12.96		
<b>POSTES NORD &amp; SUD</b>		
<b>59</b>	GB 0/14 c14 <b>EB 14 assise 35/50 et EB 14 assise 35/50 à 10% d'agrégats d'enrobés (1)</b>	
<u>Exigences générales et fondamentales</u>		
<b>P.C.G.</b>		
— Pourcentage minimal de vides		V <sub>minBR</sub> %
— Pourcentage maximal de vides		V <sub>max0</sub> %
— Pourcentage minimal de vides remplis par le bitume		APD %
— Pourcentage maximal de vides remplis par le bitume		APD %
<b>Tenue à l'eau</b>		
— Sensibilité à l'eau		ITSR <sub>20</sub> %
<b>Résistance à l'abrasion par pneumatiques à crampons</b>		APD -
<b>Comportement au feu</b>		APD -
<b>Température du mélange</b>		150 à 190 °C
<b>Granularité : passant au tamis de :</b>		
	20 mm	100 %
	16 mm	100 %
	14 mm	96 %
	12.5 mm	90 %
	10 mm	80 %
	8 mm	68 %
	6.3 mm	57 %
	4 mm	46 %
	2 mm	33 %
	1 mm	23 %
	0.5 mm	17 %
	0.250 mm	13 %
	0.1 mm	9 %
	0.1 mm	6.4 %
<b>Teneur en liant</b>		TL 4.7 %
<b>Résistance aux déformations permanentes (orniérage)</b>		
— grand modèle : pourcentage de profondeur d'ornièr		P <sub>10</sub> %
— petit modèle : pente d'orniérage		APD mm
— petit modèle : pourcentage de profondeur d'ornièr		APD %
<b>Caractéristiques fondamentales</b>		
<b>Module de rigidité</b>		S <sub>min11000</sub> Mpa
<b>Fatigue</b>		E <sub>FAI</sub> pdef
<b>Substances dangereuses</b>		Valeurs seuils en vigueur sur le lieu d'utilisation : ces enrobés ne contiennent pas de substances dangereuses au sens de la réglementation applicable en France à la date de la rédaction du présent document.

(1) : La formulation de cet enrobé comporte au plus 10% d'agrégats d'enrobé. La circulaire des Ministères de l'Aménagement du Territoire et de l'Environnement (MATE) et du Ministère de l'Équipement des transports et du Logement (METL) n° 2001-39 du 18 juin 2001 indique qu'il n'y a aucun inconvénient technique à réutiliser, dans la limite de 10% des agrégats d'enrobés. Dans ce cas, elle autorise à ne pas effectuer les études de caractérisation des agrégats et de formulation de cet enrobé. Cette règle est applicable pour tous les enrobés exceptés les cas d'application suivants :

- ▶ bétons bitumineux semi-grenus en couche de roulement sous trafic > T1
- ▶ bétons bitumineux minces en couche de roulement sous trafic > T3

## Appendix 6. EB14-GB Class 4 Base control



**PROCÈS VERBAL D'ESSAIS SUR ENROBES BITUMEUX**

N° AFFAIRE:  N° DE PV: **Fab 003**

ITINERAIRE CONCERNE: **Planche expérimentale A350 n°2**

DEMANDEUR: **AIRBUS**

Essais réalisés: Extraction de liant et détermination du module de richesse  
(Méthode asphaltoanalyser: IIEH 08)

Type de mélange hydrocarboné: **EB 14 assise 35/50** Norme de référence: **NF EN 13108-1**  
**GB 0/14 c14**

Centrale d'enrobage: **ENROBES TOULOUSE** Poste sud  
Entreprise de mise en œuvre: **MALET**

FORMULATION DE L'ENROBE: **59**

Centre d'Études  
Techniques  
de l'Équipement  
du Sud-Ouest



Laboratoire  
Régional  
des Ponts  
et Chaussées  
de Toulouse

Unité SISEC

CONSTITUANTS	PRODUCTEUR	POURCENTAGE(%)			
		Fétude*	Fa	Fb	Fc
.0 / 2	Garonne/Ariege	30,50%			
.2 / 6	Garonne/Ariege	22,90%			
.6 / 10	GARONNE	20,00%			
.10/14	GARONNE	20,00%			
Filler d'apport	LA Provencale	1,90%			
Bitume	35/50	4,70%			

\* Formulation définie au moment de l'étude(Fa,Fb,Fc:formules ajustées en cours de chantier)

COUCHE DE: **Fondation / Base**

MVRE(T/m3)	<b>2,506</b>
MVRG(T/m3)	<b>2,695</b>
Module de richesse(K) Ext	
Module de richesse(K) Int	<b>3,05</b>



Complexe Scientifique  
de Rangueil  
1 avenue de Colonel Roche  
31400 Toulouse  
téléphone :  
05 62 25 97 97  
télécopie :  
05 62 25 97 98  
mél : dl.cete-ss  
@equipement.gouv.fr

ECHANTILLONS PRELEVES SUR CHANTIER					
	N°1	N°2	N°3	N°4	N°5
MODE DE PRELEVEMENT: P:poche C:carotte	P	P	P	P	P
OPERATEUR:	J AZAM	J AZAM	J AZAM	J AZAM	G Castille
ITINERAIRE					
PR OU PK	1ère couche			2ème couche	
DATES	03-sept.	03-sept.	04-sept.	04-sept.	04-sept.
HEURES	10h00	14h00	10h	11h30	15h00
T° DU PRELEVEMENT:	160°C	152°C	155°C	165°C	
CONDITIONS METEOROLOGIQUES: NC:non conforme C:conforme	C	C	Petite pluie	C	C
OBSERVATIONS					



Unité Technique L.N.E.C. - Contrôles Châssis

## MELANGES HYDROCARBONES

Résultats d'essais (Code :IEH08 )

N° Procès Verbal :

N° Affaire:

TYPE D'ENROBES:

Fab 003

0

EB 14 assiste 35/50

Couche de :

Fondation / Base

Tamis (mm)	C. THEORIQUE (% passant)	N° de tamis					Moyenne	Ecart Absolu	Spécifications Min. / Max.	Conformité
		N°1	N°2	N°3	N°4	N°5				
16	99,7	100,0					100,0	0,30		
14	96,4	97,7	97,2	98,6	96,0	98,6	97,6	1,23		
12,5	89,8	93,5	93,7	93,1	90,6	94,0	93,0	3,17		
10	80,1	82,9	81,3	80,4	76,4	83,9	81,0	0,91		
8	68,0	72,7	69,1	69,6	61,6	72,2	69,0	1,04		
6,3	56,8	64,8	58,6	59,7	51,7	62,3	59,4	2,61		
4	45,9	52,7	46,1	48,2	39,1	50,1	47,2	1,35		
2	32,9	40,8	35,1	37,5	29,9	36,6	36,0	3,07		
1	23,2	28,9	24,6	26,5	21,0	25,1	25,2	2,03		
0,5	16,9	21,1	17,6	18,7	15,0	17,9	18,1	1,15		
0,250	12,5	15,7	12,9	12,8	11,1	13,5	13,2	0,69		
0,063	6,4	8,6	7,1	6,4	6,2	7,6	7,2	0,79		
% Blume Int	4,70%	5,02%	4,66%	4,60%	4,53%	4,93%	4,79%	0,00		
K ( Int)	3,05	2,97	2,98	2,87	2,85	2,99	2,93	-0,12		
W%										

Observations sur la fabrication

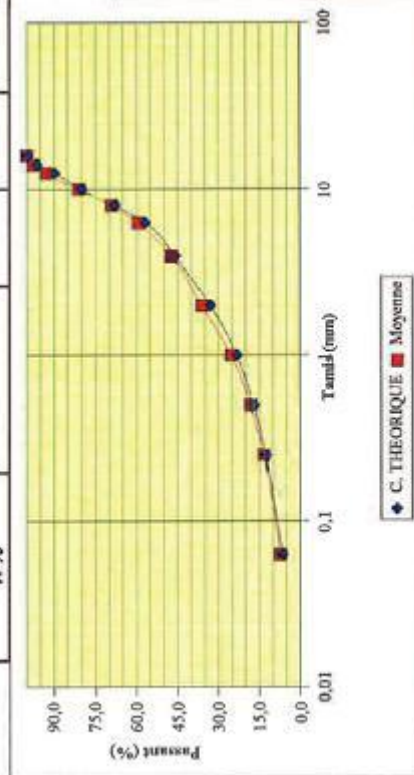
Résultats convenables dans les limites de la tolérance

Toulouse le 7 SEP. 2009  
Liamo noirs - enrobés chimie

Jean-Christophe FABRE  
Ingénieur-Docteur

Le chargé de Programme de Contrôle

Jean-Christophe FABRE



## Appendix 7. Sections A,B,C,E and F asphalt material (EB14-BBA C Class 3 Surface) specifications



ENROBÉS-TOULOUSE

32/42

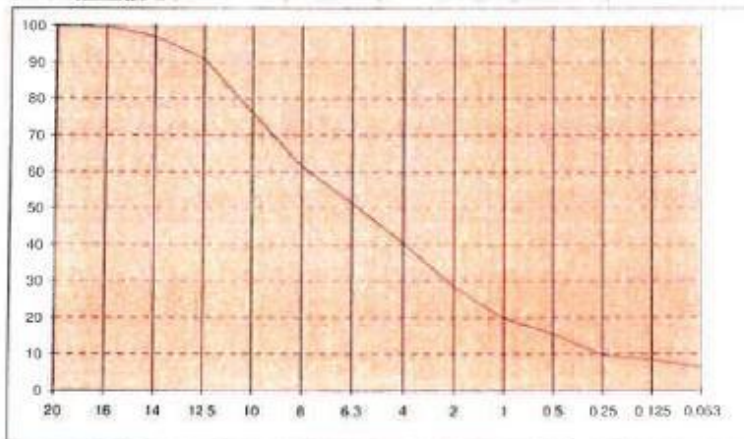
### FICHE DE SYNTHESE

POSTES NORD & SUD

Formule n° 43 EB 14 rou/lat 35/50 (BBA C 0/14 c13) NF EN 13108-1

DATE DE L'ETUDE : 05/07/2005

COUPURES	FORMULE	PROVENANCES	CARACTERISTIQUES DE LA FORMULE	
0/2l alluvion. Code a Ang1	25.6%	GARONNE/ARIEGE	M.V.R.g. (kg/m <sup>3</sup> )	2707
2/6 cl alluvion. Code BIII Ang 1	20.8%	GARONNE/ARIEGE	M.V.R.E. (kg/m <sup>3</sup> )	2492
6/10 cl alluvion. Code BIII Ang 1	24.6%	GARONNE	Surface Spécifique (m <sup>2</sup> /kg)	11.09
10/14 cl alluvion. Code BIII Ang 1	21.8%	GARONNE	Module de richesse K	3.53
Filler Calcaire	1.9%	La Provençale	* pourcentages indiqués qui pourront être modifiés pour respecter la courbe granulométrique de l'étude	
Liant hydrocarboné	5.30%	Bitume 35/50		



# Tamis	% Passants
20	100
16	99.7
14	97.1
12.5	90.9
10	76.2
8	61.6
6.3	51.4
4	40.4
2	28.4
1	19.8
0.5	15.4
0.25	9.8
0.125	8.3
0.063	6.3

CARACTERISTIQUES MECANQUES DE L'ENROBE					
ESSAI DURIEZ	Spécif	ESSAI P.C.G.	Spécif	ESSAI D'ORNIERAGE	Spécif
M.V.A. (kg/m <sup>3</sup> )	2362	10 girations	14.6	1000 cycles	4.2
Compacité (%)	94.8	25 girations	11.1	3000 cycles	5.2
Rc à sec (Mpa)	12.46	40 girations	9.3	10000 cycles	6.4
rc à l'eau (Mpa)	11.26	80 girations	6.7	30000 cycles	7.7
rc/Rc	0.90	200 girations	3.3	% vides	7.0

ESSAI MODULE COMPLEXE	Spécif	ESSAI TRACTION DIRECTE	Spécif	ESSAI DE FATIGUE	Spécif
Module à 15°C	11951 Mpa	Module à 15°C		Déformation	

### OBSERVATIONS

Cette formule peut contenir jusqu'à 10% d'agrégats d'enrobés de classe c.

### UTILISATION

<b>Domaine d'emploi:</b>	Couches de roulement et de liaison sur chaussées aéronautiques		
<b>Etat du support:</b>	Support dont les déformations n'excèdent pas 2 cm sous la règle de 3 m. Température mini de 5°C		
<b>Mise en œuvre:</b>	Epaisseur 7 à 9 cm	Température à la livraison 150°C	Observations
<b>Compactage:</b>	Compacteur à pneumatiques	Compacteur vibrant	

## Appendix 8. Sections A,B,C,E and F asphalt material (EB14-BBA C Class 3 Surface) control



**PROCES VERBAL D'ESSAIS SUR ENROBES BITUMINEUX**

N° AFFAIRE:  N° DE PV: **Fab 005**

ITINERAIRE CONCERNE: **Planche expérimentale A350** SECTEUR :  
POLE :

DEMANDEUR: **AIRBUS**

Essais réalisés: **Extraction de liant et détermination du module de richesse**  
(Méthode asphaltoanalysator:IEH 08)

Type de mélange hydrocarboné: **EB 14 roulement 35/50** Norme de référence:  
**BBAc 0/14 c13** **NF EN 13108-1**

Centrale d'enrobage: **ENROBES TOULOUSE Poste sud**  
Entreprise de mise en œuvre: **MALET**

FORMULATION DE L'ENROBE: **N°43**

Centre d'Études  
Techniques  
de l'Équipement  
du Sud-Ouest



Laboratoire  
Régional  
des Ponts  
et Chaussées  
de Toulouse

ENR 01/02

CONSTITUANTS	PRODUCEUR	POURCENTAGE(%)			
		Fétude*	Fa	Fb	Fc
0 / 2	Garonne/Ariege	25,60%			
2 / 6	Garonne/Ariege	20,80%			
6 / 10	GARONNE	24,60%			
10/14	GARONNE	21,80%			
Filler d'apport Argiliant	LA Provencale	1,90%			
Bitume	35/50	5,30%			

\* Formulation définie au moment de l'étude(Fa,Fb,Fc:formules ajustées en cours de chantier)

COUCHE DE: **Roulement**

MVRE(T/m3)	<b>2,492</b>
MVRG(T/m3)	<b>2,707</b>
Module de richesse(K) Ext	<b>3,53</b>
Module de richesse(K) Int	

cofrac



ESSA15  
Accréditation  
N°: 3-4106  
pour le  
contrôle  
sur demande



Complexe Scientifique  
de Rangueil  
Laboratoire du Colonel Roche  
31400 Toulouse  
téléphone :  
05 62 25 97 97  
télécopie :  
05 62 25 97 96  
mél : dl.cole-ro  
@equipement.gouv.fr

ECHANTILLONS PRELEVES SUR CHANTIER								
	N°1	N°2	N°3	N°4	N°5	N°6	N°7	N°8
MODE DE PRELEVEMENT: P:poche C:carotte	P	P	P	P	P	P	P	P
OPERATEUR:	J AZAM	J AZAM	J AZAM	J AZAM	J AZAM	J AZAM	J AZAM	J AZAM
ITINERAIRE	Planche expérimentale A350							
DATES	22-sept.	22-sept.	22-sept.	22-sept.	22-sept.	22-sept.	23-sept.	23-sept.
HEURES	10h00	10h30	11h00	11h30	14h00	15h00	9h30	10h00
T° DU PRELEVEMENT:	160°C	162°C	159°C	159°C	140°C	160°C	150°C	154°C
CONDITIONS METEOROLOGIQUES: NC:non conforme C:conforme	C	C	C	C	C	C	C	C
OBSERVATIONS	Planche A		Planche B		Planche C N°5 sur 1ère couche ; N°6 sur 2ème		Planche F	



## Appendix 9. Section D asphalt material (EB14-BBME C Class 3 Surface) product specifications

		39/42
Année d'apposition du marquage : 08 N° identification de l'organisme notifié : 0333 N° certificat : 0333-CPD-420100		
<b>EN 13108-1</b>		
<b>Enrobés bitumineux pour routes et autres zones de circulation</b>		
<b>ENROBES-TOULOUSE</b>		
3 CHEMIN DE COTE GOUBARD - 31270 VILLENEUVE-TOLOSANE Tél : 05.61.72.05.08 Fax : 05.61.72.12.96		
<b>POSTES NORD &amp; SUD</b>		
<b>56</b>	BBME 0/14 cl3 EB 14 roullial 20/30 et EB 14 roullial 20/30 à 10% d'agrégats d'enrobés (1)	
<u>Exigences générales et fondamentales</u>		
<b>P.C.G.</b>		
— Pourcentage minimal de vides	$V_{min4}$	%
— Pourcentage maximal de vides	$V_{max0}$	%
— Pourcentage minimal de vides remplis par le bitume	APD	%
— Pourcentage maximal de vides remplis par le bitume	APD	%
<b>Tenue à l'eau</b>		
— Sensibilité à l'eau	ITSR <sub>60</sub>	%
<b>Résistance à l'abrasion par pneumatiques à crampons</b>	APD	-
<b>Comportement au feu</b>	APD	-
<b>Température du mélange</b>	170 à 190	°C
<b>Granularité : passant au tamis de :</b>		
20 mm	100	%
16 mm	99	%
14 mm	96	%
12.5 mm	89	%
10 mm	77	%
8 mm	66	%
6.3 mm	55	%
4 mm	40	%
2 mm	28	%
1 mm	20	%
0.5 mm	16	%
0.250 mm	12	%
0.125 mm	9	%
0.063 mm	6.5	%
<b>Teneur en liant</b>	TL 5.3	%
<b>Résistance aux déformations permanentes (orniérage)</b>		
— grand modèle : pourcentage de profondeur d'ornièrè	P <sub>5</sub>	%
— petit modèle : pente d'ornièrè	APD	mm
— petit modèle : pourcentage de profondeur d'ornièrè	APD	%
<b>Caractéristiques fondamentales</b>		
<b>Module de rigidité</b>	$S_{min12000}$	Mpa
<b>Fatigue</b>	$k_{GVR}$	µdef
<b>Substances dangereuses</b>	Valeurs seuils en vigueur sur le lieu d'utilisation : ces enrobés ne contiennent pas de substances dangereuses au sens de la réglementation applicable en France à la date de la rédaction du présent document.	

(1) : La formulation de cet enrobé comporte au plus 10% d'agrégats d'enrobé. La circulaire des Ministères de l'Aménagement du Territoire et de l'Environnement (MATE) et du Ministère de l'Équipement des transports et du Logement (MRTL) n° 2001-39 du 18 juin 2001 indique qu'il n'y a aucun inconvénient technique à réutiliser, dans la limite de 10% des agrégats d'enrobés. Dans ce cas, elle autorise à ne pas effectuer les études de caractérisation des agrégats et de formulation de cet enrobé.

Cette règle est applicable pour tous les enrobés exceptés les cas d'application suivants :

- ▶ bétons bitumineux semi-grenus en couche de roulement sous trafic > T1
- ▶ bétons bitumineux minces en couche de roulement sous trafic > T3



40/42

**FICHE DE SYNTHESE**

**POSTES NORD & SUD**

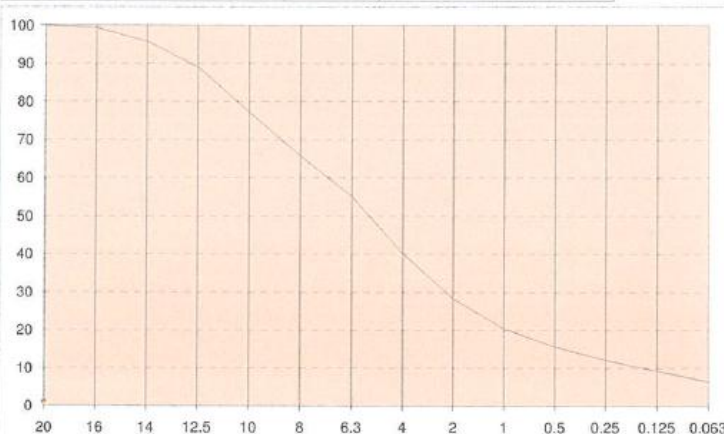
Formule n° 56 EB 14 rouf/lial 20/30 (BBME 0/14 cl3) NF EN 13108-1

DATE DE L'ETUDE : 24/11/2008

COUPURES	FORMULE*	PROVENANCES
0/2f alluvion. Code a Ang 1	24.6%	GARONNE/ARIEGE
2/6 cl alluvion. Code BIII Ang 1	25.6%	GARONNE/ARIEGE
6/10 cl alluvion. Code BIII Ang 1	18.9%	GARONNE
10/14 cl alluvion. Code BIII Ang 1	22.8%	GARONNE
Filler Calcaire	2.8%	La Provençale
Liant hydrocarboné	5.30%	Bitume 20/30

CARACTERISTIQUES DE LA FORMULE	
M.V.R.g. (kg/m <sup>3</sup> )	2715
M.V.R.E. (kg/m <sup>3</sup> )	2500
Surface Spécifique (m <sup>2</sup> /kg)	11.69
Module de richesse K	3.51

\* pourcentages indicatifs qui pourront être modifiés pour respecter la courbe granulométrique de l'étude.



# Tamis	% Passants
20	100
16	99.3
14	95.7
12.5	89.0
10	77.2
8	65.7
6.3	55.1
4	40.1
2	28.3
1	20.4
0.5	15.6
0.25	12.1
0.125	9.3
0.063	6.5

**CARACTERISTIQUES MECANQUES DE L'ENROBE**

ESSAI DURIEZ	Spécif	ESSAI P.C.G.	Spécif	ESSAI D'ORNIERAGE	Spécif
M.V.A. (kg/m <sup>3</sup> )	2282	10 girations	84.9	1000 cycles	2.7
Compacité (%)	93.6	25 girations	88.7	3000 cycles	3.4
Rc à sec (Mpa)	14.9	40 girations	90.6	10000 cycles	3.7
rc à l'eau (Mpa)	13.1	80 girations	93.3	30000 cycles	4.2
rc/Rc	0.88	200 girations	96.1	% vides	6.3
					5 à 8

ESSAI MODULE COMPLEXE	Spécif	ESSAI TRACTION DIRECTE	Spécif	ESSAI DE FATIGUE	Spécif
Module à 15 °C		Module à 15 °C	13107 Mpa	Déformation	
			≥ 11000		

**OBSERVATIONS**

Cette formule peut contenir jusqu'à 10% d'agrégats d'enrobés de classe c.

**UTILISATION**

<b>Domaine d'emploi:</b>	Couches de roulement et de liaison sous trafics intenses								
<b>Etat du support:</b>	Support dont les déformations n'excèdent pas 2 cm sous la règle de 3 m. Température mini de 5 °C								
<b>Mise en œuvre:</b>	<table border="1"> <thead> <tr> <th>Epaisseur</th> <th>Température à la livraison</th> <th>Observations</th> </tr> </thead> <tbody> <tr> <td>7 à 9 cm</td> <td>160 °C</td> <td></td> </tr> </tbody> </table>			Epaisseur	Température à la livraison	Observations	7 à 9 cm	160 °C	
Epaisseur	Température à la livraison	Observations							
7 à 9 cm	160 °C								
<b>Compactage:</b>	Compacteur à pneumatiques	Compacteur vibrant							

## Appendix 10. Section D asphalt material (EB14-BBME C Class 3 Surface) control



**PROCES VERBAL D'ESSAIS SUR ENROBES BITUMEUX**

N° AFFAIRE:  N° DE PV: **Fab 004**

ITINERAIRE CONCERNE: Planche expérimentale A350 n°2

DEMANDEUR: **AIRBUS**

Essais réalisés: Extraction de liant et détermination du module de richesse  
(Méthode asphaltoanalysator.IIH 08)

Type de mélange hydrocarboné: **EB roul 20/30** Norme de référence:  
**BBME 0/14 cl3** **NF EN 13108-1**

Centrale d'enrobage: ENROBES TOULOUSE Poste sud  
Entreprise de mise en œuvre: MALET

FORMULATION DE L'ENROBE: 56

CONSTITUANTS	PRODUCTEUR	POURCENTAGE(%)			
		Fétude*	Fa	Fb	Fc
.0 / 2f	Garonne/Ariege	24,60%			
.2 / 6	Garonne/Ariege	25,60%			
.6 / 10	GARONNE	18,90%			
.10/14	GARONNE	22,80%			
Filler d'apport	LA Provencale	2,80%			
Bitume	20/30	5,30%			

\* Formulation définie au moment de l'étude(Fa,Fb,Fc:formules ajustées en cours de chantier)

COUCHE DE:

MVRE(T/m3)	2,500
MVRG(T/m3)	2,715
Module de richesse(K) Ext	
Module de richesse(K) Int	3,51

ECHANTILLONS PRELEVES SUR CHANTIER					
	N°1	N°2	N°3	N°4	N°5
MODE DE PRELEVEMENT:	P	P			
Poche Coarotte					
OPERATEUR:	J AZAM	J AZAM			
ITINERAIRE	Planche D				
PR OU PK					
DATES	22-sept.	22-sept.			
HEURES	9h00	9h30			
T° DU PRELEVEMENT:	150°C	155°C			
CONDITIONS METEOROLOGIQUES:	C	C			
NC:non conforme C:conforme					
OBSERVATIONS					

Centre d'Études  
Techniques  
de l'Équipement  
du Sud-Ouest



Laboratoire  
Régional  
des Ponts  
et Chaussées  
de Toulouse

Unité LHEC



Complexe Scientifique  
de Rangueil  
1 avenue de Colonel Roche  
31400 Toulouse  
téléphone :  
05 62 25 97 97  
télécopie :  
05 62 25 97 98  
e-mail : dlc.cete-so  
@equipement.gov.fr

Unité Technique L.N.E.C. - Contrôles Chimiques

## MELANGES HYDROCARBONES

Résultats d'essais (Code : IEH08 )

N° Procès Verbal : **Fab 004**

N° Affaire: **0**

TYPE D'ENROBES: **EB rout 20/30**

Couche de: **Roulement**

N° Numéro d'échantillon

Tamais (mm)	C. THEORIQUE (% passant)	N°1	N°2	N°3	N°4	N°5	Moyenne	Ecart Absolu	Specifications Min.	Specifications Max.	Conformité
16	99,7	100,0	100,0				100,0	0,30			
14	96,4	97,2	96,8				97,0	0,60			
12,5	89,8	91,8	90,5				91,2	1,35			
10	80,1	77,4	77,8				77,6	-2,49			
8	68,0	64,0	66,0				65,0	-3,02			
6,3	56,8	52,2	53,7				53,0	-3,82			
4	45,9	39,7	39,4				39,5	-6,37			
2	32,9	29,3	28,8				29,1	-3,83			
1	23,2	21,5	21,1				21,3	-1,93			
0,5	16,9	16,3	16,0				16,1	-0,78			
0,250	12,5	12,5	12,3				12,4	-0,10			
0,063	6,4	7,3	7,2				7,2	0,84			
% Blème Int	5,30%	5,90%	5,65%				5,77%	0,00			
K ( Int)	3,51	3,64	3,49				3,57	0,06			
W%											

Observations sur la fabrication

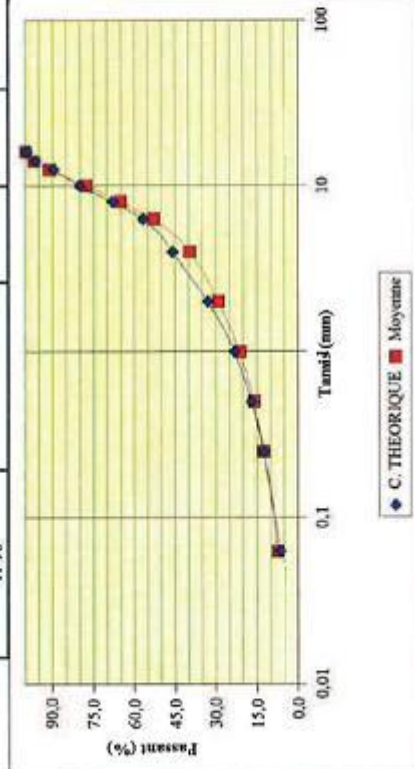
Combe un peu creuse en 2/4 - Le module de  
richesse est respecté -  
bons résultats

Toulouse le, **23 SEP 2009**

Le chargé de Programme  
de contrôle

Le Chef de P.U.T.  
Liens noirs - enrobés - chemo

**Jean-Charles FABRE**  
Ingénieur-Routeur





## Appendix 11. Section G asphalt material (EB14-BB C Surface) product specifications

				30, Avenue de Lorient - 31 081 TOULOUSE cedex Tél: 05.34.00.82.00 Fax: 05.34.00.82.01												
FICHE TECHNIQUE ETUDE DE FORMULATION																
DESTINATAIRE : MALET TOULOUSE SUD			DATE : 22/10/2008													
CHANTIER : Piste Expérimentale AIRBUS			N° DOSSIER : 104 0 612													
ENROBE : BBA C 0R14		CLASSE : 3		COUCHE : Roulement												
				REF NORME : NF EN 13108-1												
1). Origine des constituants																
a) GRANULATS (nature pétrographique, MVFG...):		Alluvionnaire Billoux														
0/2F	Sablères MALET	MB : 0,5	Rca :	FS :	MVRG 2741 Kg/m <sup>3</sup>											
2/0,3C	Sablères MALET			MSF : AS : 16	MVRG 2746 Kg/m <sup>3</sup>											
0,3/10C	Sablères MALET	LA :	MDE :	MBF : AS : 14	MVRG 2736 Kg/m <sup>3</sup>											
10/14C	Sablères MALET	LA : 20	MDE : 11	MBF : AS : 11	MVRG 2733 Kg/m <sup>3</sup>											
Granulats de catégorie :		B III a		( Prescription norme : *** )												
b) Fines d'apport :		Filler calcaire		Provenance : OMYA MEAC MVRG 2700 Kg/m <sup>3</sup>												
c) Liant :		Classe : 35/50		Provenance : SHELL												
				Pénétrabilité : 39 1/10mm												
				TBA : 53,8 °C												
d) Additif :		Nature :		Dosage :												
				Densité : Kg/m <sup>3</sup>												
2). Composition																
	%Exc	%Int	Caractéristiques du mélange													
0/2F	38	35,8	MVRG :	2740	Surf. spécifique : $\Sigma = 13,763 \text{ m}^2/\text{Kg}$											
2/0,3C	15	14,1	MVPE méthode par calcul :	2496												
0,3/10C	20	18,8	MVPE méthode à feux :	2463	Module de Richesse : K = 3,86											
10/14C	24	22,6			Teneur en liant minimale : $\geq$											
Filler calc. :	3	2,8														
Blume :	6,3	5,9														
3). Squelette minéral théorique																
Tamis # mm	20	16	14	12,5	10	8	6,3	4	2	1	0,500	0,315	0,250	0,200	0,160	0,125
% Passante	100,0	99,6	95,4	88,7	78,8	64,9	56,2	47,7	38,0	25,0	10,1	15,6	14,0	12,5	8,80	7,98
4). Résultats de l'étude de formulation.																
a) Essai de compactage à la presse à cisaillement giratoire (NF EN 12 697-31):																
Nombre de girations	10	20	40	80	60	80	100	120	180	200	Pente = 3,85					
% de vides obtenus	12,0					3,8				0,3						
Valeurs prescrites (NF EN 13108-1)						3 à 7%										
b) Essai de compression simple LCPC (NFP 88-281-1): Essai DURIEZ dilaté																
MVA LCPC / % de vides		Performances mécaniques														
MVA :	% de vides :	R :	MPa	r :	MPa											
					nFC											
		Valeur prescrite NF EN 13108-1 : $\geq 0,80$														
c) Essai d'ornièrage (NF EN 12 697-22) :																
Nbr. de compactage	% de vides moy.	Spécif. norme	Profondeur ornière	SPECIFICATIONS												
		NF EN 13108-1		Chantier												
FORT	4,8 %	V% compris entre 4% et 7%	13,07 %	9 à 14% à 10 000 cycles												
d) Module de rigidité (NF EN 12 697-26) :																
		Essai de traction indirecte			Essai de traction directe											
Spécifications % de vides NF EN 13108-1	% de vides éprouvette	NF EN 13108-1	Module de rigidité $S_{20}$ à 15°		NF EN 13108-1	Module de rigidité à 15°										
***	***	Module $S_{20}$ (Mpa)	***	Mpa	Module (Mpa)	*** Mpa										
		$\geq 9000$			$\geq 11000$											

## Appendix 12. Section G Asphalt material (EB14-BB C Surface) control



**PROCES VERBAL D'ESSAIS SUR ENROBES BITUMMEUX**

N° AFFAIRE:  N° DE PV: **Fab 006**

ITINERAIRE CONCERNE: Planche expérimentale A350 SECTEUR :  
POLE :

DEMANDEUR: AIRBUS

Essais réalisés: Extraction de liant et détermination du module de richesse  
(Méthode asphaltoaalysator:IEH 08)

Type de mélange hydrocarboné: **EB 14 roul 35/50 très ornierant** Norme de référence:  
**BBAC 0/14 Très Ornierant**

Centrale d'enrobage: ENROBES TOULOUSE Poste sud  
Entreprise de mise en œuvre: MALET

FORMULATION DE L'ENROBE:

CONSTITUANTS	PRODUCTEUR	POURCENTAGE(%)			
		Fétude*	Fa	Fb	Fc
.0 / 2F	Sablière Malet	35,80%			
.2 / 6	Sablière Malet	14,10%			
.6 / 10	Sablière Malet	18,80%			
.10/14	Sablière Malet	22,60%			
Filler d'apport					
Argiliant	LA Provencale	2,8			
Bitume	35/50	5,90%			

\* Formulation définie au moment de l'étude(Fa,Fb,Fc:formules ajustées en cours de chantier)

COUCHE DE:

MVRE(T/m3)	<b>2,496</b>
MVRG(T/m3)	<b>2,740</b>
Module de richesse(K) Ext	
Module de richesse(K) Int	<b>3,88</b>

ECHANTILLONS PRELEVES SUR CHANTIER					
	N°1	N°2	N°3	N°4	N°5
MODE DE PRELEVEMENT: P:pochs C:carotte	P	P			
OPERATEUR:	G CASTILLE				
ITINERAIRE					
DATES	23-sept.	23-sept.			
HEURES	11h30	11h45			
T° DU PRELEVEMENT:	154°C	-			
CONDITIONS METEOROLOGIQUES: NC:non conforme C:conforme	C	C			
OBSERVATIONS	Planche G				

Centre d'Études  
Techniques  
de l'Équipement  
du Sud-Ouest



Laboratoire  
Régional  
des Ponts  
et Chaussées  
de Toulouse

Unité LNEC

cofrac



ESSAIS  
Accreditation  
N°: 1-4906  
portée  
concordée  
sur demande



Complexe Scientifique  
de Rangueil  
1 avenue du Colonel Roche  
31400 Toulouse  
téléphone :  
05 62 25 97 97  
télécopie :  
05 62 25 97 88  
mél : dlr.cste-se  
cequipemat.gour.fr

Unité Technique L.N.E.C. - Comités Chantiers

## MELANGES HYDROCARBONES

Résultats d'essais (Code : JEH08 )

N° Procès Verbal :  
N° Affaire:

TYPE D'ENROBES:

Fab 006  
0

EB 14 roal 35/50 très ornierant

Couche de :

Roulement

Numéro d'échantillon

Tamis (mm)	C. THEORIQUE (% passant)	N°1	N°2	N°3	N°4	N°5	Moyenne	Ecart Absolu	Specifications Min.	Specifications Max.	Conformité
16	99,5	100,0	100,0				100,0	0,50			
14	95,4	98,2	98,5				98,3	2,94			
12,5	88,7	93,0	92,4				92,7	3,97			
10	76,6	80,3	79,1				79,7	3,11			
8	64,9	67,1	67,1				67,1	2,20			
6,3	56,2	56,3	56,3				56,3	0,10			
4	47,7	46,6	46,2				46,4	-1,29			
2	38,0	37,5	37,4				37,4	-0,58			
1	25,9	27,0	27,2				27,1	1,20			
0,5	19,1	20,2	20,3				20,3	1,16			
0,250	14,0	15,5	15,8				15,7	1,68			
0,063	8,0	8,9	8,2				8,6	0,63			
% Bitume Int	<b>5,90%</b>	<b>6,11%</b>	<b>6,05%</b>				<b>6,08%</b>	<b>0,00</b>			
K ( Int )	<b>3,88</b>	<b>3,66</b>	<b>3,68</b>				<b>3,67</b>	<b>-0,21</b>			
W%											

Observations sur la fabrication

*Bien*

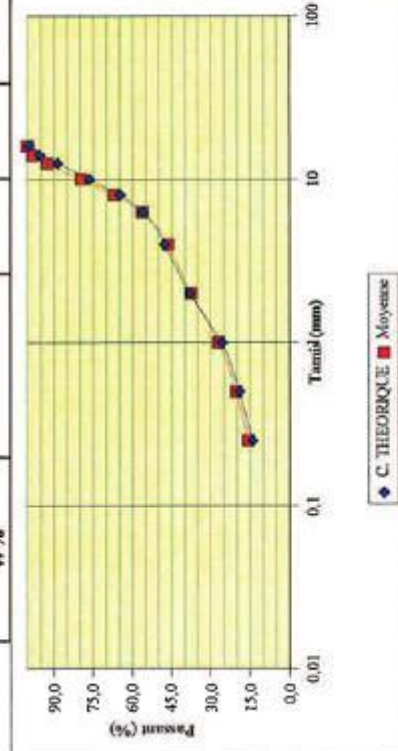
Toulouse le 23 SEP 2009

Le chargé de Programme de Contrôle

*M. AZAM*

Le Chef de U.T.  
Liants noirs - enrobés - chantiers

*Jean-Claude FABRE*  
Ingénieur-Chantier



**Appendix 13. Schematics of the simulator**

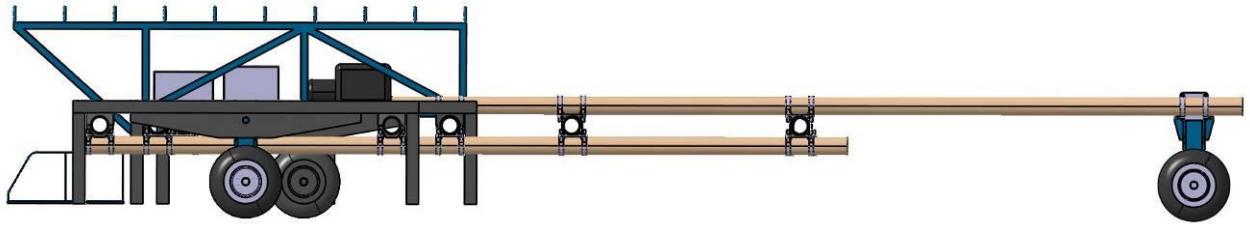


**Figure 54: Side view of the simulator**

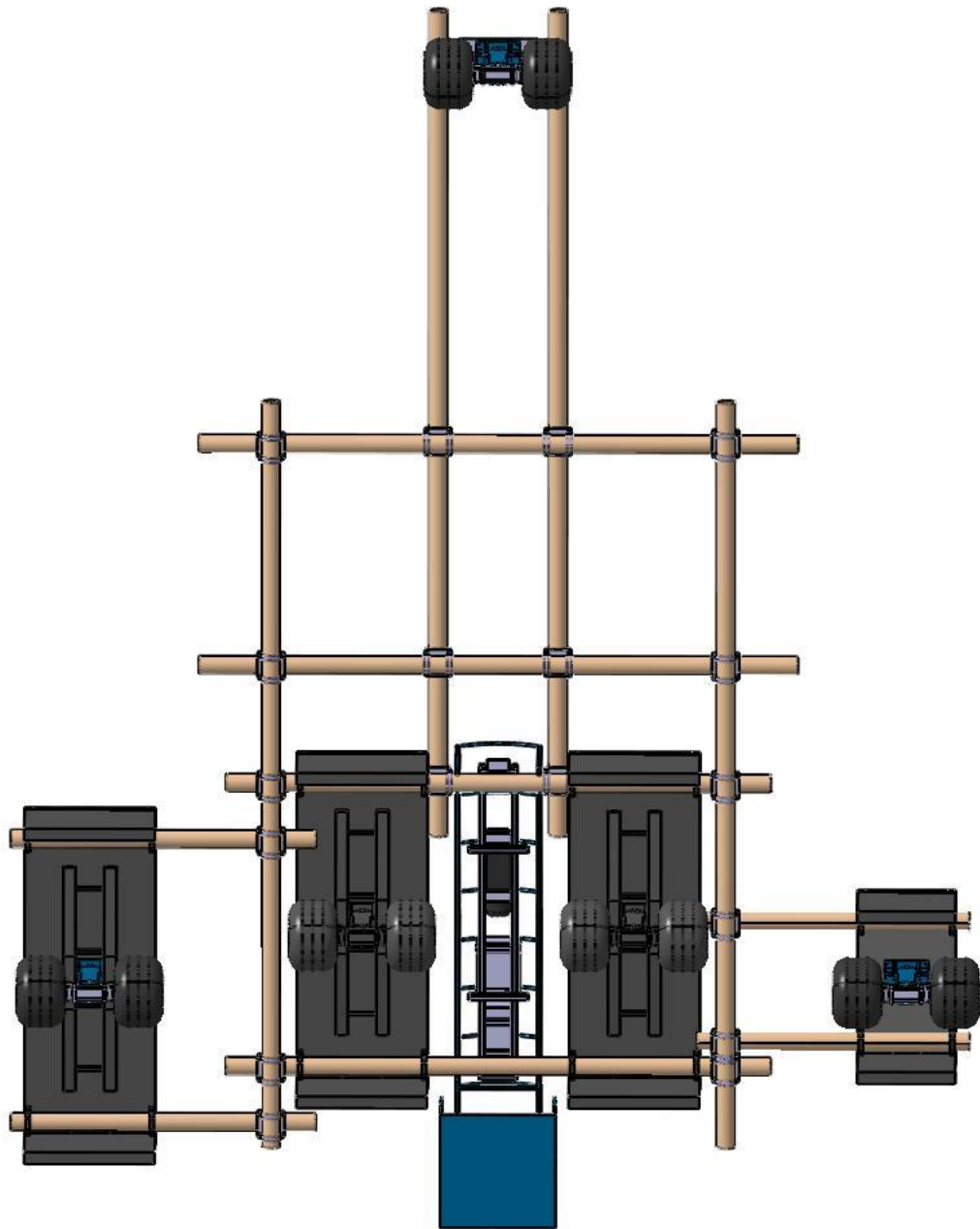


**Figure 55: Bottom view of the simulator**

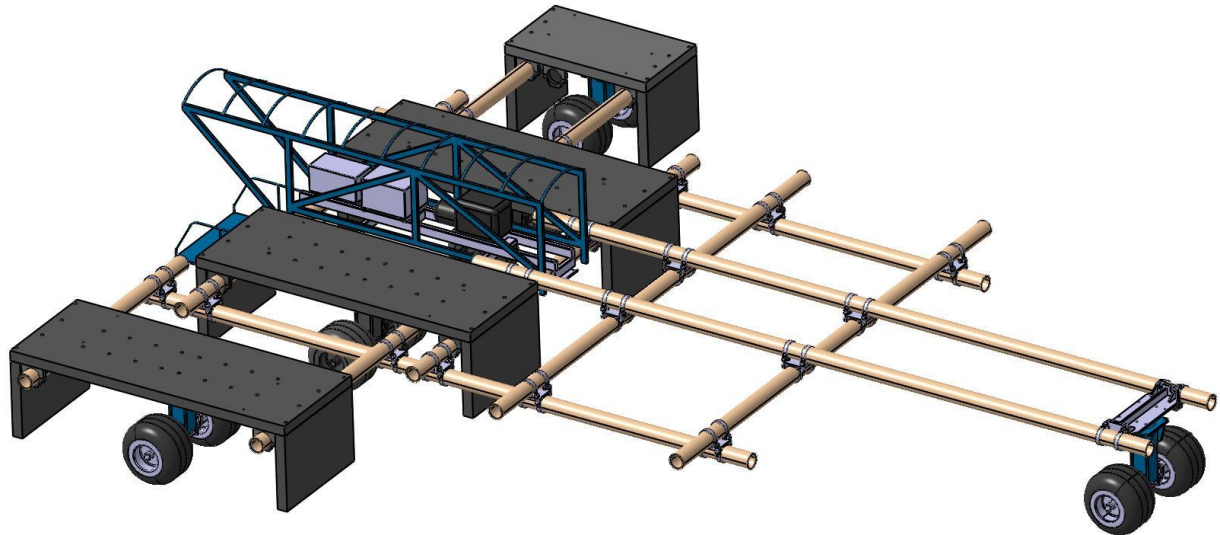


Figure 56: Top view of the simulator

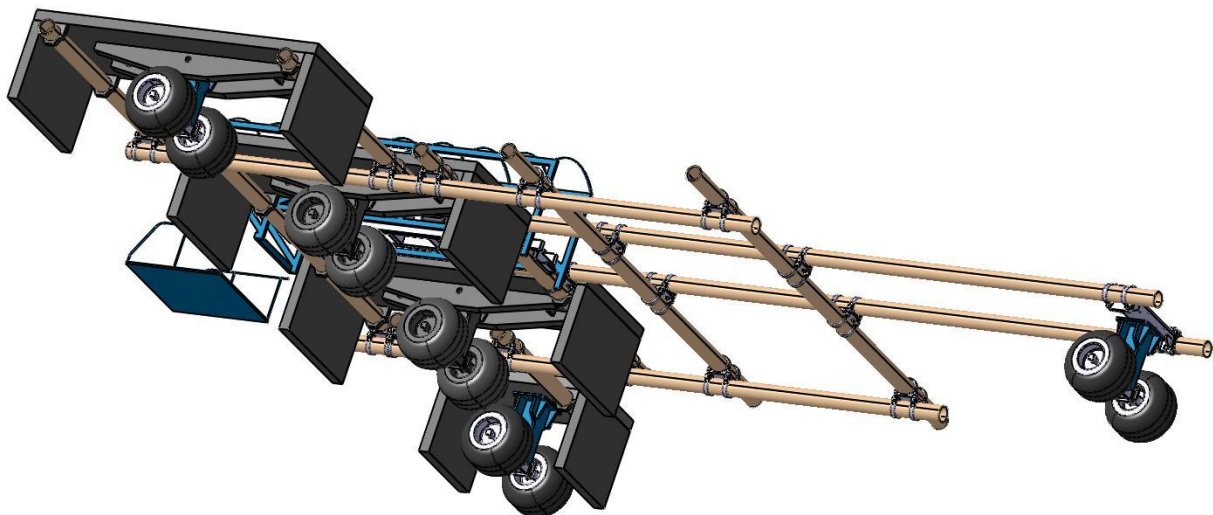


Figure 57: Bottom view of the simulator

## Appendix 14. Dynaplaque, measurement of dynamic modulus of ground

The Dynaplaque is presented on the LCPC's website:

[http://www.lcpc.fr/en/produits/materiels\\_mlpc/fiche.dml?id=105&type=abcaire](http://www.lcpc.fr/en/produits/materiels_mlpc/fiche.dml?id=105&type=abcaire),

This equipment which fits with the French standard NF P 94-117-2 is used to:

- Measure deformability of earthworks subgrade and selected fill,
- Determine their homogeneity when works realized,
- Assess lift and fatigue behaviour of structures such as car parks, site roads,

Dynaplaque 2 is an impulse generator applying a dynamic load to the ground to be tested equivalent in intensity and duration to that caused by the passage of a 13 tonne axle at 60 km/h, by means of weight falling on a shock absorber spring placed on a load plate. The deflection of the ground and the impact force are measured by sensors built into the plate. The combination of these two parameters allows the dynamic strain modulus of the structure at the test point to be calculated. If a great number of shocks is applied to a given point, the evolution of dynamic modulus allows the fatigue behaviour of the ground tested to be assessed. The new dynaplaque 2 has numerous advantages over the first generation, namely:

- direct measurement of the dynamic modulus,
- increase of measuring range toward higher rigidities (from 100 MPa to 250 MPa),
- elimination of calibration of springs and overall calibration on varied sites.

In addition, it maintains all the strains points which have made the first generation equipment successful: simple and quick implementation by one person, high measuring rate: 20 to 30 tests per hour, mobility on site and road, great speed of operation, with results immediately workable thanks to data acquisition and processing. The apparatus is permanently mounted on light truck, preferably 4-wheel drive, to make clearance of obstacles easier.

**Table 19: Dynaplaque specifications**

<b>Measurement storage capacity</b>	1 week intensives tests
<b>Dynamic modulus range</b>	20 to 250 MPa
<b>Falling weight</b>	120kg
<b>Maximum force</b>	100kN
<b>Test rate</b>	20 to 30 per hour (3 shocks per test)
<b>Fall height</b>	0.50 m
<b>Path of displacement</b>	15 mm



**Figure 58: Picture of the Dynaplaque**

## Appendix 15. Portancemetre, continuous capacity measurement

The Portancemetre is presented on the LCPC's website:

[http://www.lcpc.fr/en/produits/materiels\\_mlpc/fiche.dml?id=153&type=abcaire](http://www.lcpc.fr/en/produits/materiels_mlpc/fiche.dml?id=153&type=abcaire)

The Portancemetre is a high performance equipment used for continuous measurement of capping layers modulus. The hydraulic power unit for the vibrating of the measurement wheel is placed on board of the vehicle, a 4x4 pick up (not provided). The test is conducted from the driver's compartment where the data acquisition and processing system is placed.

The vibrating wheel and the reaction frame are hung inside a skeletal trailer. Both are fitted with vertical axis accelerometers. A hydraulic system operates lowering machinery for the reaction frame vibrating wheel set. The rotation of the unbalance device is generated by a hydraulic motor. An associated calculation algorithm determines the vertical effort inspecting the ground and its corresponding deflection.

The included software package for measurement result processing can either be run on situ, once as soon as the survey is completed, or delayed, on a desktop computer.

Table 20 gives the Portancemetre specifications.

**Table 20: Portancemetre specifications**

<b>Range of use</b>	30 to 300 MPa
<b>Vibrating mass</b>	600 kg
<b>Full wheel load</b>	1000 kg
<b>Wheel width</b>	200 mm
<b>Vibration frequency</b>	35 Hz
<b>Basic sample</b>	1 m
<b>Advance survey speed</b>	3.6 km/h
<b>Maximum installed power available</b>	19 kw



**Figure 59: Picture of the Portancemetre**

**Appendix 16. Evolution curves of rutting depth measured by the transverse-profilometer**

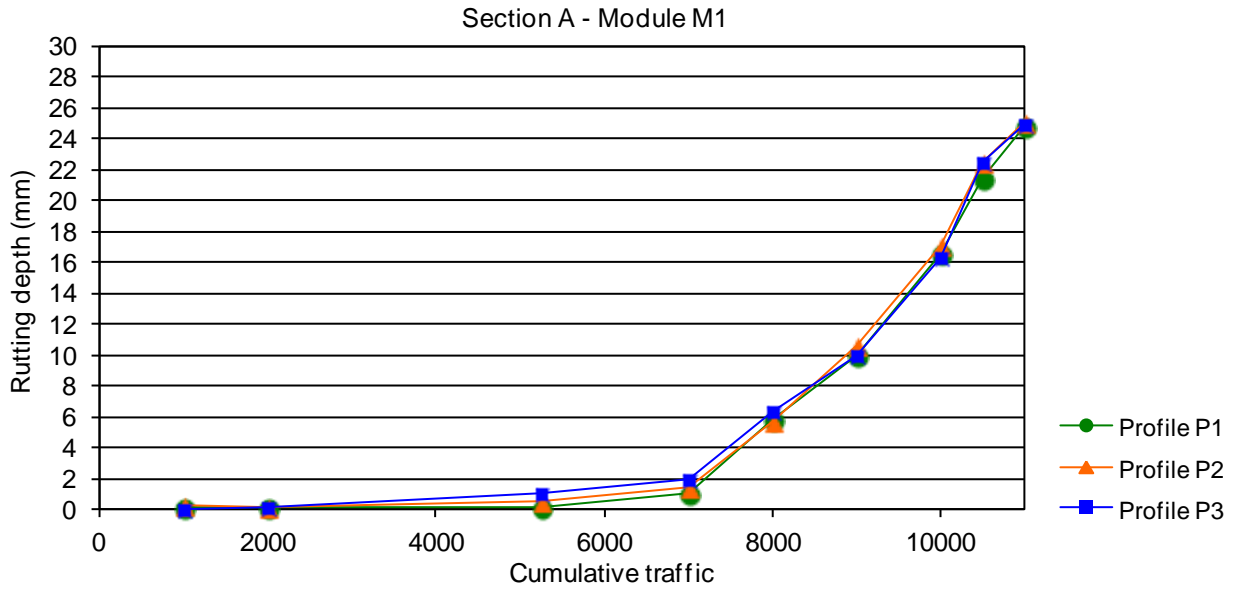


**Figure 60: Evolution curve of rutting measured on section A, configuration M1**

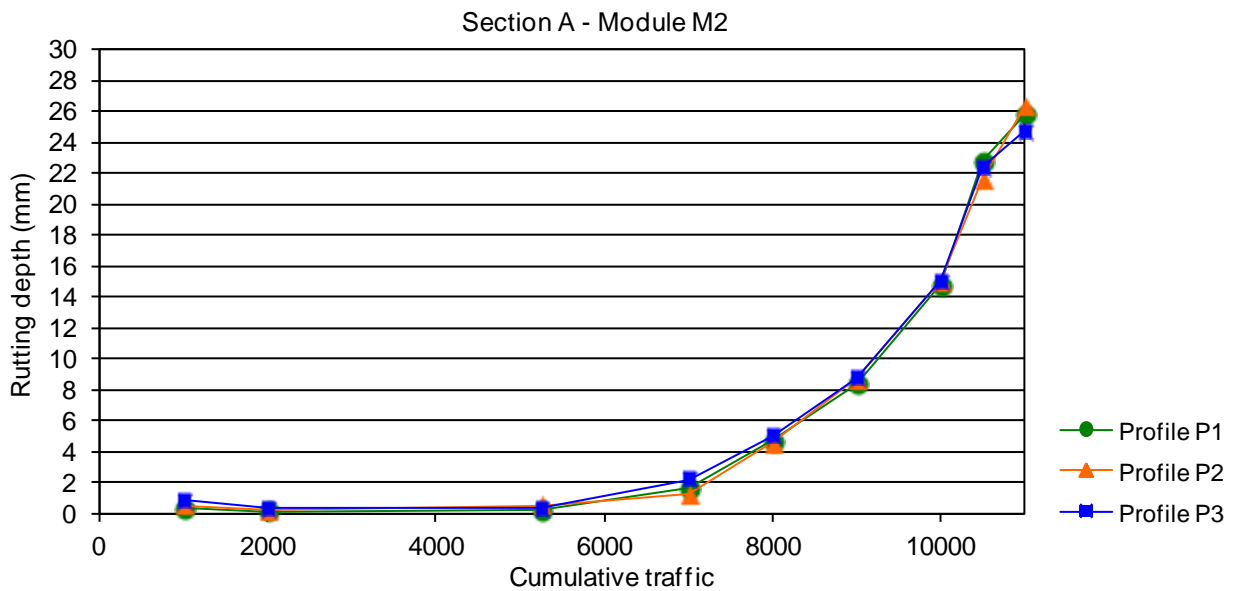


**Figure 61: Evolution curve of rutting measured on section A, configuration M2**



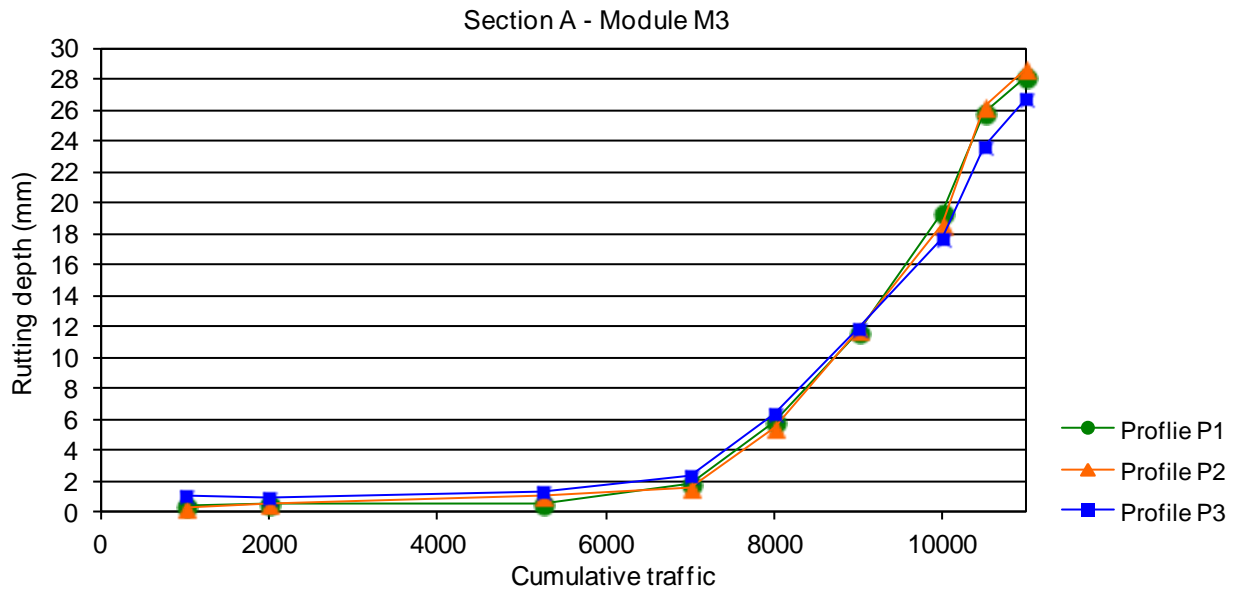


**Figure 62: Evolution curve of rutting measured on section A, configuration M3**

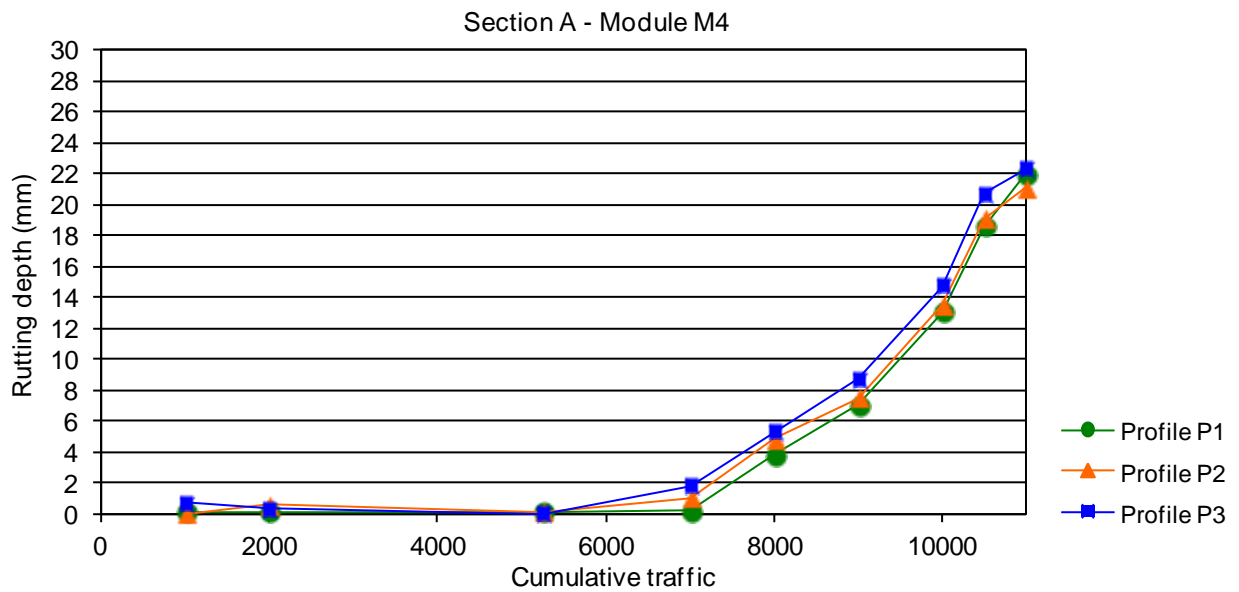


**Figure 63: Evolution curve of rutting measured on section A, configuration M4**

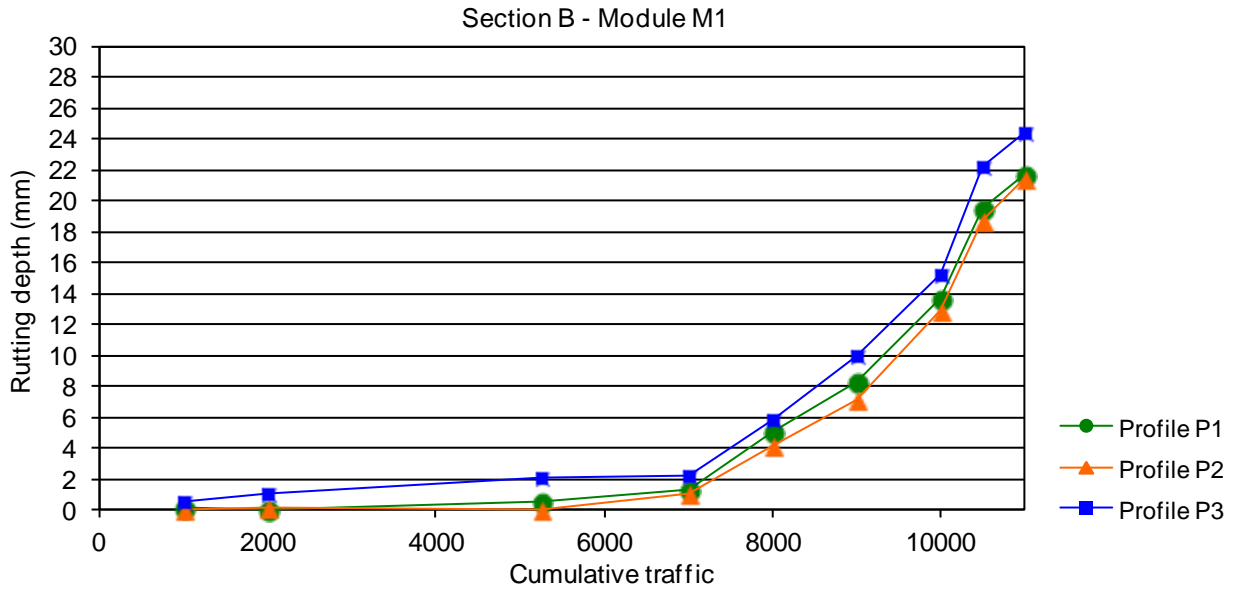


Figure 64: Evolution curve of rutting measured on section B, configuration M1

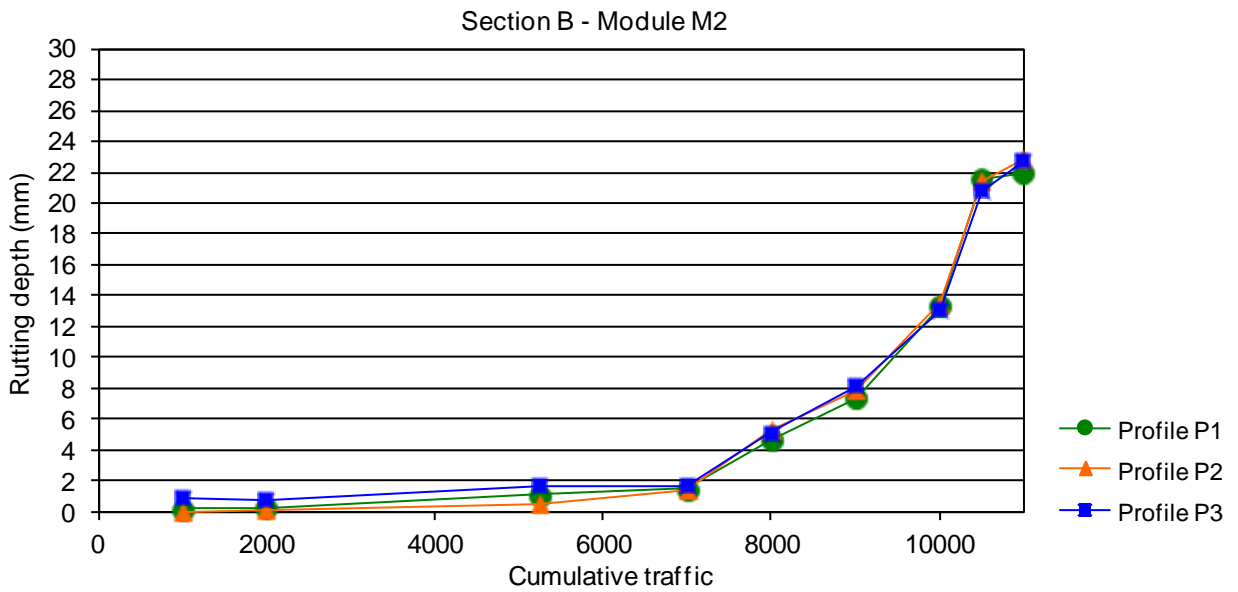


Figure 65: Evolution curve of rutting measured on section B, configuration M2

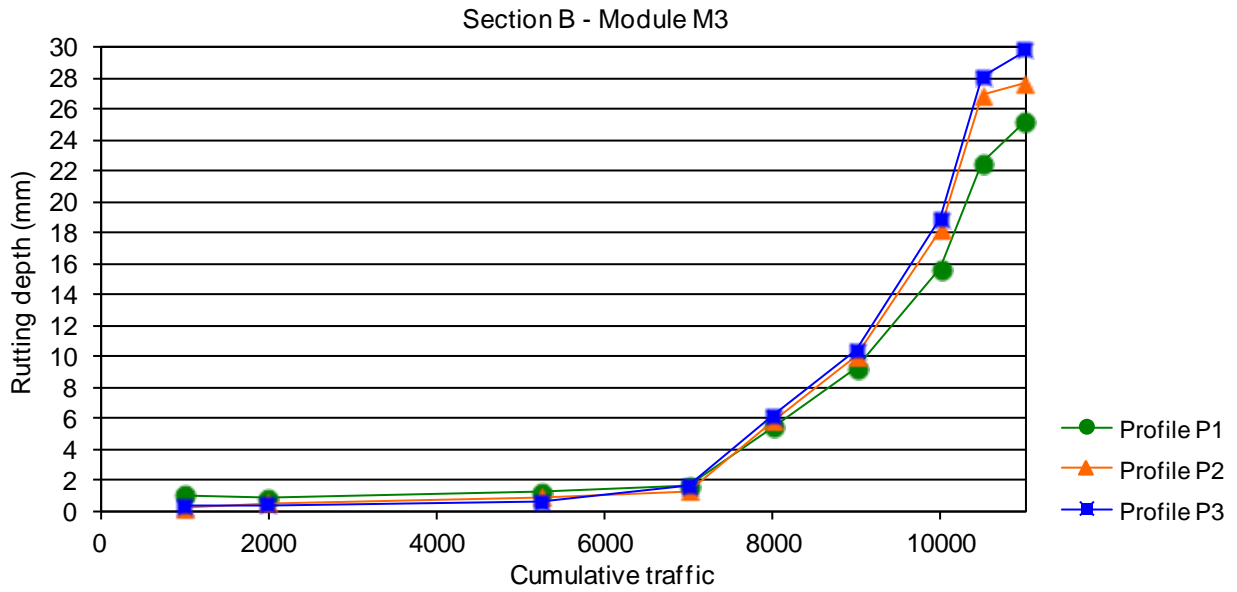


Figure 66: Evolution curve of rutting measured on section B, configuration M3

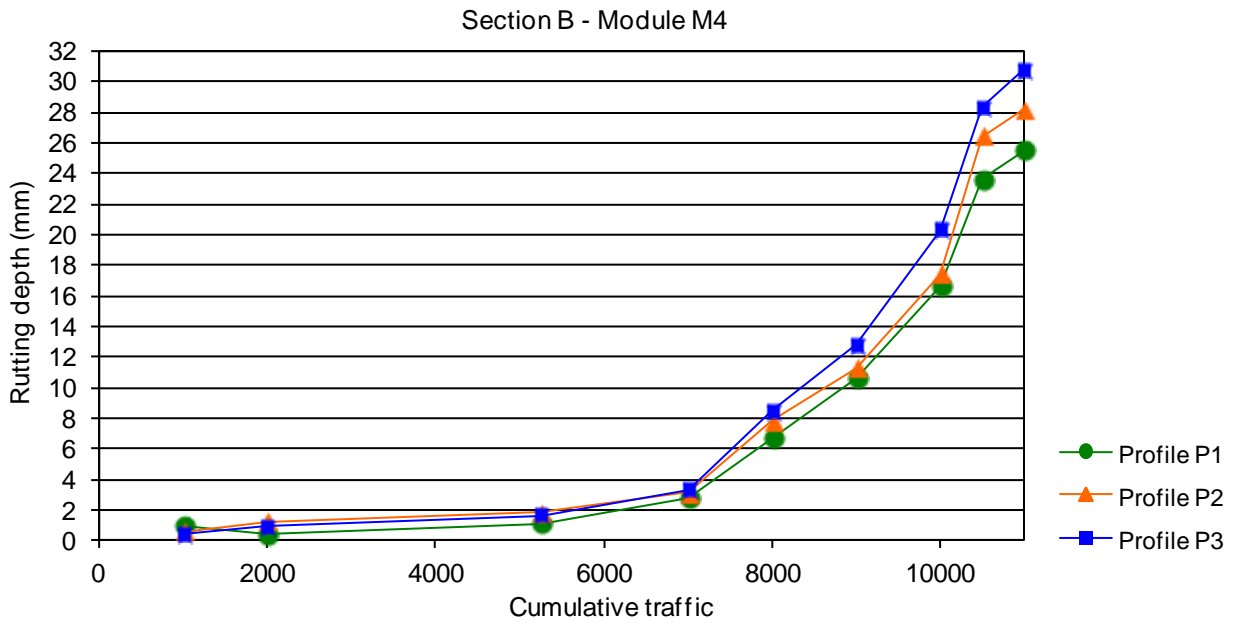


Figure 67: Evolution curve of rutting measured on section B, configuration M4

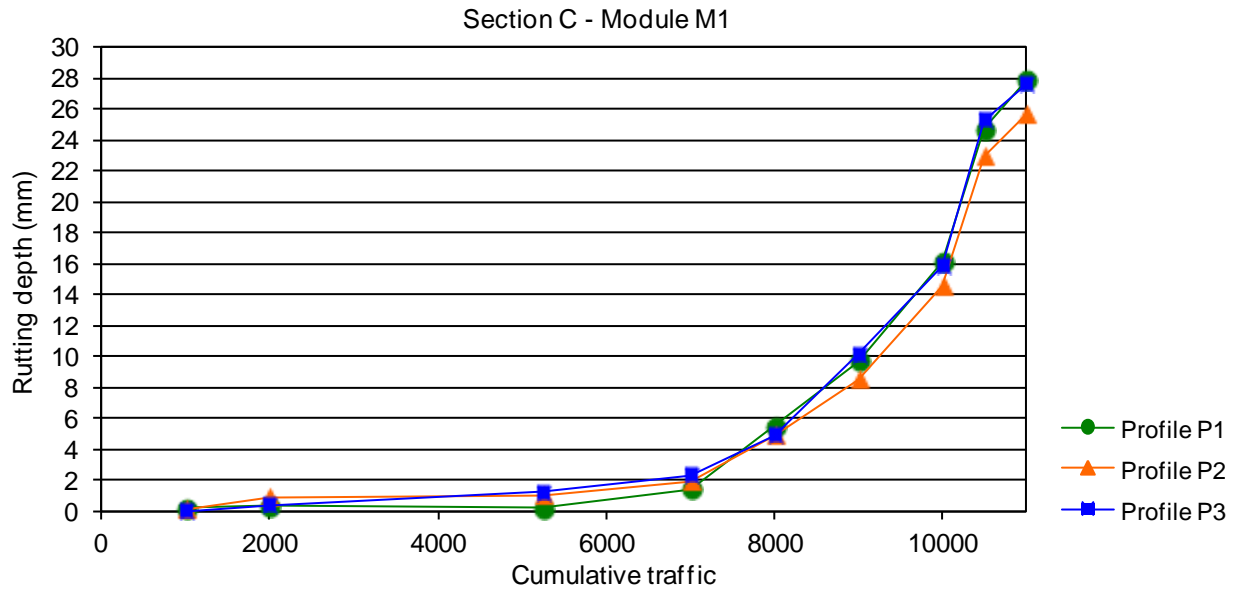


Figure 68: Evolution curve of rutting measured on section C, configuration M1

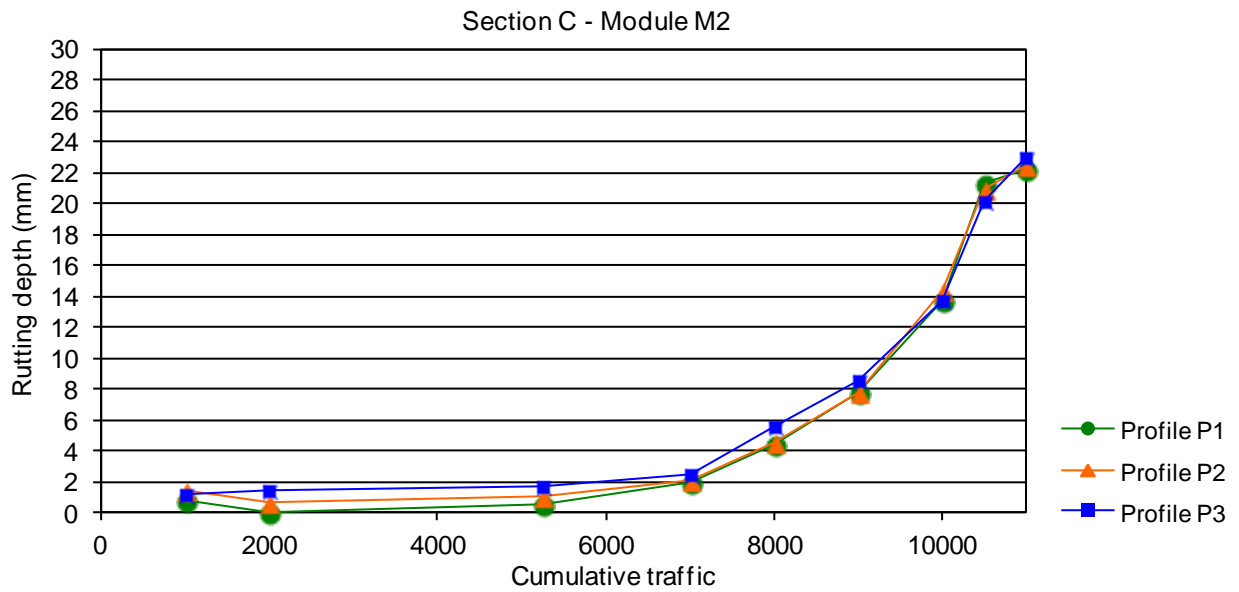
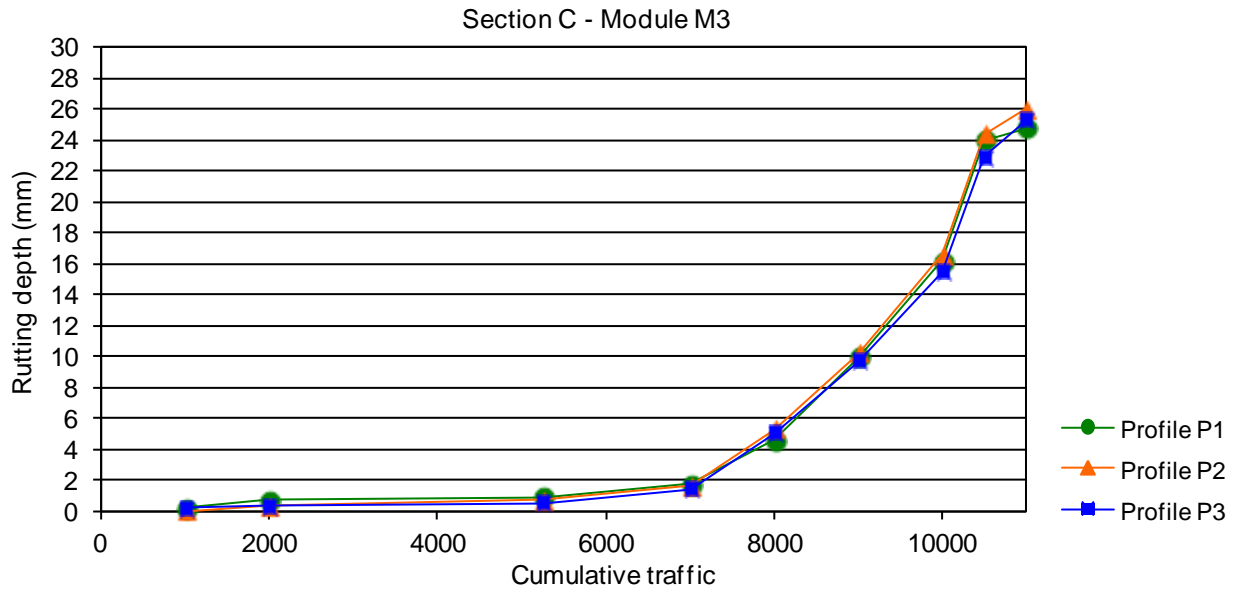
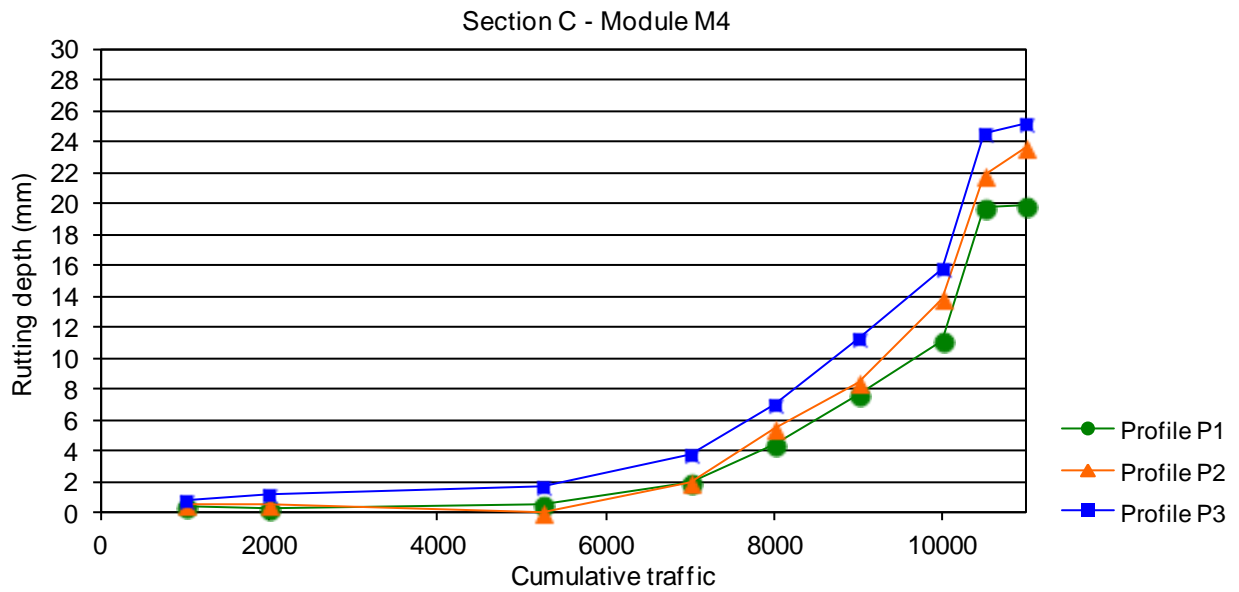


Figure 69: Evolution curve of rutting measured on section C, configuration M2



**Figure 70: Evolution curve of rutting measured on section C, configuration M3**



**Figure 71: Evolution curve of rutting measured on section C, configuration M4**

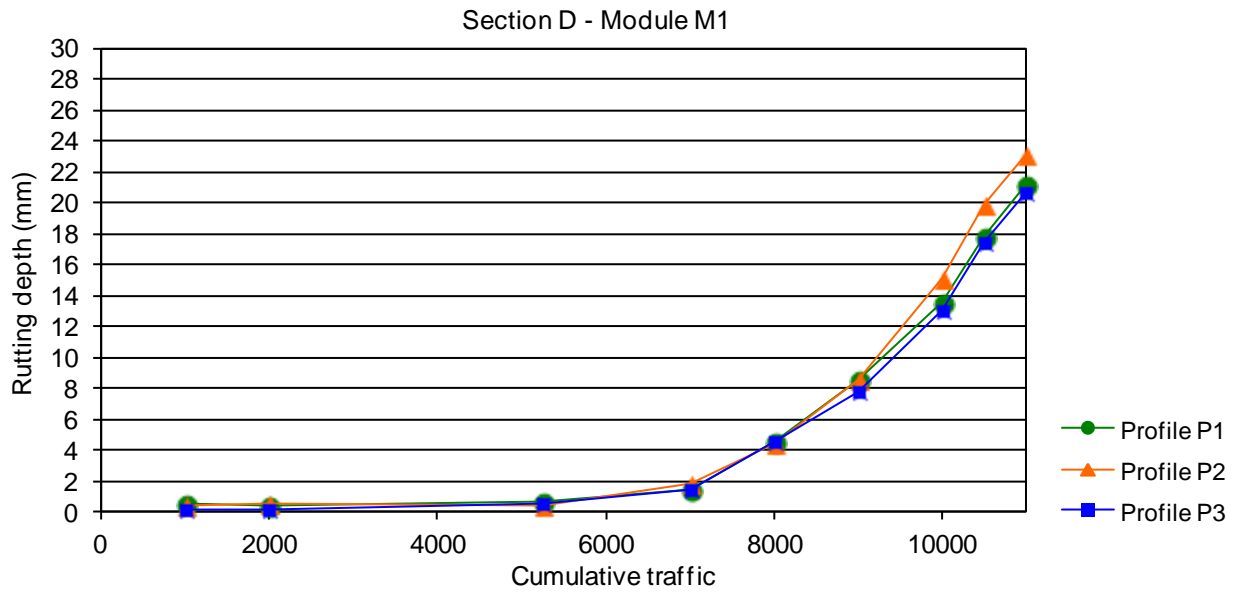


**Figure 72: Evolution curve of rutting measured on section D, configuration M1**

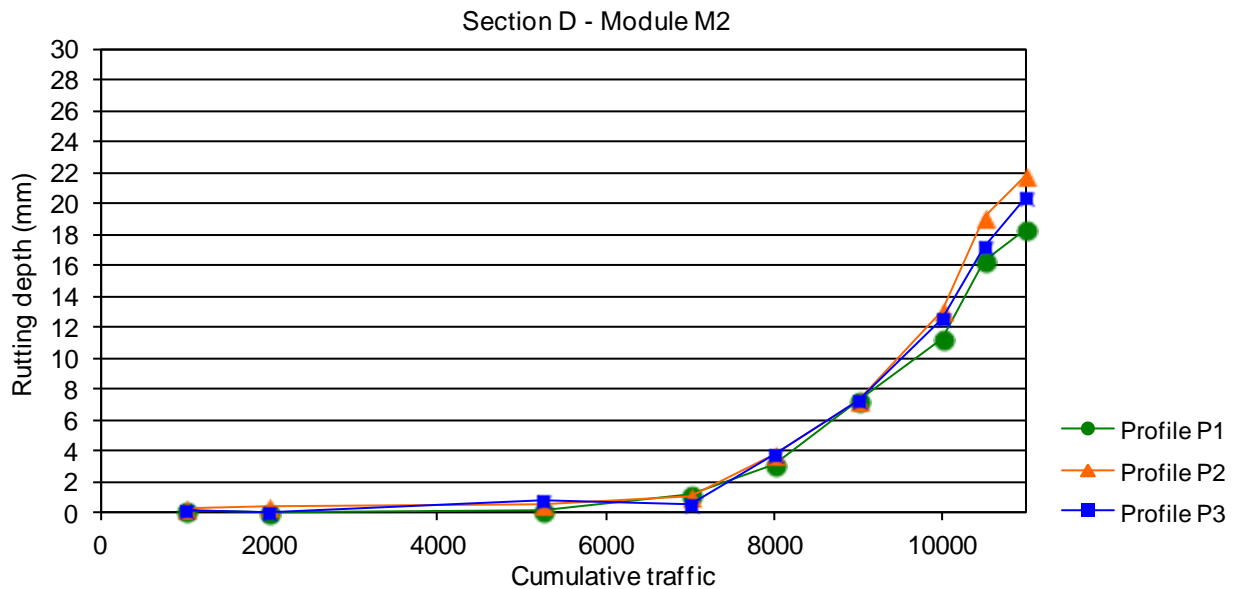


**Figure 73: Evolution curve of rutting measured on section D, configuration M2**

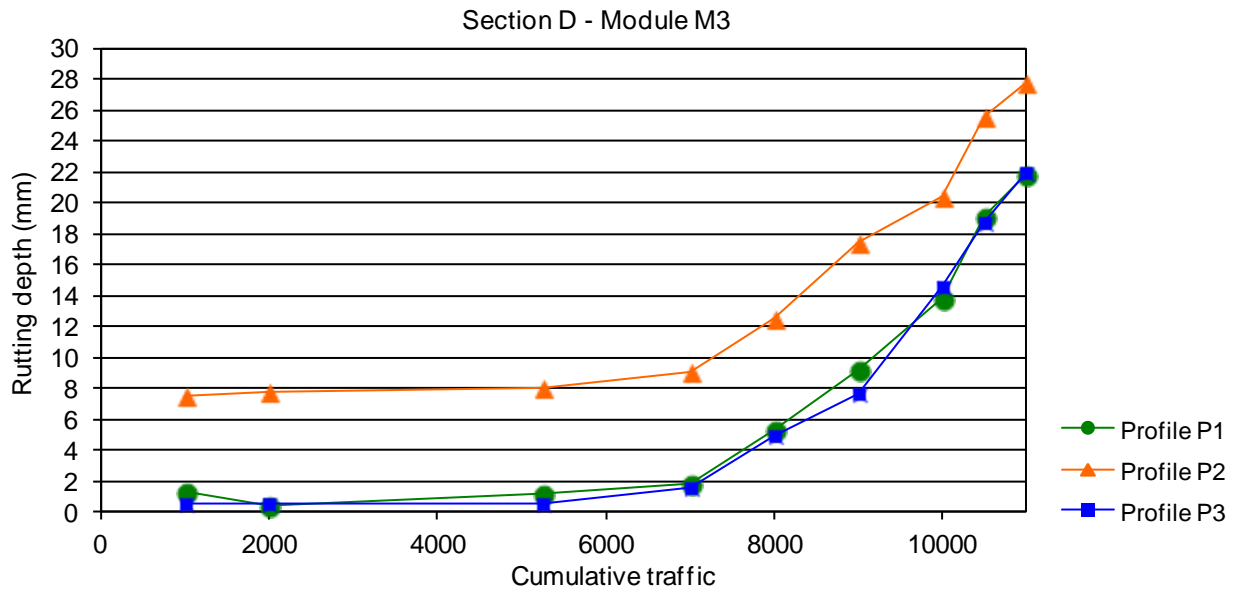


**Figure 74: Evolution curve of rutting measured on section D, configuration M3**

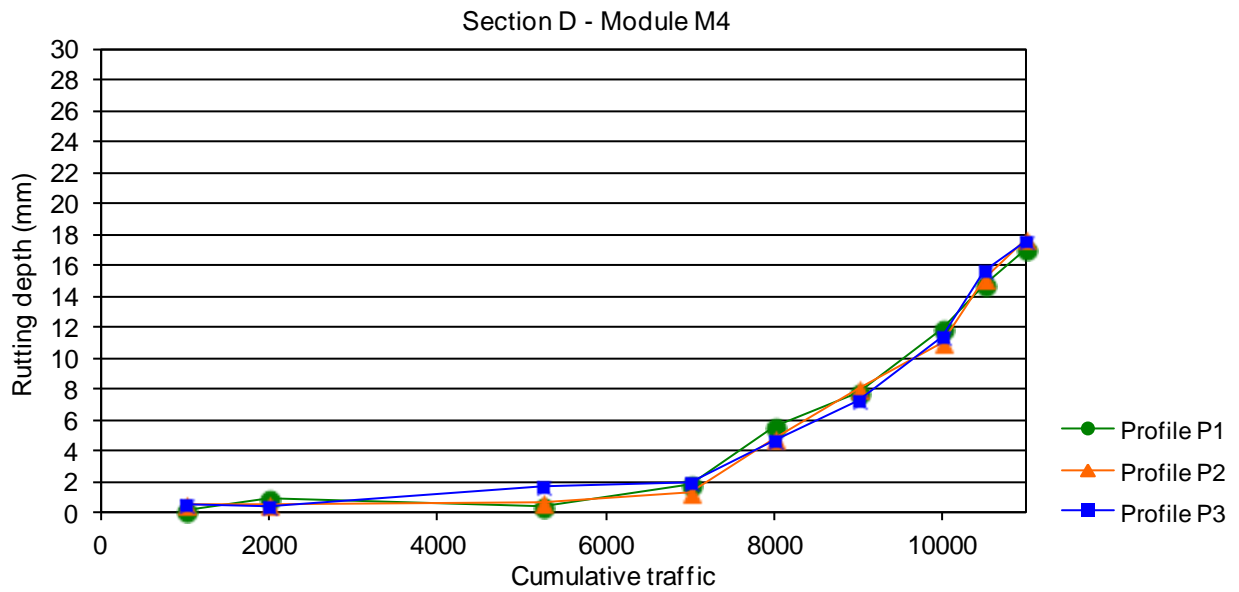


**Figure 75: Evolution curve of rutting measured on section D, configuration M4**

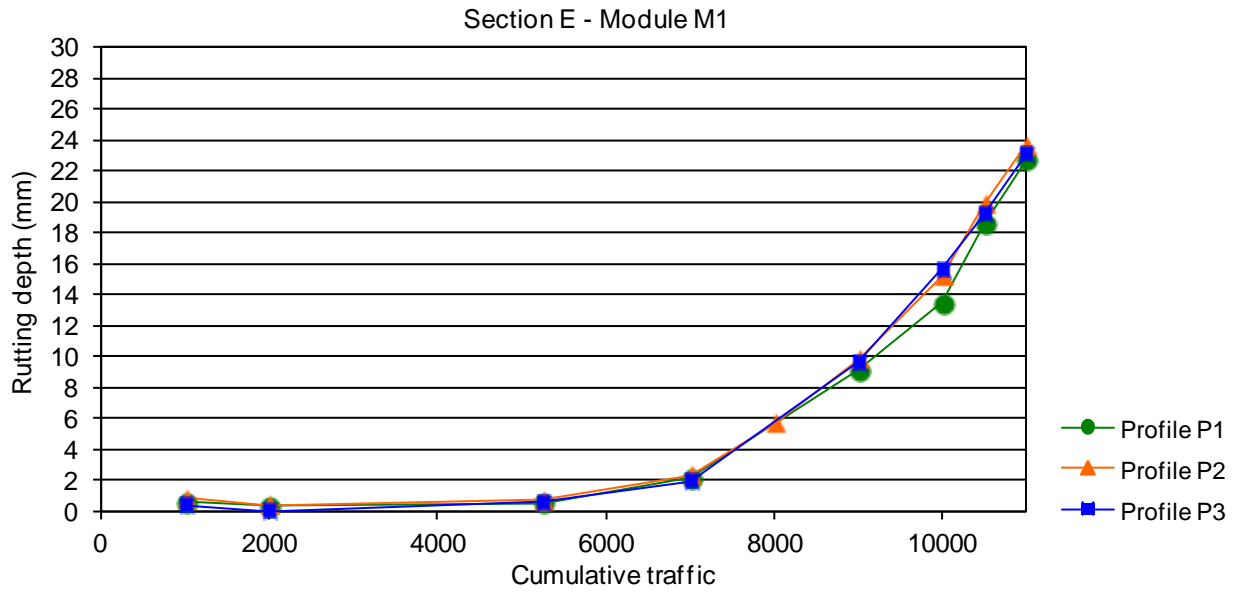


Figure 76: Evolution curve of rutting measured on section E, configuration M1

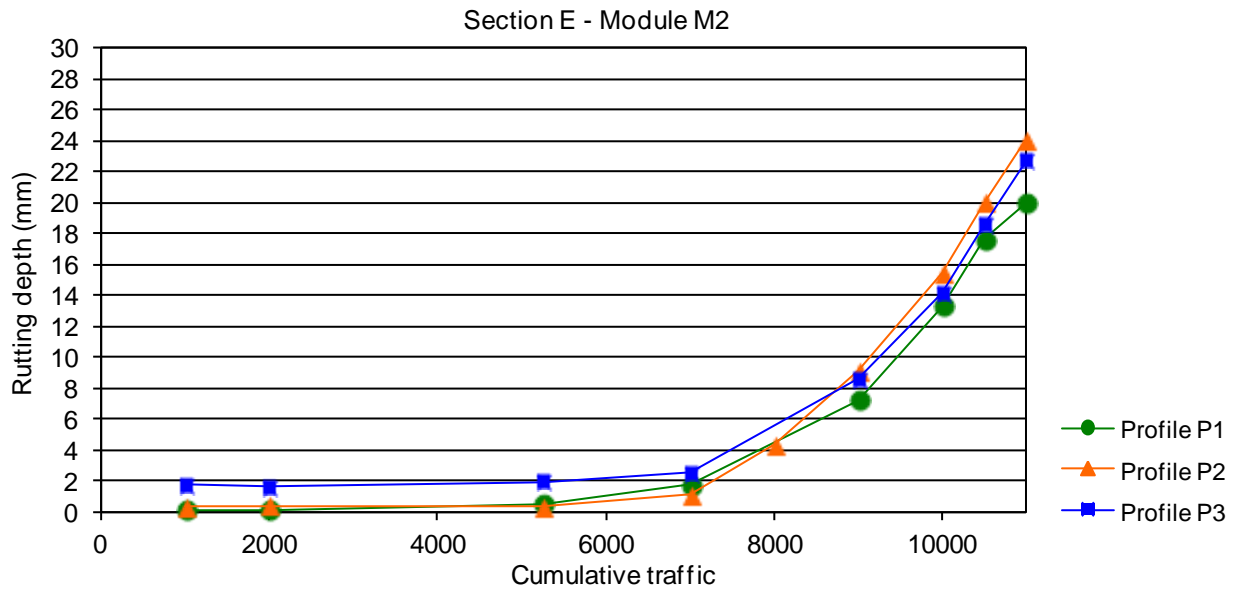


Figure 77: Evolution curve of rutting measured on section E, configuration M2



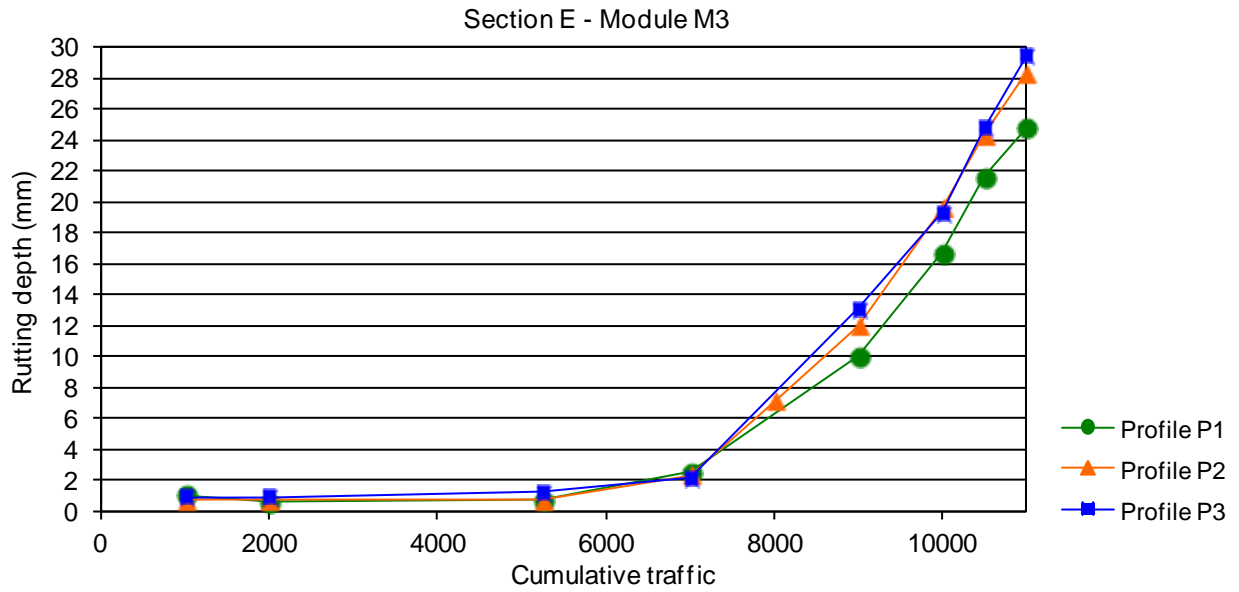


Figure 78: Evolution curve of rutting measured on section E, configuration M3

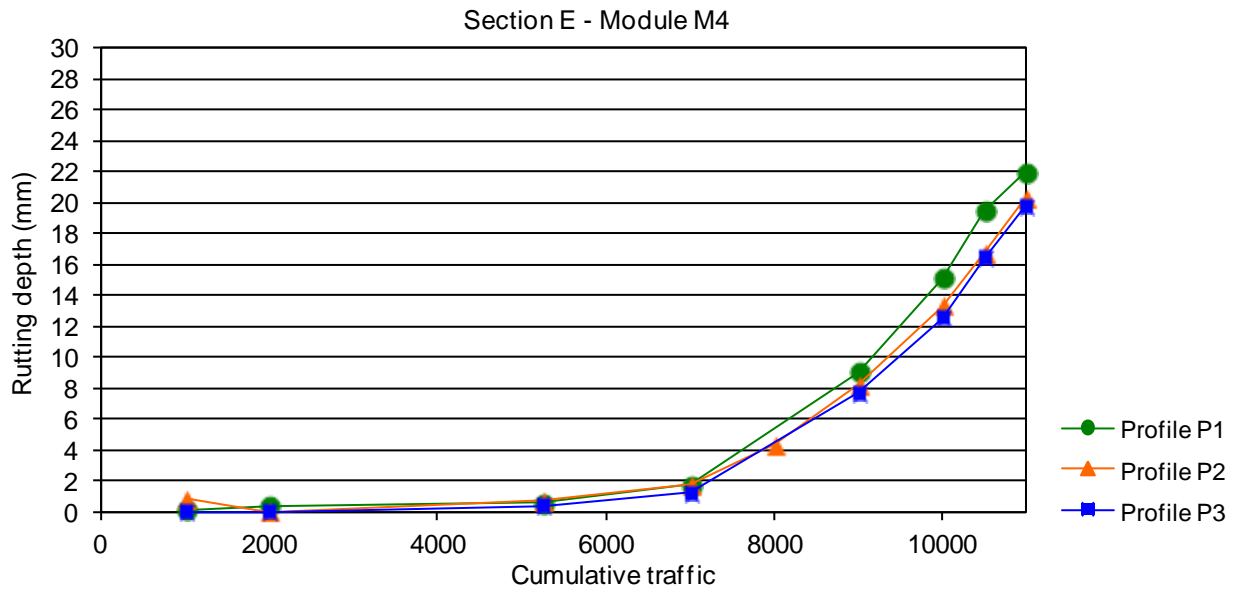


Figure 79: Evolution curve of rutting measured on section E, configuration M4

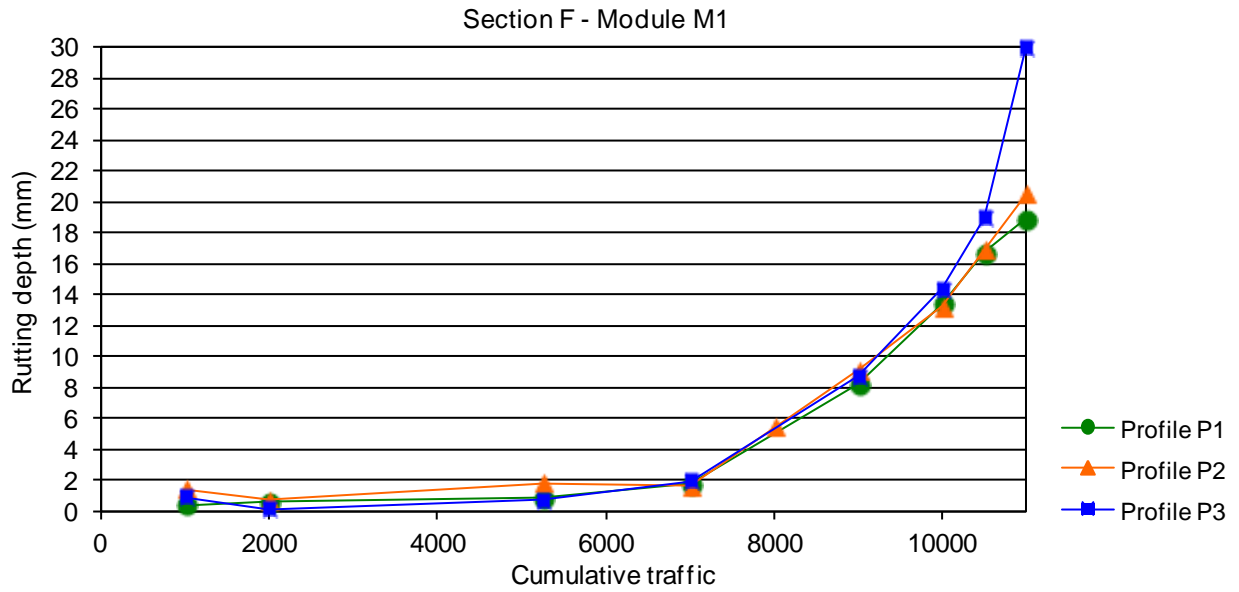


Figure 80: Evolution curve of rutting measured on section F, configuration M1

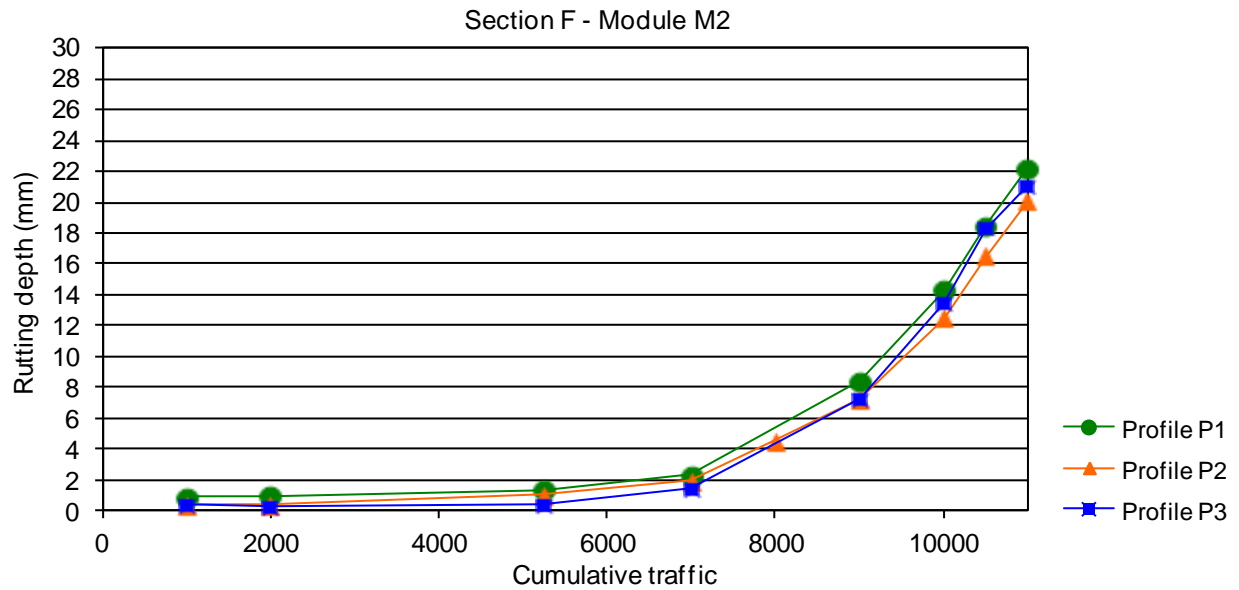
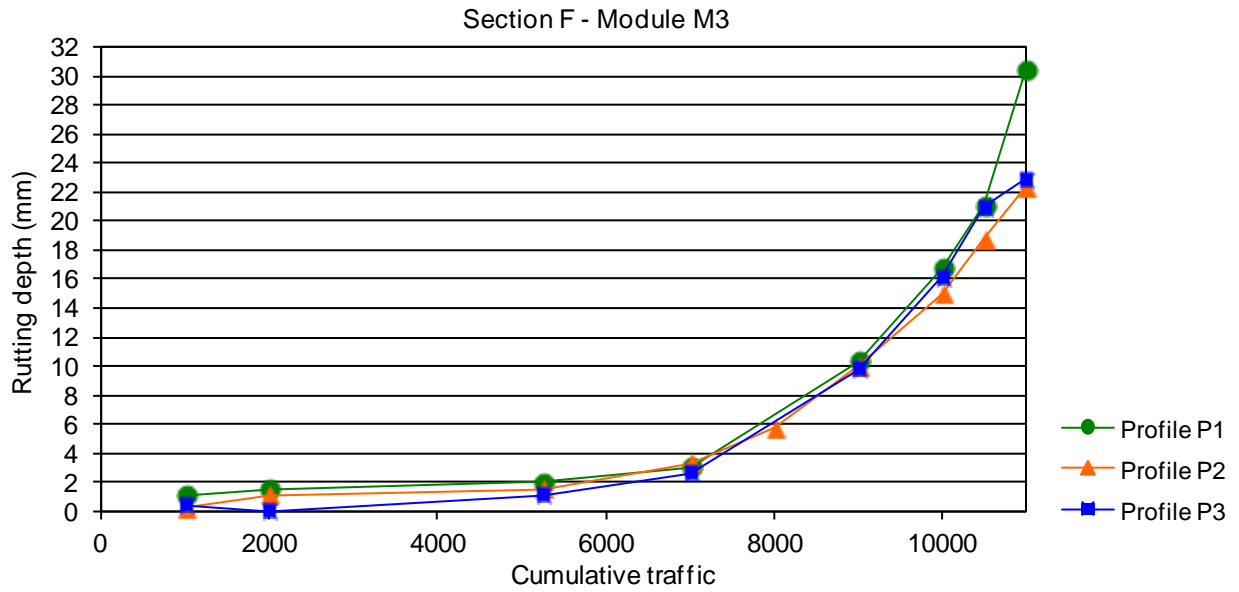
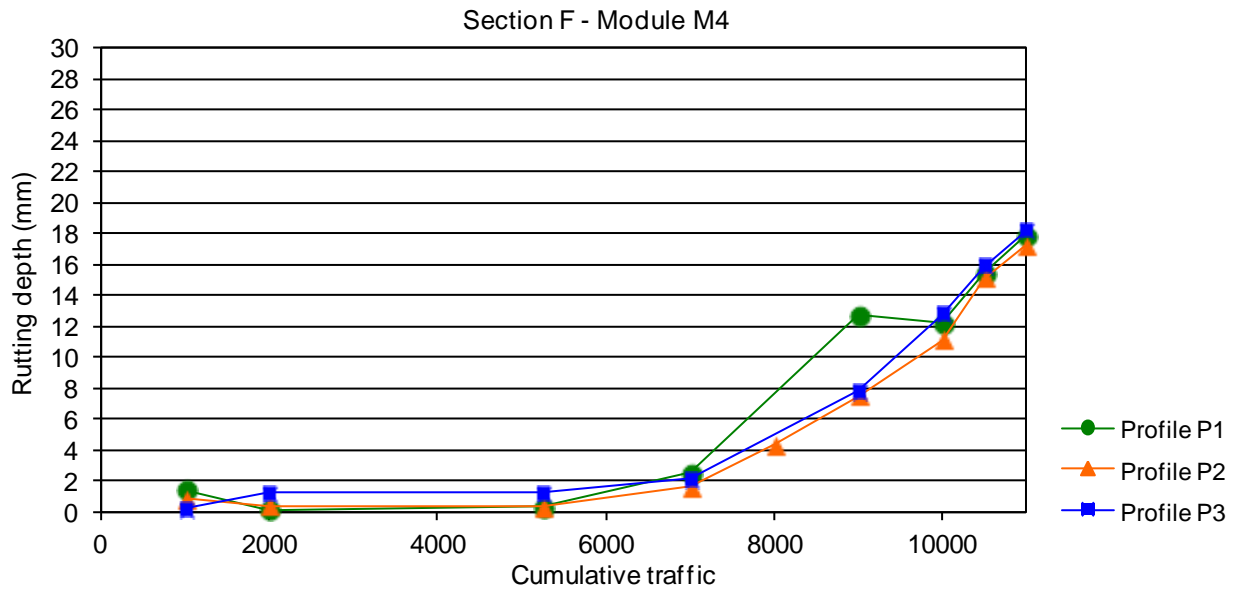


Figure 81: Evolution curve of rutting measured on section F, configuration M2



**Figure 82: Evolution curve of rutting measured on section F, configuration M3**



**Figure 83: Evolution curve of rutting measured on section F, configuration M4**

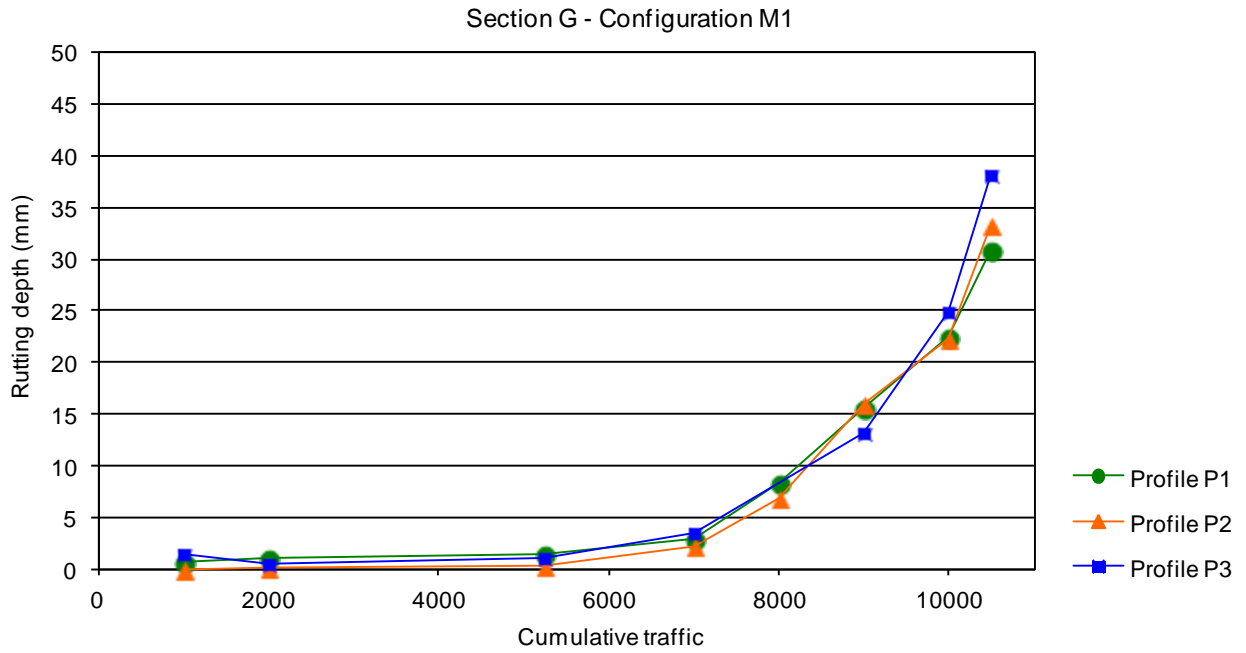


**Figure 84: Evolution curve of rutting measured on section G, configuration M1**

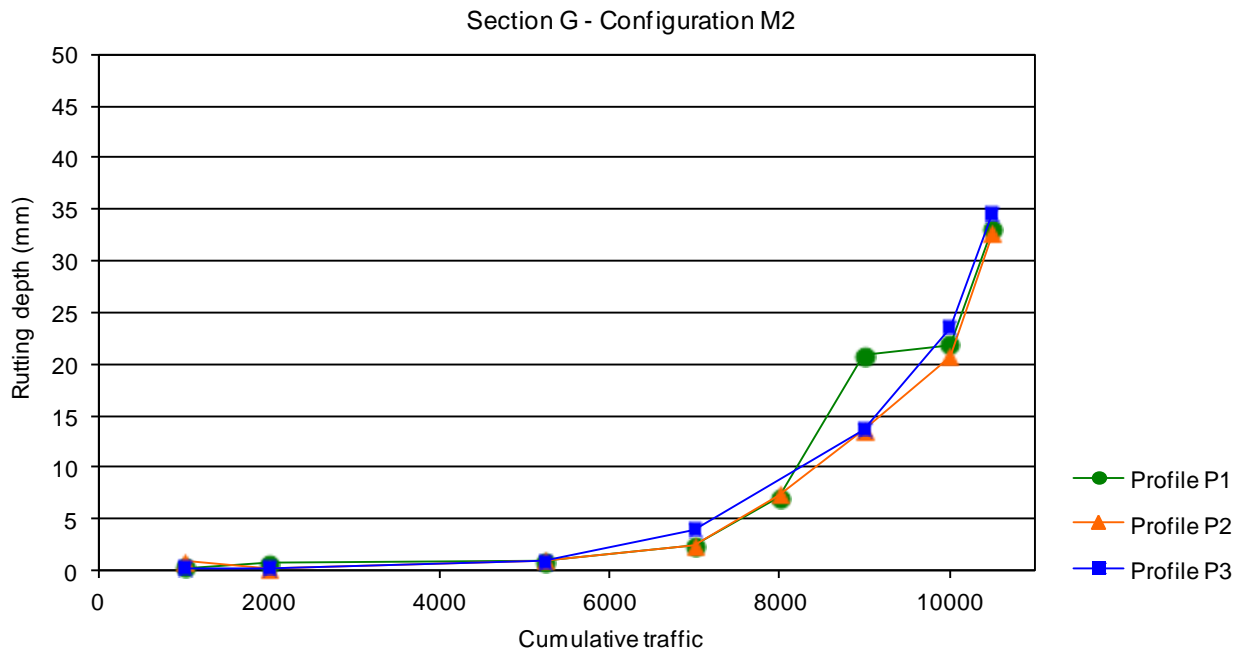


**Figure 85: Evolution curve of rutting measured on section G, configuration M2**

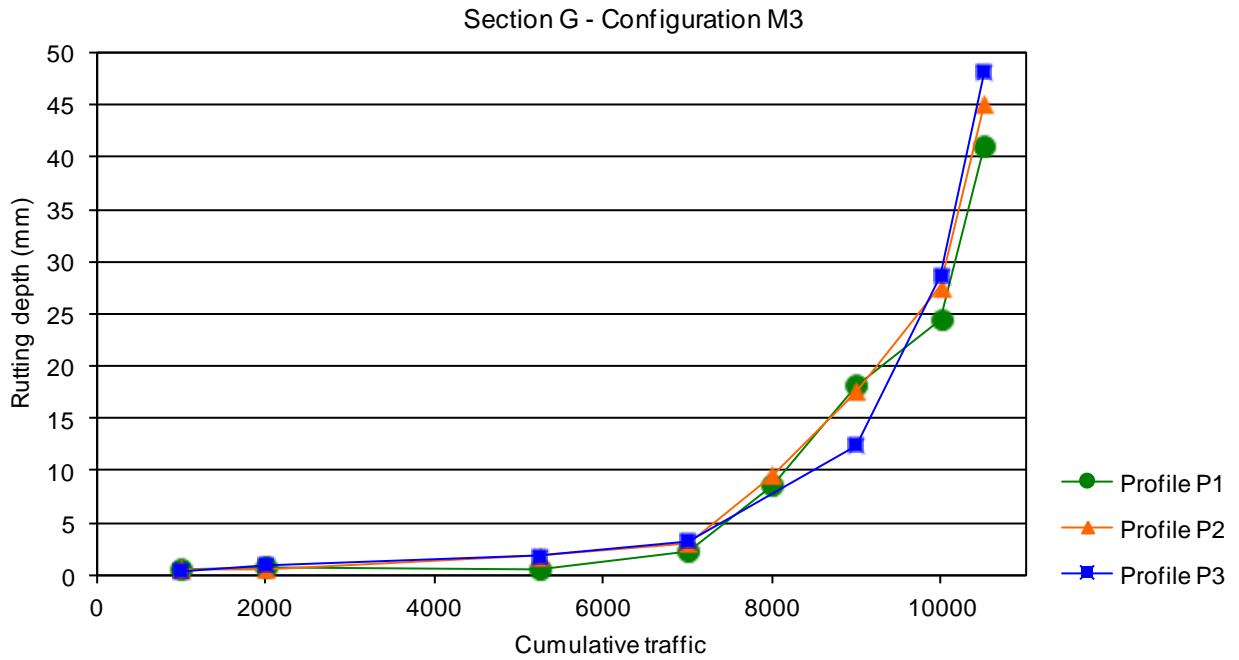


**Figure 86: Evolution curve of rutting measured on section G, configuration M3**

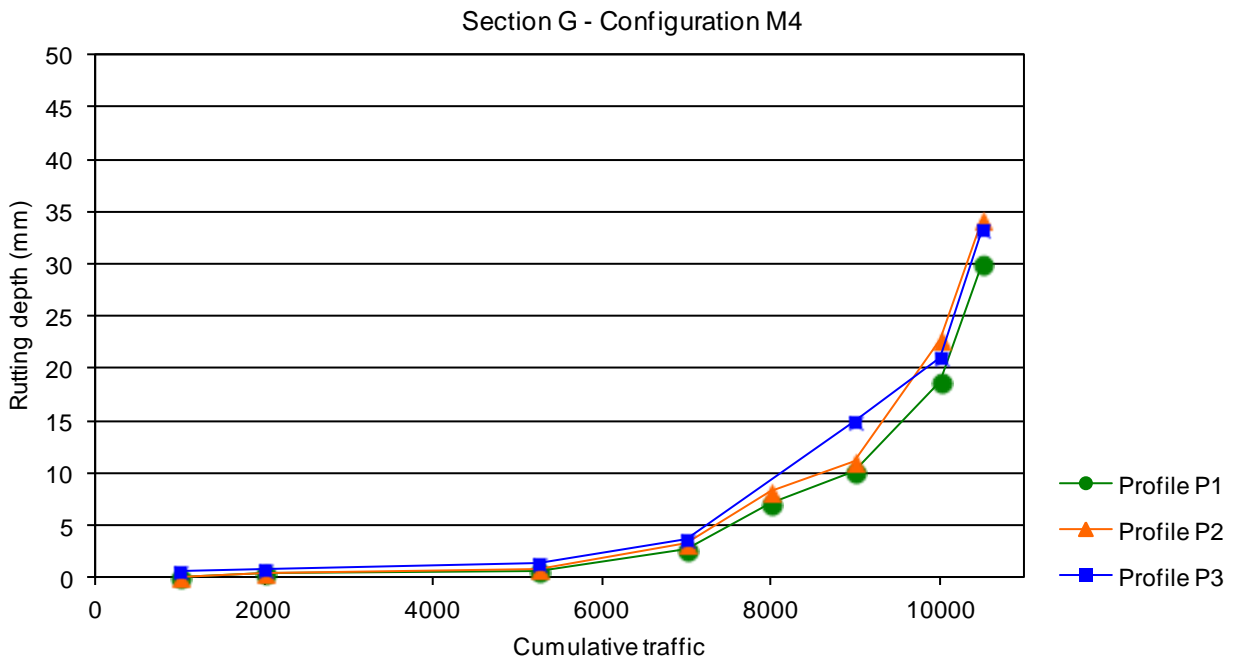


**Figure 87: Evolution curve of rutting measured on section G, configuration M4**





Ressources, territoires, habitats et logement  
Énergies et climat Développement durable  
Prévention des risques Infrastructures, transports et mer

## Présent pour l'avenir

---

service technique de l'Aviation civile  
31, avenue du Maréchal Leclerc  
94381 BONNEUIL-SUR-MARNE CEDEX  
Tél. 33 (0) 1 49 56 80 00  
Fax 33 (0) 1 49 56 82 19

Site de Toulouse  
9, avenue du Docteur Maurice Grynfolgel - BP 53735  
31037 TOULOUSE CEDEX  
Tél. 33 (0) 1 49 56 83 00  
Fax 33 (0) 1 49 56 83 02

Centre de test de détection d'explosifs  
Centre d'essais de lancement de missiles - BP 38  
40602 BISCARROSSE CEDEX  
Tél. 33 (0) 5 58 83 01 73  
Fax 33 (0) 5 58 78 02 02